

For Official Use

NEA/NSC/DOC(2012)11

Organisation de Coopération et de Développement Économiques
Organisation for Economic Co-operation and Development

24-May-2012

English - Or. English

**NUCLEAR ENERGY AGENCY
NUCLEAR SCIENCE COMMITTEE**

NEA/NSC/DOC(2012)11
For Official Use

**BENCHMARK FOR UNCERTAINTY ANALYSIS IN MODELLING (UAM)
FOR DESIGN, OPERATION AND SAFETY ANALYSIS OF LWRs**

Volume II: Specification and Support Data for the Core Cases (Phase II)

Akifumi Yamaji
akifumi.yamaji@oecd.org
+33 1 45 24 10 83

JT03322246

Complete document available on OLIS in its original format

This document and any map included herein are without prejudice to the status of or sovereignty over any territory, to the delimitation of international frontiers and boundaries and to the name of any territory, city or area.

English - Or. English

NUCLEAR ENERGY AGENCY

NUCLEAR SCIENCE COMMITTEE

NEA COMMITTEE ON SAFETY OF NUCLEAR INSTALLATIONS

**BENCHMARK FOR UNCERTAINTY
ANALYSIS IN MODELLING (UAM) FOR
DESIGN, OPERATION AND SAFETY
ANALYSIS OF LWRs**

*Volume II: Specification and Support Data
for the Core Cases (Phase II)*

Version 1.0 (Draft Specification)

T. Blyth, M. Avramova, K. Ivanov

E. Royer, E. Sartori, O. Cabellos

May 2012

OECD Nuclear Energy Agency

Foreword

In recent years there has been an increasing demand from nuclear research, industry, safety and regulation for best-estimate predictions to be provided with their confidence bounds. Consequently, an "in-depth" discussion on "Uncertainty Analysis in Modelling" was organised at the 2005 OECD/NEA Nuclear Science Committee (NSC) meeting, which led to a proposal for launching an Expert Group on "Uncertainty Analysis in Modelling" and endorsing the organisation of a workshop with the aim of defining future actions and a programme of work.

As a result, the NEA/OECD Uncertainty Analysis in Modelling (UAM) workshop took place in Pisa, Italy, on April 28-29, 2006. The major outcome of the workshop was to prepare a benchmark work programme with steps (exercises) that would be needed to define the uncertainty and modelling tasks. The other proposals made during the meeting were to be incorporated under the different steps (exercises) within the overall benchmark framework for the development of uncertainty analysis methodologies for multi-physics (coupled) and multi-scale simulations.

Following the results of the UAM-2006 workshop, the OECD/NEA NSC at its June 2006 meeting endorsed the creation of an Expert Group on Uncertainty Analysis methods in Modelling (EGUAM) under the auspices of the Working Party on Scientific issues in Reactor Systems (WPRS). Since the expert group addresses multi-scale / multi-physics aspects of uncertainty analysis, it works in close co-ordination with the benchmark groups on coupled neutronics/thermal-hydraulics simulations and on coupled core-plant problems. It also co-ordinates its activities with the Group on Analysis and Management of Accidents (GAMA) of the Committee on Safety of Nuclear Installations (CSNI). The expert group has the following mandate:

1. To elaborate a state-of-the-art report on current status and needs of sensitivity and uncertainty analysis (SA/UA) in modelling, with emphasis on multi-physics (coupled) and multi-scale simulations.
2. To identify the opportunities for international co-operation in the uncertainty analysis area that would benefit from co-ordination by the NEA/NSC.
3. To create a roadmap along with a schedule and organisation for the development and validation of methods and codes required for uncertainty analysis including the benchmarks adequate to meet those goals.

The NEA/NSC has endorsed this activity to be undertaken with the Pennsylvania State University (PSU) as the main co-ordinator and host with the assistance of the Scientific Board. The NSC/NEA has renewed and updated at the beginning of February 2011 the mandate of the EGUAM. The expert group will provide advice to the WPRS and the nuclear community on the scientific development needs (data and methods, validation experiments, scenario studies) of sensitivity and uncertainty methodology for modelling of different reactor systems and scenarios.

The main activity will be focused on uncertainties in modelling LWR transients. In this context the objectives will be:

- a) To determine modelling uncertainties for reactor systems under steady-state and transient conditions, quantifying the impact of uncertainties for each type of calculation in the multi-physics analysis, i.e.
 - a. neutronics calculations;
 - b. thermal hydraulics modelling;
 - c. fuel behaviour.
- b) For each of these types of calculation the major sources of uncertainty will be determined, arising from;

- a. data (e.g. nuclear data, geometry, materials);
 - b. numerical methods;
 - c. physical models.
- c) To develop and test methods for combining the above sources of uncertainty for each type of calculation so as to yield uncertainty assessment for the coupled multi-physics analyses;
 - d) To develop a benchmark framework, which combines information from available integral facility and NPP experimental data with analytical and numerical benchmarking;
 - e) Where available, experimental data will be used to test the individual types of calculation as well as coupled multi-physics simulations.

To summarise, in addition to LWR best-estimate calculations for design and safety analysis, the modelling aspects of Uncertainty Analysis (UA) and Sensitivity Analysis (SA) are to be further developed and validated on scientific grounds in support of their performance. There is a need for efficient and powerful UA and SA methods suitable for such complex coupled multi-physics and multi-scale simulations. The proposed benchmark sequence will address this need by integrating the expertise in reactor physics, thermal-hydraulics and reactor system modelling as well as uncertainty and sensitivity analysis, and will contribute to the development and assessment of advanced/optimised uncertainty methods for use in best-estimate reactor simulations. Such an effort can be undertaken within the framework of a programme of international co-operation that would benefit from the co-ordination of the NEA/NSC and from interfacing with the CSNI activities. More information can be found at: <http://www.oecd-nea.org/science/egrsltb/UAM>.

Version 1.0 of the Volume II: Specification and Support Data for Core Cases (Phase II) of the OECD LWR UAM benchmark incorporates suggestions and corrections proposed by the benchmark participants at the following meetings:

- UAM-3 workshop, held from April 29 to May 1, 2009 in Pennsylvania, USA,
- UAM-4 workshop, held from April 14 to April 15, 2010 in Pisa, Italy,
- UAM-5 workshop, held from April 13 to April 15, 2011 in Stockholm, Sweden.

It is advisable that participants note that the information in this document is subject to future changes following further discussions at the benchmark workshops and feedback from the participants.

Acknowledgements

Special appreciation goes to the report reviewers, which are the members the Scientific Board of UAM Expert Group:

Scientific Board and Technical Committee

| <i>Name</i> | <i>Organisation</i> | <i>Country</i> | <i>Role</i> |
|-------------------|---------------------|----------------|------------------------|
| Kostadin IVANOV | PSU | USA | Co-ordination and host |
| Thomas DOWNAR | U-Michigan | USA | Member |
| Yassin HASSAN | Texas A&M | USA | Member |
| Mark WILLIAMS | ORNL | USA | Member |
| Martin ZIMMERMANN | PSI | Switzerland | Member |
| Oscar CABELLOS | UPM | Spain | Member |
| Francesco D'AURIA | U-Pisa | Italy | Member |
| Tomasz KOZLOWSKI | U-Illinois | USA | Chair of EGUAM, NSC |
| Sören KLIEM | HZDR | Germany | Member |
| Andreas PAUTZ | GRS | Germany | Member |
| Eric ROYER | CEA | France | Member |
| Hideaki UTSUNO | JNES | Japan | Member |
| Maria AVRAMOVA | PSU | USA | Member |
| Ivo KODELI | IJS | Slovenia | Member |
| Enrico SARTORI | Consultant | France | Member |
| Jim GULLIFORD | OECD/NEA | | Secretariat |

The authors would like acknowledge specifically the contribution of providing experimental test data for definition of test cases of Dr. S. Kliem from HZDR and Dr. J. Gulliford from OECD/NEA.

The authors wish to express their sincere appreciation for the outstanding support offered by Professor F. D'Auria (U-Pisa), Dr. S. Langenbuch (GRS), and E. Royer (CEA) by preparing a document on the expected impact and benefits of the OECD LWR UAM benchmark activity for LWR safety and licensing (Technology Relevance of the "Uncertainty Analysis In Modelling" Project for Nuclear Reactor Safety, NEA/NSC/DOC (2007)15).

TABLE OF CONTENTS

FOREWORD 3

ACKNOWLEDGEMENTS 5

LIST OF FIGURES 7

LIST OF TABLES 9

CHAPTER 1: INTRODUCTION 12

1.1 OBJECTIVE 12

1.2 DEFINITION OF BENCHMARK PHASES AND EXERCISES 13

1.3 CONTENT OF THIS DOCUMENT 14

CHAPTER 2: DEFINITION OF EXERCISE II-1: FUEL PHYSICS 16

2.1 DISCUSSION OF INPUT, PROPAGATED, AND OUTPUT UNCERTAINTIES 17

2.2 TEST PROBLEMS 20

CHAPTER 3: DEFINITION OF EXERCISE II-2: TIME-DEPENDENT NEUTRONICS 50

3.1 DISCUSSION OF INPUT, TARGET, AND OUTPUT UNCERTAINTIES 50

3.2 TEST PROBLEMS 52

CHAPTER 4: DEFINITION OF EXERCISE II-3: BUNDLE THERMAL-HYDRAULICS 86

4.1 DISCUSSION OF INPUT, TARGET AND OUTPUT UNCERTAINTIES 87

4.2 TEST PROBLEMS 90

CHAPTER 5: REQUESTED OUTPUT 117

5.1 INTRODUCTION 117

5.2 RESULTS FOR EXERCISE II-1 117

5.3 RESULTS FOR EXERCISE II-2 120

5.4 RESULTS FOR EXERCISE II-3 123

CHAPTER 6: CONCLUSIONS 126

REFERENCES 128

List of Figures

| | |
|--|----|
| Figure 2.1: PB-2 Fuel Pin Image | 21 |
| Figure 2.2: PB-2 Power History Plot | 24 |
| Figure 2.3: PB-2 Axial Power Profile Plot | 25 |
| Figure 2.4: PB-2 Transient Power History Plot | 27 |
| Figure 2.5: TMI-1 Fuel Pin Image | 29 |
| Figure 2.6: TMI-1 Power History Plot..... | 30 |
| Figure 2.7: TMI-1 Axial Power Profile Plot..... | 31 |
| Figure 2.8: TMI-1 Transient Power History Plot..... | 32 |
| Figure 2.9: VVER-1000 Fuel Pin Image | 34 |
| Figure 2.10: VVER-1000 Power History Plot | 36 |
| Figure 2.11: VVER-1000 Axial Power Profile Plot | 37 |
| Figure 2.12: VVER-1000 Transient Power History Plot | 38 |
| Figure 2.13: IFA-432 Fuel Pin Image..... | 40 |
| Figure 2.14: IFA-432 Power History Plot..... | 40 |
| Figure 2.15: IFA-432 Axial Power Profile Plot..... | 42 |
| Figure 2.16: FK-1 Transient Power History Plot..... | 45 |
| Figure 2.17: IFA-429 Fuel Rod Image | 47 |
| Figure 2.18: IFA-429 Power History Plot..... | 48 |
| Figure 2.19: IFA-429 Axial Power Profile Plot..... | 49 |
| Figure 3.1: PB-2 FA Pin Layout | 53 |
| Figure 3.2: PB-2 Irradiation History Plot..... | 55 |
| Figure 3.3: PB-2 Mini-core Geometry | 56 |
| Figure 3.4: PB-2 Fuel Assembly Geometry | 57 |
| Figure 3.5: PB-2 Mini-core control rod movements over time..... | 58 |
| Figure 3.6: TMI-1 FA Pin Layout..... | 59 |
| Figure 3.7: TMI-1 Irradiation History Plot..... | 61 |
| Figure 3.8: TMI-1 Mini-core Geometry | 62 |
| Figure 3.9: TMI-1 mini-core reactivity versus time plot | 63 |
| Figure 3.10: VVER-1000 FA Pin Layout | 64 |
| Figure 3.11: VVER-1000 Irradiation History Plot..... | 66 |
| Figure 3.12: Color-set configuration for Kozloduy-6 | 66 |
| Figure 3.13: VVER-1000 Control Rod Position vs. Time Plot..... | 67 |
| Figure 3.14: FK-2 FA Pin Layout..... | 68 |
| Figure 3.15: FK-2 Irradiation History Plot | 71 |
| Figure 3.16: TK-3 FA Pin Layout..... | 72 |
| Figure 3.17: TK-3 Irradiation History Plot..... | 75 |
| Figure 3.18: SPERT III E-core Geometry | 76 |
| Figure 3.19: VVER-1000 FA Pin Layout | 77 |
| Figure 3.20: VVER-1000 Irradiation History Plot..... | 79 |
| Figure 3.21: VVER-1000 Core Based on the V-1000 Facility | 80 |
| Figure 3.22: V-1000 Core Fuel Assemblies..... | 81 |
| Figure 3.23: VVER-1000 Profiled Fuel Assembly..... | 82 |
| Figure 3.24: VVER-1000 Flat Fuel Assembly..... | 82 |
| Figure 3.25: V-1000 Transient Control Rod Movement versus Time | 85 |
| Figure 4.1: PB-2 Bundle Image | 91 |

| | |
|---|-----|
| Figure 4.2: PB-2 Bundle Axial Power Profile Plot..... | 93 |
| Figure 4.3: PB-2 Bundle Transient History Plot..... | 96 |
| Figure 4.4: TMI-1 Bundle Image..... | 97 |
| Figure 4.5: TMI-1 Bundle Axial Power Profile Plot | 99 |
| Figure 4.6: TMI-1 Bundle Transient History Plot | 101 |
| Figure 4.7: VVER-1000 Bundle Image | 102 |
| Figure 4.8: VVER-1000 Bundle Axial Power Profile Plot..... | 104 |
| Figure 4.9: VVER-1000 Radial Power Profile, 1/6 Bundle Symmetry | 104 |
| Figure 4.10: VVER-1000 Bundle Transient History Plot..... | 106 |
| Figure 4.11: BFBT Bundle Image | 107 |
| Figure 4.12: BFBT Bundle Axial Power Profile Plot | 108 |
| Figure 4.13: BFBT Bundle Transient History Plot..... | 111 |
| Figure 4.14: PSBT Bundle Image..... | 112 |
| Figure 4.15: PSBT Bundle Axial Power Profile Plot..... | 114 |
| Figure 4.16: PSBT Bundle Transient History Plot | 116 |

List of Tables

| | |
|---|----|
| Table 2.1: Exercise II-1 Core Boundary Condition Variations..... | 20 |
| Table 2.2: Exercise II-1 Code Parameter Variations | 21 |
| Table 2.3: PB-2 Fuel Rod Geometry | 22 |
| Table 2.4: PB-2 Power History..... | 23 |
| Table 2.5: PB-2 Axial Power Profile | 24 |
| Table 2.6: Case 1 Manufacturing Uncertainties..... | 25 |
| Table 2.7: PB-2 Transient Power History..... | 26 |
| Table 2.8: PB-2 Transient Time Step Sizes..... | 27 |
| Table 2.9: PB-2 Transient Coolant Temperature History..... | 28 |
| Table 2.10: TMI-1 Fuel Rod Geometry..... | 28 |
| Table 2.11: TMI-1 Power History | 29 |
| Table 2.12: TMI-1 Axial Power Profile..... | 30 |
| Table 2.13: Case 2 Manufacturing Uncertainties..... | 31 |
| Table 2.14: TMI-1 Transient Power History | 32 |
| Table 2.15: TMI-1 Transient Time Step Sizes..... | 33 |
| Table 2.16: TMI-1 Transient Coolant Temperature History..... | 33 |
| Table 2.17: VVER-1000 Fuel Rod Geometry | 34 |
| Table 2.18: VVER-1000 Power History..... | 35 |
| Table 2.19: VVER-1000 Axial Power Profile | 36 |
| Table 2.20: Case 3 Manufacturing Tolerances | 37 |
| Table 2.21: VVER-1000 Transient Power History..... | 38 |
| Table 2.22: VVER-1000 Transient Time Step Sizes | 39 |
| Table 2.23: IFA-432 Fuel Rod Geometry..... | 39 |
| Table 2.24: IFA-432 Power History | 41 |
| Table 2.25: IFA-432 Axial Power Profile..... | 42 |
| Table 2.26: Case 4 Manufacturing Uncertainties..... | 43 |
| Table 2.27: FK-1 Fuel Rod Geometry | 43 |
| Table 2.28: FK-1 Transient Power History..... | 44 |
| Table 2.29: FK-1 Transient Coolant Temperature History..... | 45 |
| Table 2.30: FK-1 Transient Time Step Sizes..... | 45 |
| Table 2.31: IFA-429 Fuel Rod Geometry..... | 46 |
| Table 2.32: IFA-429 Power History | 47 |
| Table 2.33: IFA-429 Axial Power Profile..... | 48 |
| Table 2.34: Case 5 Manufacturing Tolerances | 49 |
| Table 3.1: PB-2 FA Pin Descriptions..... | 54 |
| Table 3.2: PB-2 FA Details..... | 54 |
| Table 3.3: PB-2 Fuel Rod Dimensions and Parameters..... | 54 |
| Table 3.4: PB-2 Core Boundary Conditions | 54 |
| Table 3.5: PB-2 Zr-2 Cladding Composition..... | 55 |
| Table 3.6: PB-2 Irradiation History | 55 |
| Table 3.7: PB-2 Mini-core HZP Conditions | 56 |
| Table 3.8: TMI-1 FA Pin Descriptions..... | 58 |
| Table 3.9: TMI-1 FA Details | 59 |
| Table 3.10: TMI-1 Fuel, Guide, and Instrumentation Rod Dimensions and Parameters..... | 60 |
| Table 3.11: TMI-1 Core Boundary Conditions..... | 60 |

| | |
|--|-----|
| Table 3.12: TMI-1 Zr-4 Cladding Composition | 60 |
| Table 3.13: TMI-1 Irradiation History | 60 |
| Table 3.14: VVER-1000 FA Details | 64 |
| Table 3.15: VVER-1000 Fuel Rod Dimensions and Parameters | 65 |
| Table 3.16: VVER-1000 Core Boundary Conditions | 65 |
| Table 3.17: VVER-1000 Zr+1% Nb Cladding Composition | 65 |
| Table 3.18: VVER-1000 Irradiation History | 65 |
| Table 3.19: VVER-1000 Control Rod Movement | 67 |
| Table 3.20: FK-2 FA Pin Descriptions | 68 |
| Table 3.21: FK-2 FA Details | 69 |
| Table 3.22: FK-2 Fuel Rod Dimensions and Parameters | 69 |
| Table 3.23: FK-2 Core Boundary Conditions | 69 |
| Table 3.24: FK-2 Zr-2 Cladding Composition | 70 |
| Table 3.25: FK-2 Irradiation History | 70 |
| Table 3.26: TK-3 FA Pin Descriptions | 72 |
| Table 3.27: TMI-1 FA Details | 72 |
| Table 3.28: TK-3 Fuel, Guide, and Instrumentation Rod Dimensions and Parameters | 73 |
| Table 3.29: TK-3 Core Boundary Conditions | 73 |
| Table 3.30: TK-3 Zr-4 Cladding Composition | 73 |
| Table 3.31: TK-3 Irradiation History | 74 |
| Table 3.32: SPERT III E-core Dimensions | 76 |
| Table 3.33: SPERT III E-core Initial Conditions | 76 |
| Table 3.34: VVER-1000 FA Details | 78 |
| Table 3.35: VVER-1000 Fuel Rod Dimensions and Parameters | 78 |
| Table 3.36: VVER-1000 Core Boundary Conditions | 78 |
| Table 3.37: VVER-1000 Zr+1% Nb Cladding Composition | 78 |
| Table 3.38: VVER-1000 Irradiation History | 79 |
| Table 3.39: V-1000 Core Fuel Assemblies Defined | 81 |
| Table 3.40: V-1000 Fuel Assembly Specifications | 83 |
| Table 3.41: V-1000 Fuel Rod Dimensions and Parameters | 83 |
| Table 3.42: V-1000 Zircalloy Composition | 83 |
| Table 3.43: V-1000 Stainless Steel Composition | 83 |
| Table 3.44: Control Rod Positions and Velocities for the insertion portion | 84 |
| Table 3.45: Control Rod Positions and Velocities for times of the withdrawal portion | 85 |
| Table 4.1: Exercise II-3 Core Boundary Condition Uncertainties | 87 |
| Table 4.2: Exercise II-3 Geometry Uncertainties | 88 |
| Table 4.3a: Estimated Accuracy for Void Fraction Measurements in PWR | 88 |
| Table 4.3b: Estimated Accuracy for Void Fraction Measurements in BWR | 89 |
| Table 4.4: PB-2 Bundle Geometry | 91 |
| Table 4.5: PB-2 Bundle Boundary Conditions | 92 |
| Table 4.6: PB-2 Spacer Grid Locations | 92 |
| Table 4.7: PB-2 Bundle Axial Power Profile | 92 |
| Table 4.8: PB-2 Bundle Radial Power Profile | 93 |
| Table 4.9: PB-2 Bundle Transient History | 94 |
| Table 4.10: TMI-1 Bundle Geometry | 97 |
| Table 4.11: TMI-1 Bundle Boundary Conditions | 98 |
| Table 4.12: TMI-1 Spacer Grid Locations | 98 |
| Table 4.13: TMI-1 Bundle Axial Power Profile | 98 |
| Table 4.14: TMI-1 Bundle Radial Power Profile, 1/4 Bundle Symmetry | 99 |
| Table 4.15: TMI-1 Bundle Transient History | 100 |
| Table 4.16: VVER-1000 Bundle Geometry | 102 |

| | |
|--|-----|
| Table 4.17: VVER-1000 Bundle Boundary Conditions | 103 |
| Table 4.18: VVER-1000 Spacer Grid Locations | 103 |
| Table 4.19: VVER-1000 Bundle Axial Power Profile..... | 103 |
| Table 4.20: VVER-1000 Bundle Transient History..... | 105 |
| Table 4.21: BFBT Bundle Geometry | 106 |
| Table 4.22: BFBT Bundle Boundary Conditions..... | 107 |
| Table 4.23: BFBT Spacer Grid Locations | 107 |
| Table 4.24: BFBT Bundle Axial Power Profile | 108 |
| Table 4.25: BFBT Bundle Radial Power Profile | 109 |
| Table 4.26: BFBT Bundle Transient History | 109 |
| Table 4.27: PSBT Bundle Geometry | 111 |
| Table 4.28: PSBT Bundle Boundary Conditions..... | 112 |
| Table 4.29: Spacer Grid Types and Locations..... | 113 |
| Table 4.30: PSBT Bundle Axial Power Profile | 113 |
| Table 4.31: PSBT Bundle Radial Power Profile..... | 114 |
| Table 4.32: PSBT Bundle Transient History | 115 |
| Table 5.1: Exercise II-1 Steady-State Numerical Case Results Template | 118 |
| Table 5.2: Exercise II-1 Steady-State Experimental Case Results Template | 119 |
| Table 5.3: Exercise II-1 Transient Numerical Case Results Template | 119 |
| Table 5.4: Exercise II-1 Transient Experimental Case Results Template | 120 |
| Table 5.5: Exercise II-2 Depletion Numerical Case Results Template..... | 121 |
| Table 5.6: Exercise II-2 Depletion Experimental Case Results Template..... | 122 |
| Table 5.7: Exercise II-2 Kinetics Numerical Case Results Template..... | 123 |
| Table 5.8: Exercise II-2 Kinetics Experimental Case Results Template | 123 |
| Table 5.9: Exercise II-3 Steady-state Numerical Case Results Template..... | 124 |
| Table 5.10: Exercise II-3 Transient Numerical Case Results Template | 125 |

Chapter 1: Introduction

In addition to the establishment of light-water reactor (LWR) best-estimate calculations for design and safety analysis, it is important to understand uncertainties for introducing appropriate design margins and deciding where additional efforts should be undertaken to reduce uncertainties. The need of uncertainty evaluations for LWR best-estimate calculations was discussed and addressed within the framework of the CRISSUE-S international European Union (EU) project [1] along with the identification of sources of uncertainties in coupled neutronics/thermal-hydraulics simulations. For this reason the modelling aspects of Uncertainty Analysis (UA) and Sensitivity Analysis (SA) are to be further developed and validated on scientific grounds in support of their performance. In line with recent meetings the international expert community in reactor physics, thermal-hydraulics, and uncertainty and sensitivity analysis, has decided that a first step in this direction is to define an OECD benchmark for Uncertainty Analysis in Modelling (UAM) for design, operation, and safety analysis of LWRs [2], [3], [4]. The expected impact and benefits of the OECD LWR UAM benchmark activity for LWR safety and licensing are summarised in [5]. This benchmark project is challenging and responds to needs of estimating confidence bounds for results from simulations and analysis in real applications.

Reference LWR systems and scenarios for coupled code analysis are defined to study the uncertainty effects for all stages of the system calculations. Measured data from plant operation are available for the chosen scenarios. The existing OECD/NEA/NSC coupled code transient benchmarks – such as BWR Turbine Trip (TT) [6], PWR Main Steam Line Break (MSLB) [7], VVER-1000 (V1000) Coolant Transients (CT) [8], BWR Full Bundle Test (BFBT) [9], PWR Sub-channel and Bundle Test (PSBT) [10] are used as part of the framework for adding uncertainty analysis methodologies in the best-estimate modelling for design and operation of LWRs. Such an approach facilitates the benchmark activities since many organisations have already developed input decks and tested their codes on the above-mentioned coupled code benchmarks. From these OECD LWR transient benchmark problems, the Peach Bottom 2 (PB-2) BWR Turbine Trip (TT) is proposed as the first reference system-scenario, although provisions are made to address the other LWR systems and scenarios such as TMI-1 PWR MSLB, PWR-RIA-ATWS, BWR-CRDA-ATWS (with boron modelling), VVER-1000 CT, etc. The Peach Bottom 2 BWR Turbine Trip Benchmark is well documented not only in the OECD/NEA/NRC BWR TT benchmark specifications [6] but also in a series of EPRI [11], [12] and PECO reports [13], which include design, operation, and measured steady-state and transient neutronics and thermal-hydraulics data. The fuel cycle depletion, steady-state and transient measured data, available at the integral parameter level and the local distribution level, are very important features of the Peach Bottom 2 BWR Turbine Trip. Integration with the OECD/NEA/NRC BWR BFBT and PSBT benchmarks and the uncertainty analysis exercises performed in their framework will be made. The integration of the PB-2 BWR turbine trip will also be extended to the ongoing NEA/CSNI BEMUSE-3 benchmark through the NEA internal co-operation between the NSC and CSNI Committees.

1.1 Objective

The proposed technical approach is to establish a benchmark for uncertainty analysis in best-estimate modelling and coupled multi-physics and multi-scale LWR analysis, using as bases a series of well-defined problems with complete sets of input specifications and reference experimental data. The objective is to determine the uncertainty in LWR system calculations at all stages of coupled reactor physics/thermal hydraulics calculation. The full chain of uncertainty propagation from basic data, engineering uncertainties, across different scales (multi-scale), and physics phenomena (multi-physics) is tested on a number of

benchmark exercises for which experimental data is available and for which the power plant details have been released.

The principal objectives are: a) to subdivide the complex system/scenario into several steps or exercises, each of which can contribute to the total uncertainty of the final coupled system calculation, b) to identify input, output and assumptions for each step, c) to calculate the resulting uncertainty in each step; d) to propagate the uncertainties in an integral systems simulation for which high-quality plant experimental data exist for the total assessment of the overall computer code uncertainty. As part of this effort, the development and assessment of different methods or techniques to account for the uncertainties in the calculations will be investigated and reported to the participants.

In summary, the objective of the proposed work is to define, co-ordinate, conduct, and report an international benchmark for uncertainty analysis in best-estimate coupled code calculations for design, operation, and safety analysis of LWRs. The title of this benchmark is: “OECD UAM LWR Benchmark”.

The experimental data are used as much as possible (two “interactions” with “known” experimental data are indicated above but others can be added). The benchmark team identifies Input (I), Output (O) or target of the analysis, as well as provides guidance on assumptions for each step and propagated uncertainty parameters (U). The uncertainty from one step should be propagated to the others (as much as feasible and realistic).

1.2 Definition of benchmark phases and exercises

The above-described approach is based on the introduction of 9 steps (exercises), which allows for developing a benchmark framework which mixes information from the available integral facility and NPP experimental data with analytical and numerical benchmarking. Such an approach compares and assesses current and new uncertainty methods on representative applications and simultaneously benefits from different methodologies to arrive at recommendations and guidelines. These 9 steps (exercises) are carried out in 3 phases as follows:

Phase I (Neutronics Phase)

- Exercise I-1: “Cell Physics” focused on the derivation of the multi-group microscopic cross-section libraries and their uncertainties.
- Exercise I-2: “Lattice Physics” focused on the derivation of the few-group macroscopic cross-section libraries and their uncertainties.
- Exercise I-3: “Core Physics” focused on the core steady-state stand-alone neutronics calculations and their uncertainties.

Phase II (Core Phase)

- Exercise II-1: “Fuel Physics”: Fuel thermal properties relevant to steady-state and transient performance.
- Exercise II-2: “Time-Dependent Neutronics”: Neutron kinetics and fuel depletion stand-alone performance.
- Exercise II-3: “Bundle Thermal-Hydraulics”: Thermal-hydraulic fuel bundle performance.

Phase III (System Phase)

- Exercise III-1: “Core Multi-Physics” - Coupled neutronics/thermal-hydraulics core performance (coupled steady-state, coupled depletion, and coupled core transient with boundary conditions).
- Exercise III-2: “System Thermal-Hydraulics” - Thermal-hydraulics system performance.

- Exercise III-3: “Coupled Core-System” - Coupled neutronics kinetics thermal-hydraulic core/thermal-hydraulic system performance.
- Exercise III-4: “Comparison of Best-Estimate Plus Uncertainty (BEPU) vs. Conservative Calculations”.

1.3 Content of this document

Separate specifications will be prepared for each phase in order to allow participation in the full phase or only in a subset of the exercises. Boundary conditions and necessary input information are provided by the benchmark team. The intention is to follow the calculation scheme for coupled calculations for LWR design and safety analysis established in the nuclear power generation industry and regulation. This specification document covers Phase II, which includes the second three Exercises (core) as follows:

Chapter 2 of this document provides the definition of Exercise II-1.

Chapter 3 provides the definition of Exercise II-2.

Chapter 4 provides the definition of Exercise II-3.

Chapter 5 specifies the requested output for the three exercises.

Chapter 6 provides summary and conclusions.

This phase is focused on understanding uncertainties in prediction of key reactor core parameters associated with LWR stand-alone fuel performance, thermal-hydraulics and neutron kinetics core simulation. Such uncertainties occur due to input data uncertainties, modelling errors, and numerical approximations. Phase II addresses time-dependent neutronics (kinetics and depletion), thermal-hydraulics, and fuel performance without any coupling between the three physics phenomena. Output parameters and propagated parameters are defined for exercises of Phases II for the three main types of LWRs selected in UAM (PWR, BWR and VVER). These three main LWR types are selected, based on previous benchmark experience and available data:

- PWR (TMI-1)
- BWR (Peach Bottom-2)
- VVER-1000 (Kozloduy-6, Kalinin-3)

For each exercise it is important to identify which new input uncertainties are taken into account and which input uncertainties are propagated from the previous exercise. In Phase II of the benchmark the input uncertainties are specified as follows: best-estimate values for input parameters supplemented by the variance-covariance matrices (utilised for cross-section uncertainties), and for other input uncertainties – probability distribution functions (PDF) and associated parameters. Other important parameters to be defined are the Output (O) uncertainties and propagated Uncertainty parameters (U) for each exercise. This task is directly related to the objective of each exercise. The Output (O) uncertainties are for specified output parameters for each exercise, used to test (evaluate) the utilised uncertainty method. The propagated Uncertainty parameters (U) are output parameters, which are selected to be propagated further through the follow-up exercises in order to calculate the overall resulting uncertainty. The Phase I of the benchmark adopts the following approach. For Output (O) uncertainties – requested is the best-estimate value of the parameter with associated uncertainties where the associated uncertainties are in terms of standard deviation. For propagated Uncertainty parameters (U) – requested is the best-estimate value of the parameter with associated uncertainties where the associated uncertainties are variance-covariance matrices.

For example the propagated uncertainties for Phase II are as follows:

- Exercise II-1 - U-4 (uncertainties in fuel temperature – Doppler feedback);

- Exercise II-2 - U-5 (uncertainties in time-dependent (dynamic) reactivity insertion, total power evolution and power peaking factors as well as uncertainties of criticality values, reactions and collapsed cross-sections, and nuclide concentrations with depletion in an assembly model);
- Exercise II-3 - U-6 (uncertainties in moderator temperature, density and void fraction – moderator feedback).

Chapter 2: Definition of Exercise II-1: fuel physics

Exercise II-1 is entitled “Fuel Modelling” and it is focused on evaluating uncertainties associated with modelling and prediction of one of the most important feedback parameters in coupled neutronics/thermal-hydraulic calculations - fuel temperature (Doppler feedback). Its objective is to identify and propagate input uncertainties in the standard fuel rod models (whether it is an average rod, a fuel assembly, a group of assemblies, or the whole core) used in the current thermal-hydraulics codes for steady-state and transient analysis. More sophisticated simulation tools such as fuel performance codes (for example FRAPCON and FRAPTRAN) will be utilised for obtaining reference solutions. Halden in-pile experimental fuel temperature data will be used to determine the uncertainty in the participants’ fuel rod models. The other relevant considerations in this exercise include data, models, and recommendations on the most appropriate fuel properties which reflect burn-up as well as uncertainties in fuel manufacturing.

Modelling fuel behaviour in a reactor under certain transient conditions is an important step in the calculations required to assess the safety and operation of the reactor. The models in this exercise will be single-pin models. Variations in the Doppler feedback properties of the fuel can change greatly with smaller variations in power levels. The propagation of these uncertainties throughout calculations will affect other outputs desired by the participants. There are codes that excel in transient calculations such as the Pacific Northwest National Laboratory (PNL) developed FRAPTRAN. This code can provide reference data for time-dependent rod power scenarios. It provides radial and axial temperature distributions as well as time dependence for the fuel rods analysed. It is also useful for determining physical parameters of the fuel such as diameter and fuel-cladding gap thickness, the internal pressure of the fuel rod gases, the heat transfer coefficient at the cladding surface, strains and stresses, and more details. The types of abnormal operational scenarios for which this code is useful are in reactivity-initiated accidents (RIAs) such as rod ejection/drops and loss-of-coolant accidents (LOCAs). The codes are capable of predicting deformation history of the fuel rods as a function of time-dependent rod parameters given as inputs.

Static reactor operation can also be analysed with another code from PNL: FRAPCON. This code calculates cladding and fuel temperatures, various fuel properties and dimensions, and more, based on a variety of inputs that the user specifies. Inputs include the time steps for the programme, properties of the pellet such as its dimensions and density, the nodalisation of the geometry, and the fuel properties, the mole fractions of the chemicals present in the simulation, fuel enrichment, rod dimensions, and other geometries. There are also various correlations that can be activated depending on what is most accurate for the simulation. These correlations include more detailed material properties and various models that track things such as cladding degradation. Also, many included subroutines in FRAPCON can give very detailed results for certain parameters, mostly physical properties of the fuel and cladding. During calculations, FRAPCON takes into account many phenomena such as heat conduction, deformation, mechanical interaction of cladding and fuel, fission gas release, internal gas pressure, oxidation and heat transfer through the rod to the coolant.

Proper modelling of thermal behaviour during normal and transient conditions includes surface heat transfer, the heat transfer across the fuel-to-cladding gap, thermal conductivity of fuel and cladding, power generation distribution in the fuel, and determining a solution of the conduction equation. There are various inputs required for this type of modelling and the uncertainty inherent in each of them will be examined in this exercise.

2.1 Discussion of input, propagated, and output uncertainties

Input uncertainties include the fuel pellet nodalisation, gas gap composition, as well as cladding, fuel and gap conductivities. For some of the conductivities the uncertainties of code-utilised correlations will be taken into account. The fuel conductivity has burn-up dependence, which can be treated either in a simple way or can be left for Phase III. For steady-state simulations, the input uncertainties (such as uncertainties of thermal conductivities) will be propagated to the uncertainty of Doppler temperature prediction. The output uncertainty parameter of interest in this exercise is the nodal fuel (Doppler) temperature. The definition for calculation of Doppler temperature will be provided to the participants by the benchmark team.

The input, output, and propagated uncertainties have been identified for this exercise and include the following:

Input (I) uncertainty parameters: local pin power, local pin exposure, local pressure, local bulk temperature and local surface heat transfer coefficient.

Output (O) uncertainty parameters: fuel temperature profiles, local flow area reductions, gap conductance, and axial elongation.

The propagated uncertainty (U) parameters are the same as the output ones.

Certain assumptions need to be made in order to improve the feasibility of the models. Using single pin modelling makes the input to the codes easier but it leaves out some complexities which would affect the results if included. These complexities include the exact geometry of the fuel assemblies within the core along with spacer grid effects and localised flow patterns. These assumptions will cost some accuracy but make the simulations more manageable. Uncertainty is introduced from modelling the scenario, the manufactured tolerances and dimensions, and from the code's calculation of the desired outputs.

In principle, the sources of Input (I) uncertainties in computer code simulations are identified as:

- input data uncertainties;
- geometry and nodalisation uncertainties;
- modelling uncertainties;
- code uncertainties;
- manufacturing uncertainties.

Input data uncertainties:

These uncertainties are included in parameters such as the cross-sections used by the codes or the initial and boundary conditions of the scenario. Since there is a small inherent inaccuracy in every cross-section value it will propagate this error throughout the calculations. It is difficult to remove these uncertainties since most of them are limited by scientific knowledge and some errors are typically accepted for normal analyses. The boundary conditions such as the shapes of the applied power transient or the duration of irradiation also affect results. These are sometimes difficult to model because in real life the shapes are not as smooth as the approximations that are often used in calculations.

Geometry and nodalisation uncertainties:

It is difficult to quantise a transient situation that may have been observed experimentally into a series of inputs that are suitable and realistic to model. It requires some simplifications that stray from the exact scenario in order to make the input more general. When modelling the scenario it is very difficult to exactly match all of the inputs such as coolant temperature and reactor power because these parameters can change very often and would require thousands of inputs to be modelled accurately. Usually some generalisations are made and some lines become flattened in order to simplify the input enough for practical use. During this truncation some uncertainties are introduced and the produced results will be

slightly different from the measured ones. Steady-state codes especially ignore these changes that occur over seconds/minutes because the overall case is likely on the order of hours/days. Transient code input might involve smoothing out a power pulse in order to make it symmetric or even triangular, which is not as it actually occurs.

The geometry of the fuel rods and assemblies also receive some simplifications when they are modelled. These may involve ignoring certain parameters altogether such as plenum volumes and springs in order to comply with what the input requests or does not request. Other shapes are simplified and homogenised in order to make the codes more practical and easy-to-use. The uncertainties involved with these simplifications are difficult to quantise because of all the other uncertainties in codes, but their accuracy can be increased by utilising additional nodes and time steps as well as improved geometry of the model.

Modelling uncertainties:

These uncertainties are described as the ones included in the code used for the analysis. There are some inaccuracies in the values used in the computer codes for parameters such as fuel and cladding thermal conductivity. Since many of these parameters and correlations are temperature-dependent the inaccuracies can propagate through iteration if the initial value is inaccurate. There is also the fact that the most of the codes use a 1-D scheme for temperature calculations which means it works outward from the center of the fuel to the coolant. In order to keep computation time reasonable it is important to find a balance between a small convergence value for the correlation calculations and the accuracy of the solution. Subroutines in the codes are also a source of uncertainty; they take one input parameter and perform a calculation with it to produce another. A common example of this is the calculation of the thermal conductivity based on an input temperature. During this calculation some errors are introduced as the models used are not completely accurate and are often based on best-fit lines of previously measured data. With codes that determine fuel rod failure the selection of the failure criteria used by the code is of importance. It is based on several factors such as the yield strength and the melting point of the material at the experienced temperatures. Also, many codes are capable of running very detailed calculations with the use of many optional inputs that may not be utilised by the user. Without these options specified the code is forced to output a more general solution that may lack some of the intricacies found in the measured data. Other code factors that introduce some errors are machine rounding and varying significant figures kept during code subroutines. It is difficult to quantise a transient situation that may have been observed experimentally into a series of inputs that are suitable and realistic to model. It requires some simplifications that stray from the exact scenario in order to make the input more general. When modelling the scenario it is very difficult to exactly match all of the inputs such as coolant temperature and reactor power because these parameters can change very often and would require thousands of inputs to be modelled accurately. Usually some generalisations are made and some lines become flattened in order to simplify the input enough for practical use. During this truncation some uncertainties are introduced and the produced results will be slightly different from the measured ones. Steady-state codes especially ignore these changes that occur over seconds/minutes because the overall case is likely in the order of hours/days. Transient code input might involve smoothing out a power pulse in order to make it symmetric or even triangular, which is not as it actually occurs. Modelling a changing axial power ratio is often necessary when the void fraction changes in a BWR and it can be done but the transitions will not be as smooth or continuous as they are in experiments. Differences in measured versus calculated temperatures may arise also from the code's treatment of cladding build-up such as oxidation and other corrosion that may appear on the outside of the fuel rods. The amount of burn-up in the rods at the time of the transient can also add some uncertainties depending on how accurately the code can model this past irradiation and accommodate for it.

Code uncertainties:

There are some inaccuracies in the values used in the PNL codes for parameters such as fuel and cladding thermal conductivity. Since many of these parameters are temperature-dependent the inaccuracies

can propagate through iteration if the initial value is inaccurate. There is also the fact that the codes use a 1-D scheme for temperature calculations which means it works outward from the center of the fuel to the coolant. Other uncertainty is introduced from the user's selection of time steps, nodes, and convergence criteria. In order to keep computation time reasonable it is important to find a balance between a small convergence value and the accuracy of the solution. Transients that occur over very short durations may be poorly modelled because of the code's ability to model rapid transients may be limited. Subroutines in the codes are also a source of uncertainty; they take one input parameter and perform a calculation with it to produce another. A common example of this is the calculation of the thermal conductivity based on an input temperature. During this calculation some errors are introduced as the models used are not completely accurate and are often based on best-fit lines of previously measured data. With codes that determine fuel rod failure the selection of the failure criteria used by the code is of importance. It is based on several factors such as the yield strength and the melting point of the material at the experienced temperatures. Also, many codes are capable of running very detailed calculations with the use of many optional inputs that may not be utilised by the user. Without these options specified the code is forced to output a more general solution that may lack some of the intricacies found in the measured data. Other code factors that introduce some errors are machine rounding and varying significant figures kept during code subroutines.

Manufacturing uncertainties:

Other uncertainties arise from the values as provided by the manufacturers of the fuels and equipment used in the reactor. There are design tolerances due to machining precision that are built into each of the pieces of equipment and each fuel rod used in the reactor. Since it is not possible to measure each fuel pellet accurately the dimensions provided by the manufacturer are sufficient for most calculations but it is important to understand that these values do carry some errors. The significance of these errors can grow depending on the model setup and the types of equations used. Some of these manufacturing parameters are cladding Inner Diameter (ID)/Outer Diameter (OD), fuel pellet OD, pellet/cladding roughness, enrichment, yield strength (and several other material properties), fill gas composition/pressure, as well as the coolant properties. Of these geometry parameters, it was determined in "Predictive Bias and Sensitivity in NRC Fuel Performance Codes" that the ones with the largest effect on fuel temperature are the fuel pellet density and the pellet roughness. The roughness is especially important in determining the effective heat transfer coefficient from the coolant to the cladding and also from the fill gas to the fuel pellets. Of the material properties, changing the thermal conductivity of the fuel had a very large effect on the resulting fuel temperature.

Other uncertainties arise from the values used by the participants as provided by the manufacturers of the fuels and equipment used in the reactor. There are design tolerances due to machining precision that are built into each of the pieces of equipment and each fuel rod used in the reactor. Since it is not possible to measure each fuel pellet accurately the dimensions provided by the manufacturer are sufficient for most calculations but it is important to understand that these do carry some errors. The significance of these errors can grow depending on the model setup and the types of equations used. Some of these manufacturing parameters are cladding ID/OD, fuel pellet OD, pellet/cladding roughness, enrichment, yield strength (and several other material properties), fill gas composition/pressure, and coolant properties. Of these geometry parameters, it was determined in "Predictive Bias and Sensitivity in NRC Fuel Performance Codes" that the ones with the largest effect on fuel temperature are the fuel pellet density and the pellet roughness. The roughness is especially important in determining the effective heat transfer coefficient from the coolant to the cladding and also from the fill gas to the fuel pellets. Of the material properties, changing the thermal conductivity of the fuel had a very large effect on the resulting fuel temperature.

2.2 Test problems

The test problems included in this exercise cover three different types of reactors (the BWR, PWR, and VVER-1000) as well as two types of cases (transient and steady-state) for both experimental and numerical tests. The numerical test cases involve different stand-alone neutronics single pin-cell test problems, designed for the purposes of the Exercise I-1 utilising information from the previous OECD coupled code benchmarks for each of the representative reactors- BWR PB-2, PWR TMI-1, and Kozloduy-6 (Kalinin-3) VVER-1000.

For Exercise II-1 the available experimental data have been identified using the CRISSUE-S database. The Halden in-pile fuel temperature data have been examined for appropriate transient fuel thermal property data. For the steady-state cases, FRAPCON is utilised to generate reference results relevant to the studies in this exercise while for transient cases, FRAPTRAN is used to generate reference solutions and study the problem definition for transient simulations.

The first six cases listed (cases 1a through 3b) are the numerical cases, which means that they are based on experiments but the dimensions and other important parameters have been modified in order to represent the three reactors of interest in this phase (PB-2, TMI-1, and Kozloduy-6). There is a steady-state irradiation case and a transient case for each of these three reactors. The steady-state cases provide small changes in the power over a large amount of time, often on the scale of months.

The transient cases (cases 4a through 6b) are often quick pulses in the order of milliseconds, and the total duration of the simulation is usually a few seconds or less. Some of the experimental transient cases occur after a long period of irradiation, such that the fuel rod will have a specified value of burn-up at the onset of the scenario, such as 65 GWd/MTU.

For the steady-state cases, the main parameter of interest is the centerline fuel temperature at various burn-up steps. For some experiments, fuel temperature was not directly measured so cladding temperature is also relevant. There are several dimensions and values that the users are asked to modify in order to determine the effect of the changes on the resulting temperatures. The transient cases also focus on determining the temperature profile at each time step of the simulation.

The major uncertainty input parameters, their ranges of change and associated PDFs are summarised below. These parameters involve manufacturing uncertainties, uncertainties in the boundary conditions, and uncertainties in the parameters in the code models.

The manufacturing uncertainties are specified for each test case. Uncertainties of boundary conditions are the same for all test cases as shown in Table 2.1. The uncertainties of boundary conditions (these include the coolant flow rate and temperature, as well as the reactor pressure and power level) have normal distribution around the average value.

Table 2.1: Exercise II-1 Core Boundary Condition Variations

| Parameter | BWR | PWR | VVER |
|---------------------------|------------|------------|-------------|
| Coolant flow rate | ±2.0% | ±2.0% | ±2.0% |
| Coolant inlet temperature | ±10 K | ±10 K | ±10 K |
| Core pressure | ±3.0% | ±3.0% | ±3.0% |
| Power | ±5.0% | ±5.0% | ±5.0% |

The users are also asked to modify the inputs to their codes or the source of their codes in order to represent some code and model uncertainties. The code and model uncertainties are given in Table 2.2 and follow normal distribution also.

Table 2.2: Exercise II-1 Code Parameter Variations

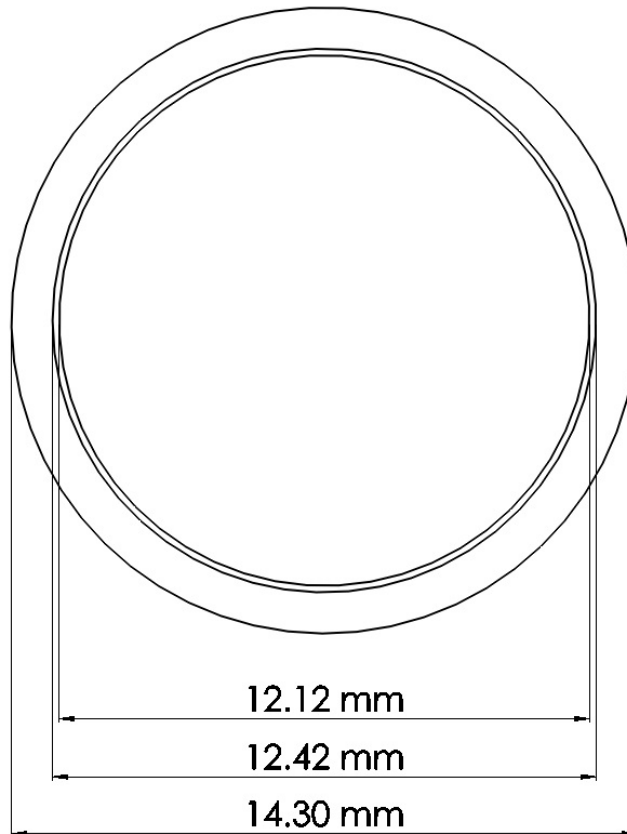
| Parameter | BWR | PWR | VVER |
|-------------------------------|-------------|-------------|-------------|
| Fuel thermal conductivity | ±0.5 W/m-K | ±0.5 W/m-K | ±0.5 W/m-K |
| Fuel thermal expansion | ±15% | ±15% | ±15% |
| Cladding thermal conductivity | ±5 W/m-K | ±5 W/m-K | ±5 W/m-K |
| Cladding thermal expansion | ±30% | ±30% | ±30% |
| Gas conductivity | ±0.02 W/m-K | ±0.02 W/m-K | ±0.02 W/m-K |
| Heat transfer coefficient | ±5.0% | ±5.0% | ±5.0% |

The uncertainties in nodalisation and time steps will not be studied during this exercise, but if the user chooses to implement a different nodalisation scheme, then that should be noted in the results. The nodalisation can have a significant effect on the propagated uncertainty parameters and its variation could be studied further.

Case 1a – Steady-state BWR numerical test problem

This case is modelled after a PNL assessment case written for the FK-1 reactor. It has been modified for application to the PB-2 reactor, a typical BWR representative. The case should be run with the parameters listed below, and then with the variations provided by the manufacturing tolerances for a BWR. The participants should apply the code uncertainties in order to determine their effects as well.

The geometry of the PB-2 Fuel rod is defined in Table 2.3 and shown in Figure 2.1.

Figure 2.1: PB-2 Fuel Pin Image

The irradiation history to be used for this case is fairly flat and involves a brief ramp-up in the beginning to get to power as given in Table 2.4 and shown in Figure 2.2. The power is given as a linear heat rate, which can be applied in conjunction with the axial power profile. The axial power profile applied to this BWR test problem is provided in Table 2.5 and shown in Figure 2.3. The axial nodalisation consists of 17 axial nodes.

Table 2.3: PB-2 Fuel Rod Geometry

| Geometry | Value |
|--|-------------------|
| Cladding OD | 14.30 mm |
| Cladding ID | 12.42 mm |
| Cladding wall thickness | 0.940 mm |
| Fuel pellet OD | 12.12 mm |
| Pellet-cladding radial gap thickness | 0.15 mm |
| Total fuel column length | 3657.6 mm |
| Fuel pellet height | 10.67 mm |
| Fuel enrichment (atom percent) | 3.0% |
| % of theoretical density (10.96 g/cc) | 95.1% |
| Pellet surface roughness | 2.0 μm |
| Cladding type | Zr-2 |
| Cladding surface roughness | 0.5 μm |
| Fill gas type | Helium |
| Fill gas pressure | 0.69 MPa |
| Fuel rod pitch | 18.75 mm |
| Coolant pressure | 7.14 MPa |
| Coolant inlet temperature | 550 K |
| Coolant mass flux around rod | |
| Heat transfer coefficient for coolant | |
| # of time steps | 50 |
| # of axial nodes in pellet | 17 |
| # of equal volume radial rings in pellet | 45 |

Table 2.4: PB-2 Power History

| Time step - | Time (days) | Power (kW/m) | Time step - | Time (days) | Power (kW/m) |
|----------------|----------------|-----------------|----------------|----------------|-----------------|
| 1 | 0.0 | 0.00 | 26 | 1 050 | 16.55 |
| 2 | 0.1 | 3.28 | 27 | 1 100 | 16.55 |
| 3 | 0.2 | 6.56 | 28 | 1 150 | 16.55 |
| 4 | 0.3 | 9.84 | 29 | 1 200 | 16.55 |
| 5 | 0.4 | 13.12 | 30 | 1 250 | 13.39 |
| 6 | 50 | 15.70 | 31 | 1 300 | 13.39 |
| 7 | 100 | 15.70 | 32 | 1 350 | 13.39 |
| 8 | 150 | 15.70 | 33 | 1 400 | 13.39 |
| 9 | 200 | 15.70 | 34 | 1 450 | 13.39 |
| 10 | 250 | 15.70 | 35 | 1 500 | 13.39 |
| 11 | 300 | 17.32 | 36 | 1 550 | 13.39 |
| 12 | 350 | 17.32 | 37 | 1 600 | 13.39 |
| 13 | 400 | 17.32 | 38 | 1 650 | 13.39 |
| 14 | 450 | 17.32 | 39 | 1 700 | 13.39 |
| 15 | 500 | 17.32 | 40 | 1 750 | 15.16 |
| 16 | 550 | 17.32 | 41 | 1 800 | 15.16 |
| 17 | 600 | 17.32 | 42 | 1 850 | 15.16 |
| 18 | 650 | 17.32 | 43 | 1 900 | 15.16 |
| 19 | 700 | 17.32 | 44 | 1 950 | 15.16 |
| 20 | 750 | 16.55 | 45 | 2 000 | 15.16 |
| 21 | 800 | 16.55 | 46 | 2 050 | 15.16 |
| 22 | 850 | 16.55 | 47 | 2 100 | 15.16 |
| 23 | 900 | 16.55 | 48 | 2 150 | 15.16 |
| 24 | 950 | 16.55 | 49 | 2 200 | 15.16 |
| 25 | 1 000 | 16.55 | 50 | 2 230 | 15.16 |

Figure 2.2: PB-2 Power History Plot

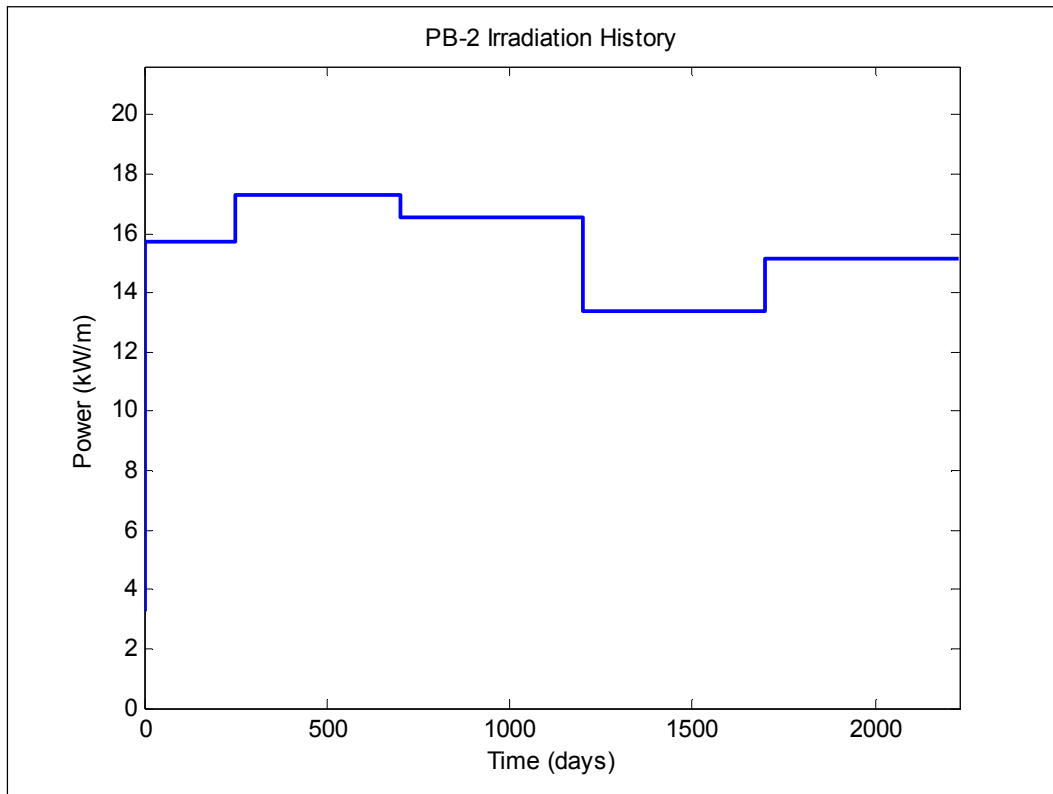
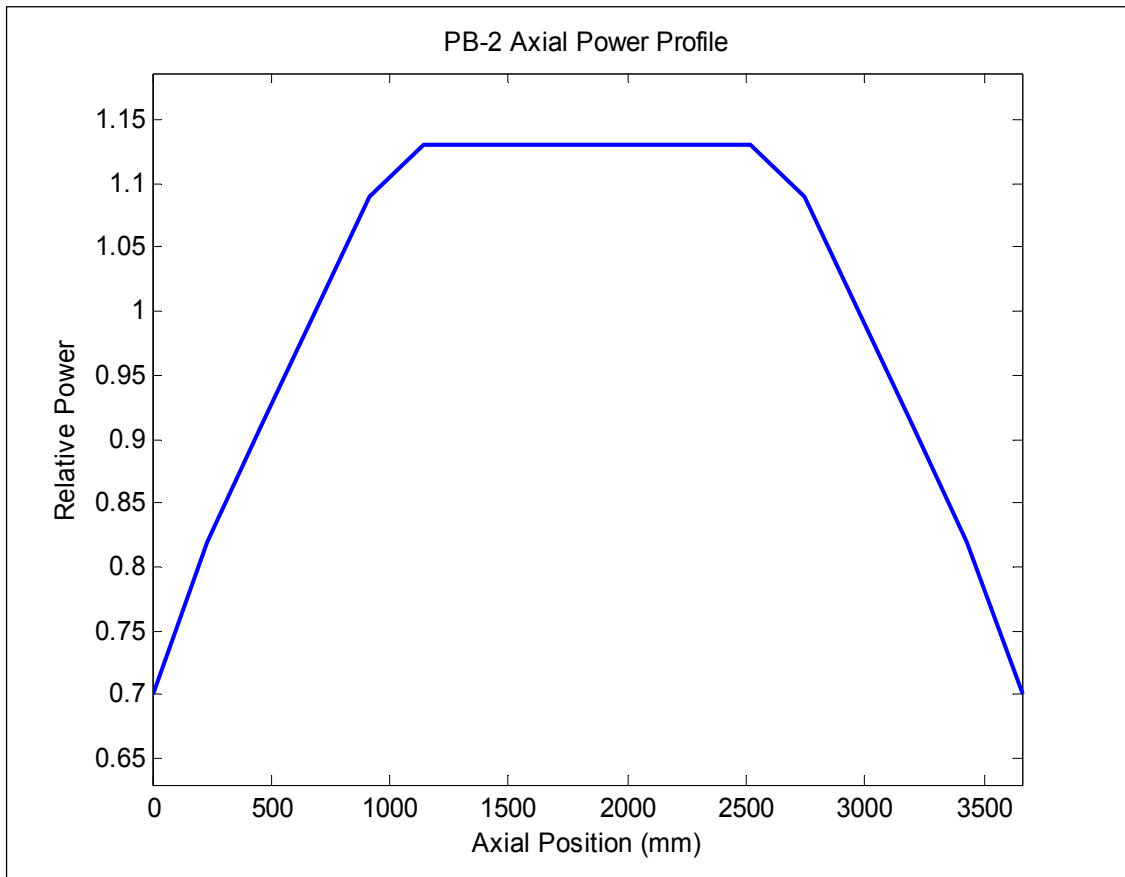


Table 2.5: PB-2 Axial Power Profile

| Location (mm) | Relative power - |
|---------------|------------------|
| 0.0 | 0.70 |
| 228.6 | 0.82 |
| 457.2 | 0.91 |
| 685.8 | 1.00 |
| 914.4 | 1.09 |
| 1143.0 | 1.13 |
| 1371.6 | 1.13 |
| 1600.2 | 1.13 |
| 1828.8 | 1.13 |
| 2057.4 | 1.13 |
| 2286.0 | 1.13 |
| 2514.6 | 1.13 |
| 2743.2 | 1.09 |
| 2971.8 | 1.00 |
| 3200.4 | 0.91 |
| 3429.0 | 0.82 |
| 3657.6 | 0.70 |

Figure 2.3: PB-2 Axial Power Profile Plot

The manufacturing uncertainties to be applied to this case are shown in the following table. These values are specific to this BWR configuration.

Table 2.6: Case 1 Manufacturing Uncertainties

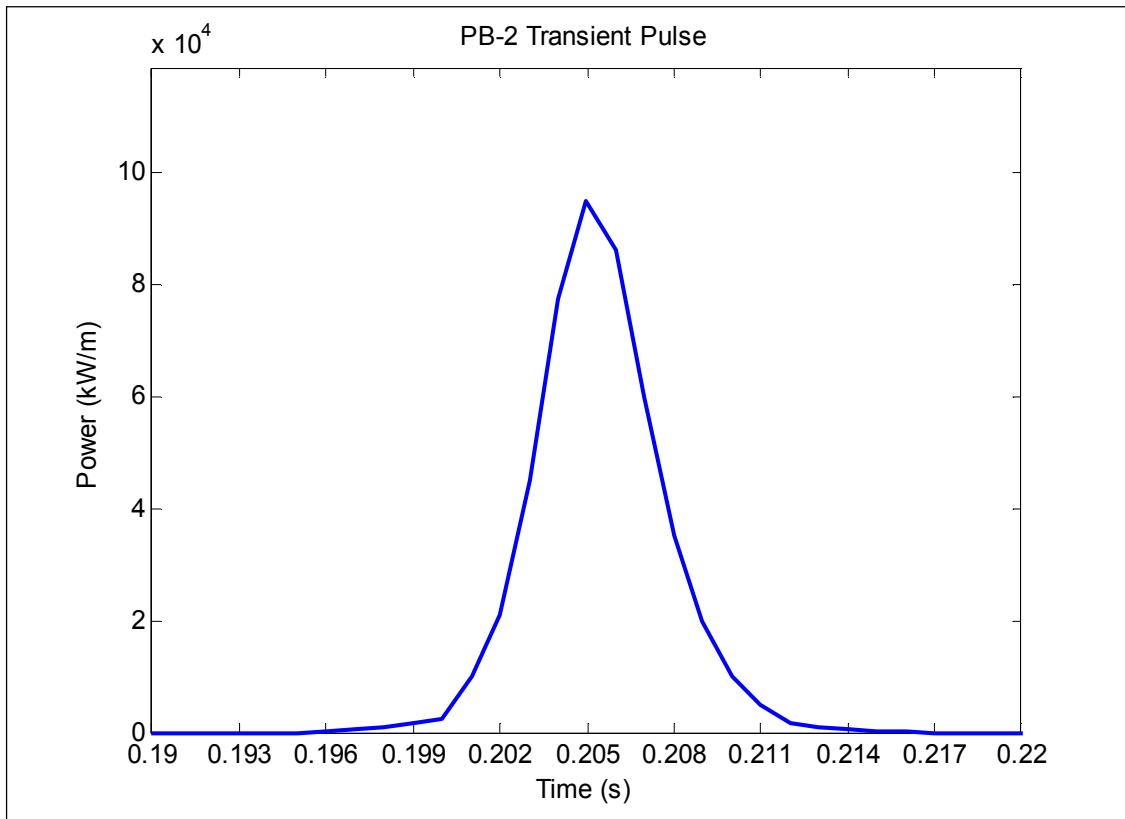
| Parameter | Lower limit | Upper limit | Distribution |
|-----------------------|-------------------|-------------------|--------------|
| Cladding ID | 12.38 mm | 12.46 mm | Normal |
| Cladding thickness | 0.936 mm | 0.944 mm | Normal |
| Cladding roughness | 0.2 μm | 0.8 μm | Normal |
| Fuel pellet OD | 12.10 mm | 12.14 mm | Normal |
| Fuel density | 10.3 g/cc | 10.5 g/cc | Normal |
| Fuel pellet roughness | 1.5 μm | 2.5 μm | Normal |
| Rod fill pressure | 0.62 MPa | 0.76 MPa | Normal |

Case 1b - Transient BWR numerical test problem

This case is also modelled on a FK-1 rod case and modified for the PB-2 reactor. It is a short-duration pulse which causes a spike in the power level of the reactor. It is simulated in this case as a single fuel pin. The geometry of the pin is the same as described in the previous case (Case 1a, Table 2.3) and the initial burn-up of the rod used in this simulation is 45.5 GWd/MTU (since it is assumed to be previously irradiated). The power history of the transient is provided in Table 2.7 and shown in Figure 2.4. The duration of the scenario is 1.00 seconds.

Table 2.7: PB-2 Transient Power History

| Time (s) | Power (kW/m) |
|----------|--------------|
| 0.000 | 0.0 |
| 0.195 | 0.0 |
| 0.196 | 200.0 |
| 0.197 | 400.0 |
| 0.198 | 1000.0 |
| 0.199 | 1500.0 |
| 0.200 | 2500.0 |
| 0.201 | 10000.0 |
| 0.202 | 21000.0 |
| 0.203 | 45000.0 |
| 0.204 | 77500.0 |
| 0.205 | 95000.0 |
| 0.206 | 86000.0 |
| 0.207 | 60000.0 |
| 0.208 | 35000.0 |
| 0.209 | 20000.0 |
| 0.210 | 10000.0 |
| 0.211 | 5000.0 |
| 0.212 | 1500.0 |
| 0.213 | 1000.0 |
| 0.214 | 500.0 |
| 0.215 | 200.0 |
| 0.216 | 100.0 |
| 0.217 | 0.0 |
| 1.000 | 0.0 |

Figure 2.4: PB-2 Transient Power History Plot

The time step sizes to be used during the simulation are defined in Table 2.8. These are important for obtaining consistent results.

Table 2.8: PB-2 Transient Time Step Sizes

| Step size | Time period |
|-----------|---------------|
| 0.001 s | 0.00 - 0.15 s |
| 0.00001 s | 0.15 - 0.25 s |
| 0.001 s | 0.25 - 1.00 s |

The coolant temperature is also provided for this case as a function of time in Table 2.9. These can be applied as boundary conditions as needed. The axial power profile and manufacturing uncertainties are the same as used in Case 1a.

Table 2.9: PB-2 Transient Coolant Temperature History

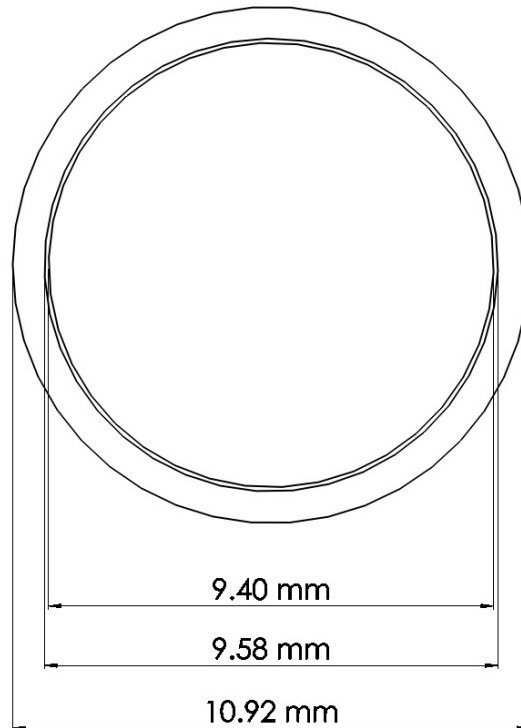
| Time (s) | Coolant T (K) |
|----------|---------------|
| 0.00 | 305 |
| 0.21 | 305 |
| 0.25 | 393 |
| 0.35 | 436 |
| 0.50 | 510 |
| 0.70 | 452 |
| 0.85 | 452 |
| 1.00 | 383 |

Case 2a – Steady-state PWR numerical test problem

This case is based on the Na-3 experiments performed at the CABRI test reactor facility. This case is modified to fit the parameters of the TMI-1 reactor. This is a single pin model of an irradiation case over a long time period. The geometry of the TMI-1 fuel pin cell is provided in Table 2.10 and shown in Figure 2.5.

Table 2.10: TMI-1 Fuel Rod Geometry

| Geometry | Value |
|--|----------------------------|
| Cladding OD | 10.92 mm |
| Cladding ID | 9.58 mm |
| Cladding wall thickness | 0.673 mm |
| Fuel pellet OD | 9.40 mm |
| Pellet-cladding radial gap thickness | 0.089 mm |
| Total fuel column length | 3657.6 mm |
| Fuel pellet height | 11.43 mm |
| Fuel enrichment (atom percent) | 4.85% |
| % of theoretical density (10.96 g/cc) | 93.8% |
| Pellet surface roughness | 2.0 μm |
| Cladding type | Zr-4 |
| Cladding surface roughness | 0.5 μm |
| Fill gas type | Helium |
| Fill gas pressure | 1 207 kPa |
| Fuel rod pitch | 14.43 mm |
| Coolant pressure | 15.51 MPa |
| Coolant inlet temperature | 561 K |
| Coolant mass flux around rod | 3 460 kg/m ² -s |
| Heat transfer coefficient for coolant | 2.0e6 W/m ² -K |
| # of time steps | 31 |
| # of axial nodes in pellet | 17 |
| # of equal volume radial rings in pellet | 45 |

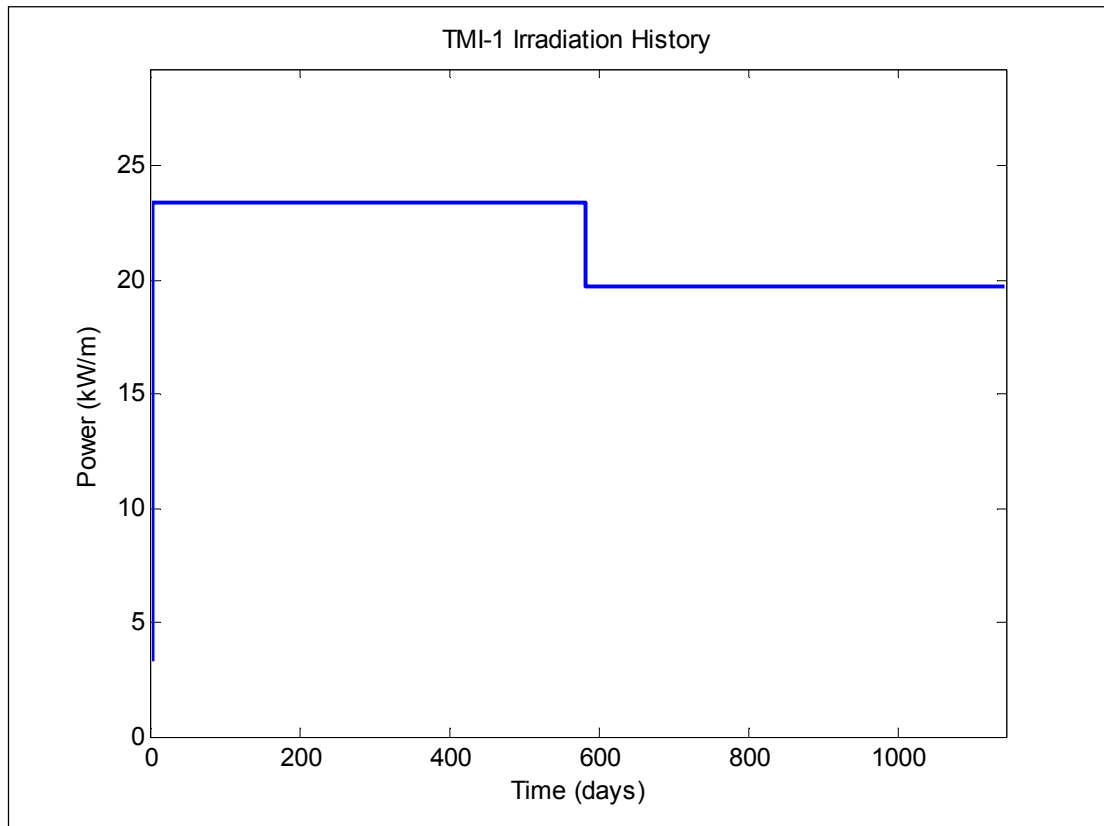
Figure 2.5: TMI-1 Fuel Pin Image

The irradiation history of this pin model is provided in Table 2.11 and Figure 2.6.

Table 2.11: TMI-1 Power History

| Time Step - | Time (days) | Power (kW/m) | Time Step - | Time (days) | Power (kW/m) |
|----------------|----------------|-----------------|----------------|----------------|-----------------|
| 1 | 0.0 | 0.00 | 17 | 500 | 23.39 |
| 2 | 0.1 | 3.28 | 18 | 550 | 23.39 |
| 3 | 0.2 | 6.56 | 19 | 580 | 23.39 |
| 4 | 0.3 | 9.84 | 20 | 600 | 19.69 |
| 5 | 0.4 | 13.12 | 21 | 650 | 19.69 |
| 6 | 0.5 | 16.40 | 22 | 700 | 19.69 |
| 7 | 0.6 | 19.69 | 23 | 750 | 19.69 |
| 8 | 50 | 23.39 | 24 | 800 | 19.69 |
| 9 | 100 | 23.39 | 25 | 850 | 19.69 |
| 10 | 150 | 23.39 | 26 | 900 | 19.69 |
| 11 | 200 | 23.39 | 27 | 950 | 19.69 |
| 12 | 250 | 23.39 | 28 | 1 000 | 19.69 |
| 13 | 300 | 23.39 | 29 | 1 050 | 19.69 |
| 14 | 350 | 23.39 | 30 | 1 100 | 19.69 |
| 15 | 400 | 23.39 | 31 | 1 143 | 19.69 |
| 16 | 450 | 23.39 | - | | |

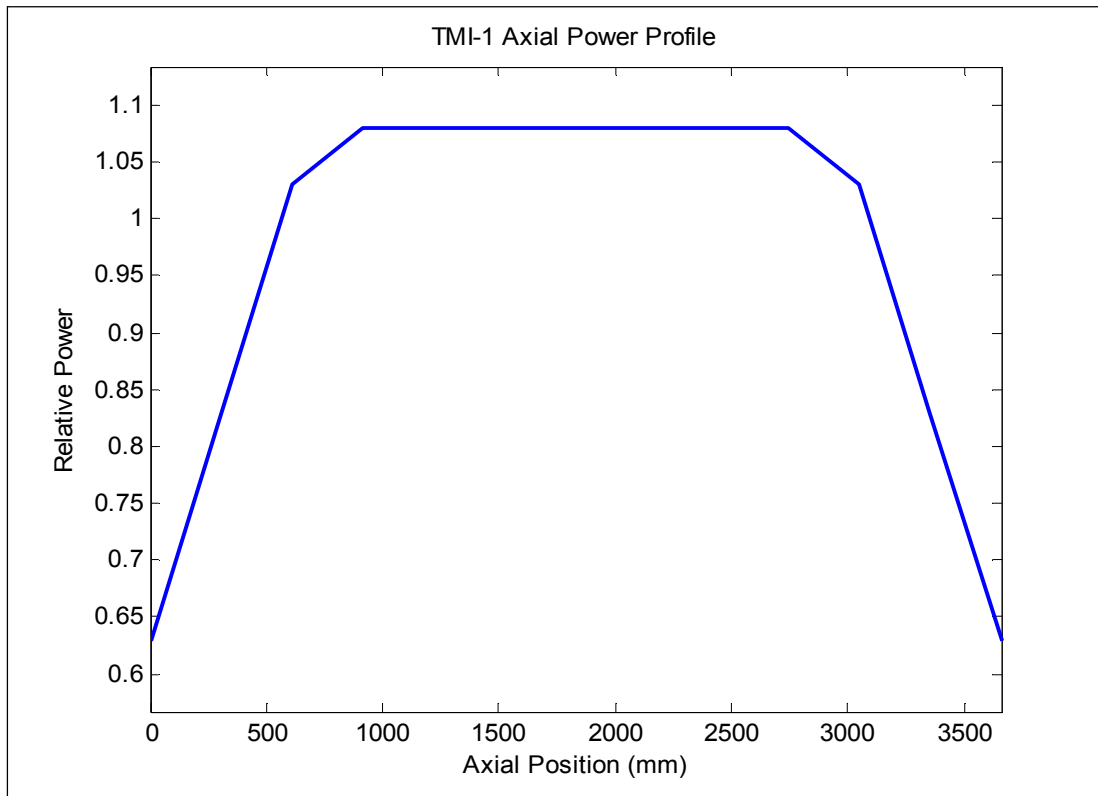
Figure 2.6: TMI-1 Power History Plot



The axial power profile of the TMI-1 fuel rod is given in Table 2.12 and is shown in Figure 2.7 as a 13- node model.

Table 2.12: TMI-1 Axial Power Profile

| Location (mm) | Relative power - |
|---------------|------------------|
| 0.0 | 0.63 |
| 304.8 | 0.83 |
| 609.6 | 1.03 |
| 914.4 | 1.08 |
| 1219.2 | 1.08 |
| 1524.0 | 1.08 |
| 1828.8 | 1.08 |
| 2133.6 | 1.08 |
| 2438.4 | 1.08 |
| 2743.2 | 1.08 |
| 3048.0 | 1.03 |
| 3352.8 | 0.83 |
| 3657.6 | 0.63 |

Figure 2.7: TMI-1 Axial Power Profile Plot

The manufacturing uncertainties to be applied to this case are shown in Table 2.13. These values are specific to this PWR numerical case configuration.

Table 2.13: Case 2 Manufacturing Uncertainties

| Parameter | Lower limit | Upper limit | Distribution |
|-----------------------------|-------------|-------------|--------------|
| Cladding thickness | 0.648 mm | 0.698 mm | Normal |
| Fuel pellet OD | 9.38 mm | 9.42 mm | Normal |
| Fuel density | 10.11 g/cc | 10.45 g/cc | Normal |
| Gap thickness | 0.089 mm | 0.113 mm | Normal |
| U ²³⁵ enrichment | 4.847 w/o | 4.853 w/o | Normal |

Case 2b – Transient PWR numerical test problem

This is a pulse modelled on the Na-3 pulse test completed at the CABRI test facility. The actual rod used is shorter than a typical PWR fuel rod found in power reactors so the dimensions have been scaled up to fit the TMI-1 reactor. The geometry of the fuel pin is the same as given in Case 2a. The duration of this transient is 0.400 seconds. The transient power history is given in Table 2.14 and Figure 2.8 while the step sizes to be used during the calculations are also provided in Table 2.15.

Table 2.14: TMI-1 Transient Power History

| Time (s) | Power (kW/m) |
|----------|--------------|
| 0.000 | 0.0 |
| 0.060 | 0.0 |
| 0.065 | 336.9 |
| 0.070 | 1347.8 |
| 0.075 | 8087.3 |
| 0.082 | 25339.6 |
| 0.084 | 18870.1 |
| 0.087 | 10782.8 |
| 0.090 | 3369.8 |
| 0.095 | 269.7 |
| 0.100 | 82.3 |
| 0.400 | 0.0 |

Figure 2.8: TMI-1 Transient Power History Plot

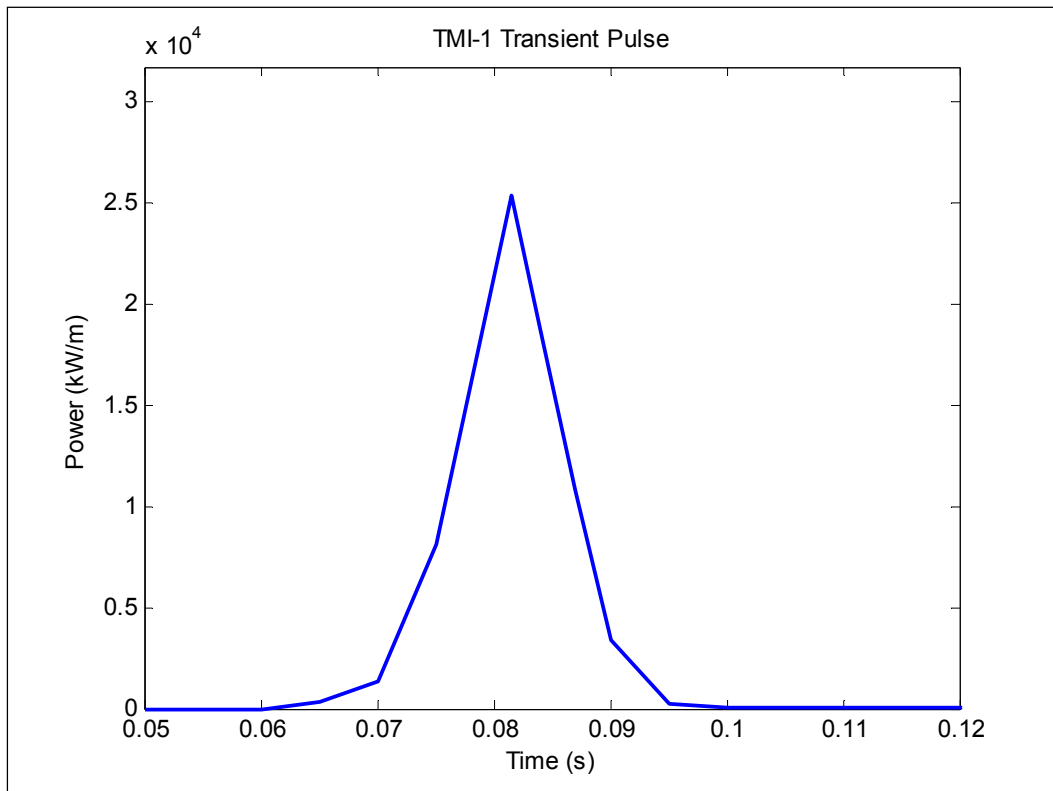


Table 2.15: TMI-1 Transient Time Step Sizes

| Step size | Time period |
|-----------|-------------------|
| 0.0001 s | 0.0000 – 0.0800 s |
| 0.00001 s | 0.0800 – 0.0815 s |
| 0.0001 s | 0.0815 – 0.1500 s |
| 0.001 s | 0.1500 – 0.4000 s |

The coolant temperature is also provided for this case as a function of time, for two locations along the fuel pin as shown in Table 2.16. The lower location is at 887.5 mm and the upper measurement is at the top, at 3 550 mm. These can be applied as boundary conditions as needed.

Table 2.16: TMI-1 Transient Coolant Temperature History

| Time (s) | Coolant T lower (K) | Coolant T upper (K) |
|----------|---------------------|---------------------|
| 0.000 | 553 | 553 |
| 0.075 | 553 | 553 |
| 0.100 | 568 | 563 |
| 0.150 | 628 | 643 |
| 0.200 | 668 | 683 |
| 0.250 | 668 | 703 |
| 0.300 | 658 | 708 |
| 0.350 | 650 | 708 |
| 0.400 | 642 | 703 |

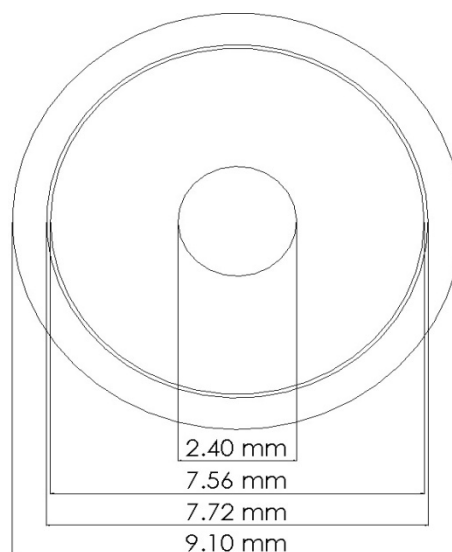
The axial power profile and manufacturing uncertainties are the same as used in Case 2a.

Case 3a – Steady-state VVER numerical test problem

This irradiation case for a VVER-1000 fuel rod has its geometry defined by Table 2.17 and shown in Figure 2.9. It is important to note that the VVER fuel pins and assemblies have hexagonal geometry as well as a central void in the fuel pellet, making the VVER cases slightly different from the other LWR cases. Some modifications to codes may be necessary in order to accurately represent these changes.

Table 2.17: VVER-1000 Fuel Rod Geometry

| Geometry | Value |
|--|-------------|
| Cladding OD | 9.10 mm |
| Cladding ID | 7.72 mm |
| Cladding wall thickness | 0.69 mm |
| Fuel pellet OD | 7.56 mm |
| Fuel pellet ID | 2.40 mm |
| Pellet-cladding radial gap thickness | 0.08 mm |
| Total fuel column length | 3 550 mm |
| Fuel pellet height | 9.1 mm |
| Fuel enrichment (atom percent) | 3.3% |
| % of theoretical density (10.96 g/cc) | 94.9% |
| Pellet surface roughness | 2 μ m |
| Cladding type | Zr-1% Nb |
| Cladding surface roughness | 0.5 μ m |
| Fill gas type | He |
| Fill gas pressure | 2.5 Mpa |
| Fuel rod pitch | 12.75 mm |
| Coolant pressure | 15.7 Mpa |
| Coolant inlet temperature | 560 K |
| Coolant mass flux around rod | |
| Heat transfer coefficient for coolant | |
| # of time steps | 41 |
| # of axial nodes in pellet | |
| # of equal volume radial rings in pellet | |

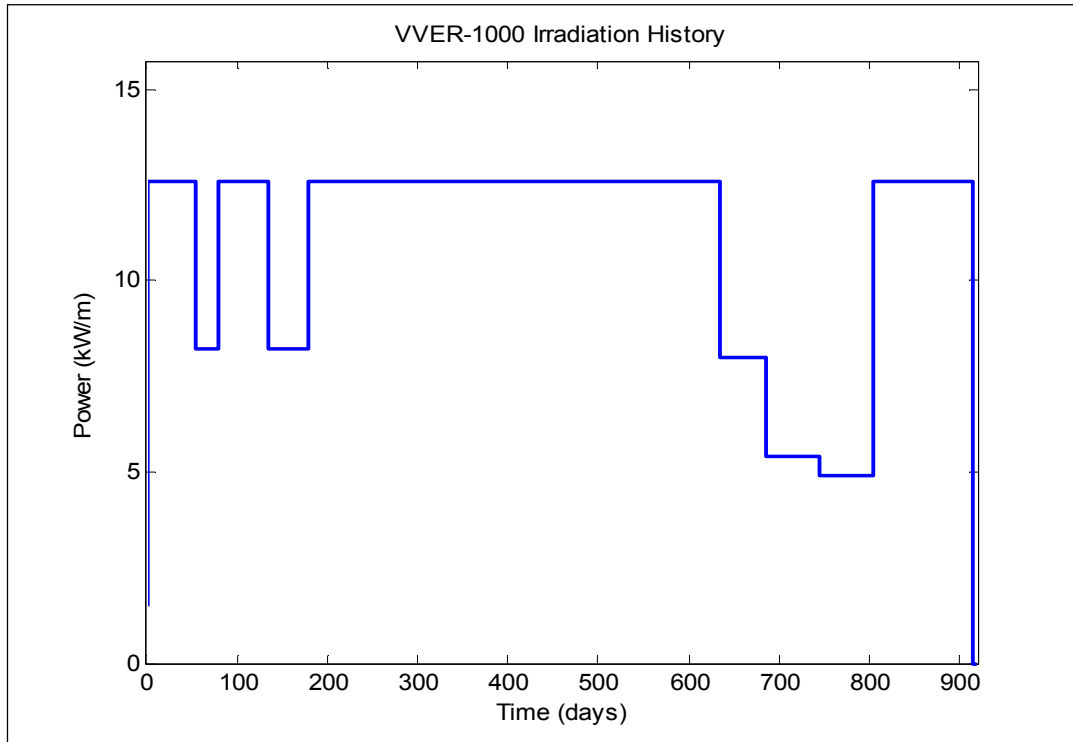
Figure 2.9: VVER-1000 Fuel Pin Image

The fuel pin model is irradiated according to the data in Table 2.18 and Figure 2.10.

Table 2.18: VVER-1000 Power History

| Time step - | Time (days) | Power (kW/m) | Time step - | Time (days) | Power (kW/m) |
|----------------|----------------|-----------------|----------------|----------------|-----------------|
| 1 | 0 | 0.0 | 22 | 350 | 12.6 |
| 2 | 0.1 | 1.5 | 23 | 400 | 12.6 |
| 3 | 0.2 | 3.0 | 24 | 450 | 12.6 |
| 4 | 0.3 | 4.5 | 25 | 500 | 12.6 |
| 5 | 0.4 | 6.0 | 26 | 550 | 12.6 |
| 6 | 0.5 | 7.5 | 27 | 600 | 12.6 |
| 7 | 0.6 | 10.0 | 28 | 635 | 12.6 |
| 8 | 5 | 12.6 | 29 | 640 | 8.0 |
| 9 | 50 | 12.6 | 30 | 685 | 8.0 |
| 10 | 55 | 12.6 | 31 | 690 | 5.4 |
| 11 | 58 | 8.2 | 32 | 700 | 5.4 |
| 12 | 80 | 8.2 | 33 | 745 | 5.4 |
| 13 | 82 | 12.6 | 34 | 750 | 4.9 |
| 14 | 100 | 12.6 | 35 | 800 | 4.9 |
| 15 | 135 | 12.6 | 36 | 805 | 4.9 |
| 16 | 140 | 8.2 | 37 | 810 | 12.6 |
| 17 | 180 | 8.2 | 38 | 850 | 12.6 |
| 18 | 185 | 12.6 | 39 | 900 | 12.6 |
| 19 | 200 | 12.6 | 40 | 915 | 12.6 |
| 20 | 250 | 12.6 | 41 | 920 | 0.0 |
| 21 | 300 | 12.6 | - | | |

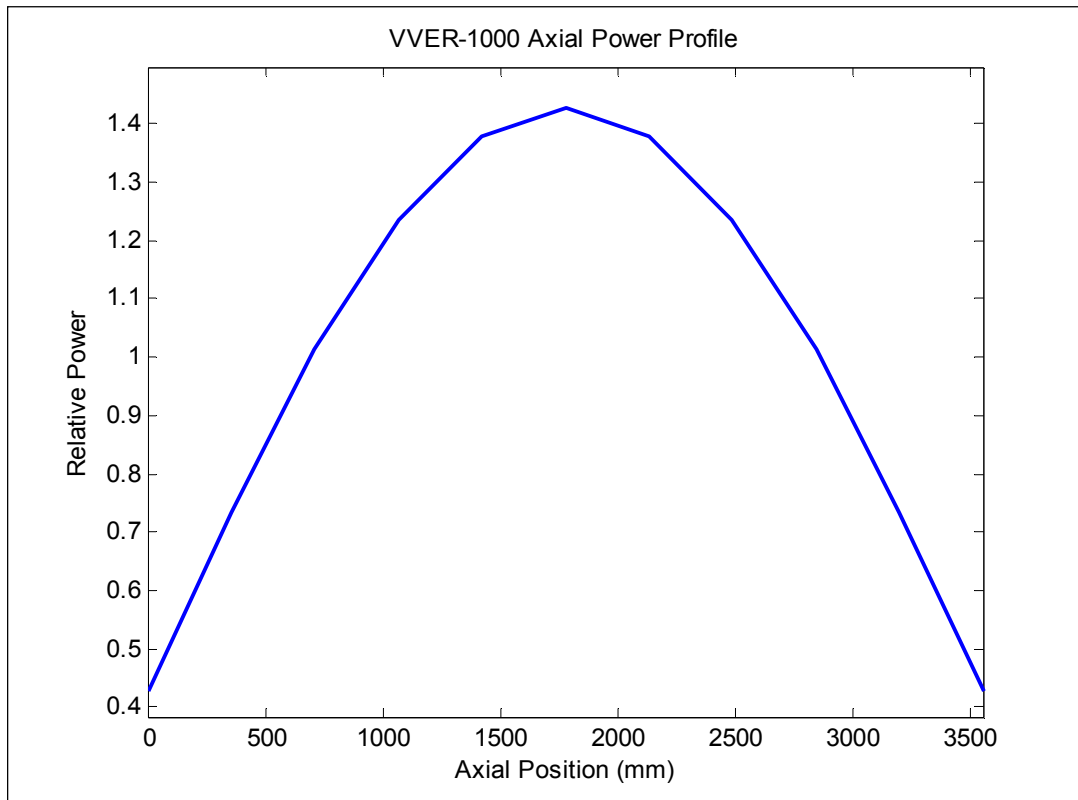
Figure 2.10: VVER-1000 Power History Plot



The axial power profile for the rod in this case is supplied in Table 2.19 and shown in Figure 2.11.

Table 2.19: VVER-1000 Axial Power Profile

| Location (mm) | Relative power - |
|---------------|------------------|
| 0.0 | 0.426 |
| 355.0 | 0.735 |
| 710.0 | 1.014 |
| 1065.0 | 1.235 |
| 1420.0 | 1.377 |
| 1775.0 | 1.426 |
| 2130.0 | 1.377 |
| 2485.0 | 1.235 |
| 2840.0 | 1.014 |
| 3195.0 | 0.735 |
| 3550.0 | 0.426 |

Figure 2.11: VVER-1000 Axial Power Profile Plot

The manufacturing uncertainties to be applied to this case are shown in Table 2.20. These values are specific to this VVER numerical case configuration.

Table 2.20: Case 3 Manufacturing Tolerances

| Parameter | Lower limit | Upper limit | Distribution |
|---------------------|-------------|-------------|--------------|
| Fuel pellet void ID | 2.40 mm | 2.70 mm | Uniform |
| Fuel pellet OD | 7.53 mm | 7.56 mm | Uniform |
| Cladding ID | 7.72 mm | 7.78 mm | Uniform |
| Cladding OD | 8.95 mm | 9.15 mm | Uniform |
| Fuel density | 10.1 g/cc | 10.7 g/cc | Uniform |
| 3.3 w/o enrichment | 3.25% | 3.35% | Uniform |
| 3.0 w/o enrichment | 2.95% | 3.05% | Uniform |

Case 3b - Transient VVER numerical test problem

This transient case is another short-duration power pulse resulting from a reactivity-initiated accident scenario which is typically a rod-ejection. The geometry of this rod is the same as in Case 3a, and the power history of the scenario is provided in Table 2.21 and is shown in Figure 2.12. The duration of the pulse is 8.00 seconds.

Table 2.21: VVER-1000 Transient Power History

| Time (s) | Power (kW/m) |
|----------|--------------|
| 0.00 | 0.10 |
| 1.20 | 0.7 |
| 1.82 | 26.2 |
| 2.22 | 52.5 |
| 2.87 | 164.0 |
| 3.35 | 383.9 |
| 3.67 | 213.3 |
| 4.06 | 75.5 |
| 4.50 | 26.2 |
| 4.92 | 13.1 |
| 6.22 | 4.9 |
| 8.00 | 1.6 |

Figure 2.12: VVER-1000 Transient Power History Plot

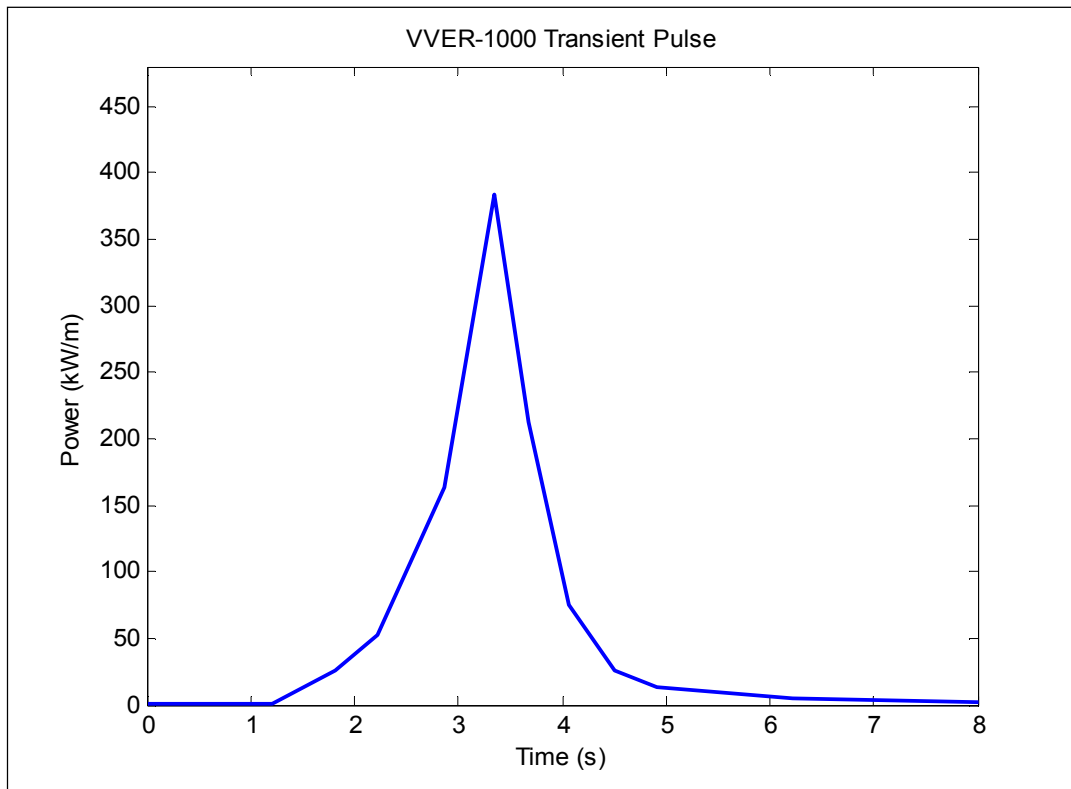


Table 2.22: VVER-1000 Transient Time Step Sizes

| Step size | Time period |
|-----------|---------------|
| 0.002 s | 0.00 - 1.50 s |
| 0.0002 s | 1.50 - 3.45 s |
| 0.00005 s | 3.45 - 4.20 s |
| 0.0005 s | 4.20 - 6.00 s |
| 0.001 s | 6.00 - 8.00 s |

The transient time steps are given in Table 2.22. The coolant temperature is not available for this case. The axial power profile and manufacturing uncertainties are the same as the one used in Case 3a.

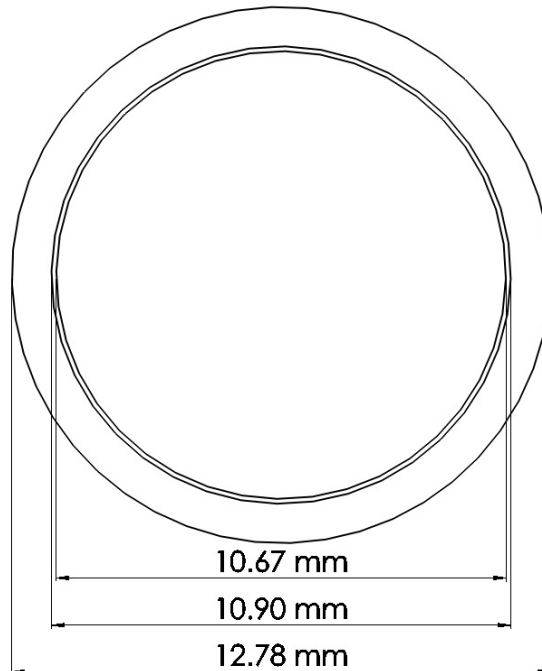
Case 4a- Steady-state BWR experimental test problem

This experimental case is the IFA-432 rod irradiation performed at the Halden reactor in Norway, a BWR. The enrichment of this rod is slightly higher (10%) than those typically found in LWRs but otherwise it is similar to a standard fuel rod. It is also shorter in length, but the diameter and materials are appropriate. The geometry of this case is provided in Table 2.23 and is shown in Figure 2.13.

Table 2.23: IFA-432 Fuel Rod Geometry

| Geometry | Value |
|--|-------------------|
| Cladding OD | 12.78 mm |
| Cladding ID | 10.90 mm |
| Cladding wall thickness | 0.94 mm |
| Fuel pellet OD | 10.67 mm |
| Pellet-cladding radial gap thickness | 0.12 mm |
| Total fuel column length | 577.9 mm |
| Fuel pellet height | 13.0 mm |
| Fuel enrichment (atom percent) | 10.0% |
| % of theoretical density (10.96 g/cc) | 95.1% |
| Pellet surface roughness | 2.0 μm |
| Cladding type | Zr-2 |
| Cladding surface roughness | 0.5 μm |
| Fill gas type | Helium |
| Fill gas pressure | 101.3 kPa |
| Fuel rod pitch | 14.22 |
| Coolant pressure | 3.46 MPa |
| Coolant inlet temperature | 513 K |
| Coolant mass flux around rod | |
| Heat transfer coefficient for coolant | |
| # of time steps | 50 |
| # of axial nodes in pellet | 11 |
| # of equal volume radial rings in pellet | 45 |

Figure 2.13: IFA-432 Fuel Pin Image



The irradiation history of this rod has been simplified in order to bring it to a manageable number of time steps as provided in Table 2.24 and shown in Figure 2.14. The original power versus time history had much variation which has been smoothed out in order to preserve the overall irradiation effect.

Figure 2.14: IFA-432 Power History Plot

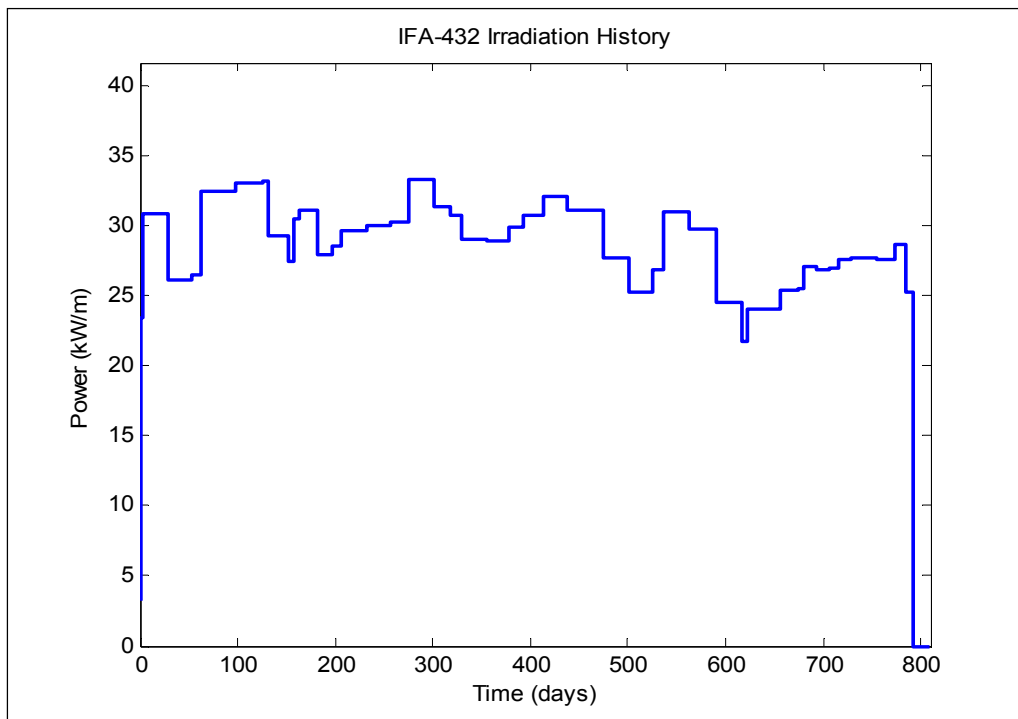


Table 2.24: IFA-432 Power History

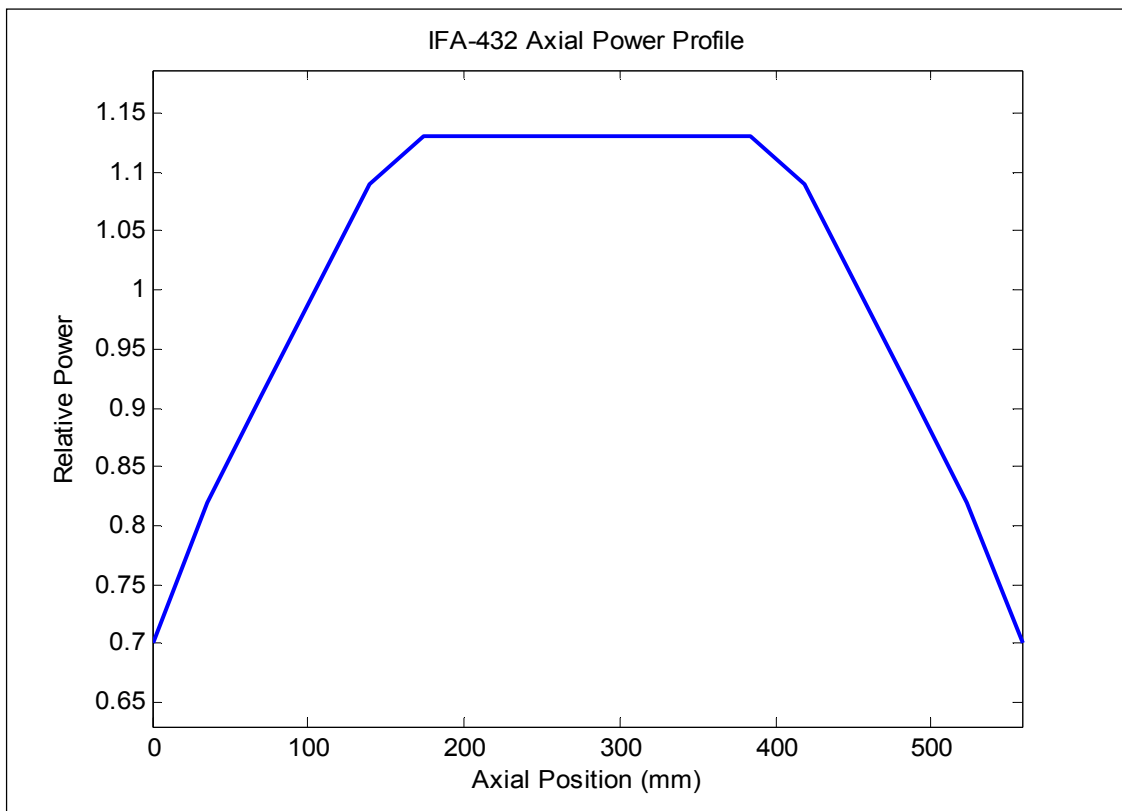
| Time step - | Time (days) | Power (kW/m) | Time step - | Time (days) | Power (kW/m) |
|----------------|----------------|-----------------|----------------|----------------|-----------------|
| 1 | 0.00 | 0.00 | 26 | 355.06 | 28.97 |
| 2 | 0.10 | 3.28 | 27 | 377.67 | 28.85 |
| 3 | 0.20 | 6.56 | 28 | 392.18 | 29.86 |
| 4 | 0.30 | 9.84 | 29 | 413.05 | 30.71 |
| 5 | 0.40 | 13.12 | 30 | 437.73 | 32.11 |
| 6 | 0.50 | 16.40 | 31 | 475.03 | 31.08 |
| 7 | 2.23 | 23.43 | 32 | 500.15 | 27.63 |
| 8 | 28.97 | 30.82 | 33 | 524.51 | 25.23 |
| 9 | 53.70 | 26.14 | 34 | 536.26 | 26.77 |
| 10 | 63.14 | 26.53 | 35 | 563.16 | 31.02 |
| 11 | 97.94 | 32.45 | 36 | 590.49 | 29.80 |
| 12 | 125.17 | 33.07 | 37 | 617.39 | 24.57 |
| 13 | 132.06 | 33.15 | 38 | 622.89 | 21.73 |
| 14 | 152.43 | 29.21 | 39 | 655.36 | 24.08 |
| 15 | 157.86 | 27.38 | 40 | 673.66 | 25.43 |
| 16 | 163.56 | 30.54 | 41 | 680.78 | 25.47 |
| 17 | 181.05 | 31.05 | 42 | 693.35 | 27.04 |
| 18 | 196.11 | 27.96 | 43 | 705.61 | 26.87 |
| 19 | 206.87 | 28.56 | 44 | 715.82 | 26.92 |
| 20 | 231.83 | 29.63 | 45 | 729.09 | 27.60 |
| 21 | 257.14 | 29.96 | 46 | 754.66 | 27.68 |
| 22 | 275.96 | 30.20 | 47 | 772.92 | 27.58 |
| 23 | 300.91 | 33.29 | 48 | 783.91 | 28.66 |
| 24 | 317.30 | 31.35 | 49 | 791.76 | 25.28 |
| 25 | 328.50 | 30.72 | 50 | 809.80 | 0.00 |

The axial power profile is an assumed shape since the original rod is fairly short axially. These values are given in Table 2.25 and shown in Figure 2.15.

Table 2.25: IFA-432 Axial Power Profile

| Location (mm) | Relative power - |
|---------------|------------------|
| 0.00 | 0.70 |
| 34.87 | 0.82 |
| 69.74 | 0.91 |
| 104.61 | 1.00 |
| 139.48 | 1.09 |
| 174.34 | 1.13 |
| 209.21 | 1.13 |
| 244.08 | 1.13 |
| 278.95 | 1.13 |
| 313.82 | 1.13 |
| 348.69 | 1.13 |
| 383.56 | 1.13 |
| 418.43 | 1.09 |
| 453.29 | 1.00 |
| 488.16 | 0.91 |
| 523.03 | 0.82 |
| 557.90 | 0.70 |

Figure 2.15: IFA-432 Axial Power Profile Plot



The manufacturing uncertainties to be applied to this case are shown in Table 2.26. These values are specific to this BWR experimental case configuration.

Table 2.26: Case 4 Manufacturing Uncertainties

| Parameter | Lower limit | Upper limit | Distribution |
|-----------------------|-------------------|-------------------|--------------|
| Cladding ID | 10.86 mm | 10.94 mm | Normal |
| Cladding thickness | 0.936 mm | 0.944 mm | Normal |
| Cladding roughness | 0.2 μm | 0.8 μm | Normal |
| Fuel pellet OD | 10.65 mm | 10.69 mm | Normal |
| Fuel density | 10.3 g/cc | 10.5 g/cc | Normal |
| Fuel pellet roughness | 1.5 μm | 2.5 μm | Normal |
| Rod fill pressure | 0.08 MPa | 0.12 MPa | Normal |

Case 4b - Transient BWR experimental test problem

This case is modelled after the FK-1 pulse test performed at the Fukushima Daini BWR. The pulse is one in a series of short-term RIA tests which were performed after an initial irradiation of the fuel. The initial burn-up is equal to 45.5 GWd/MTU. The geometry and dimensions of the FK-1 fuel rod are provided in Table 2.27.

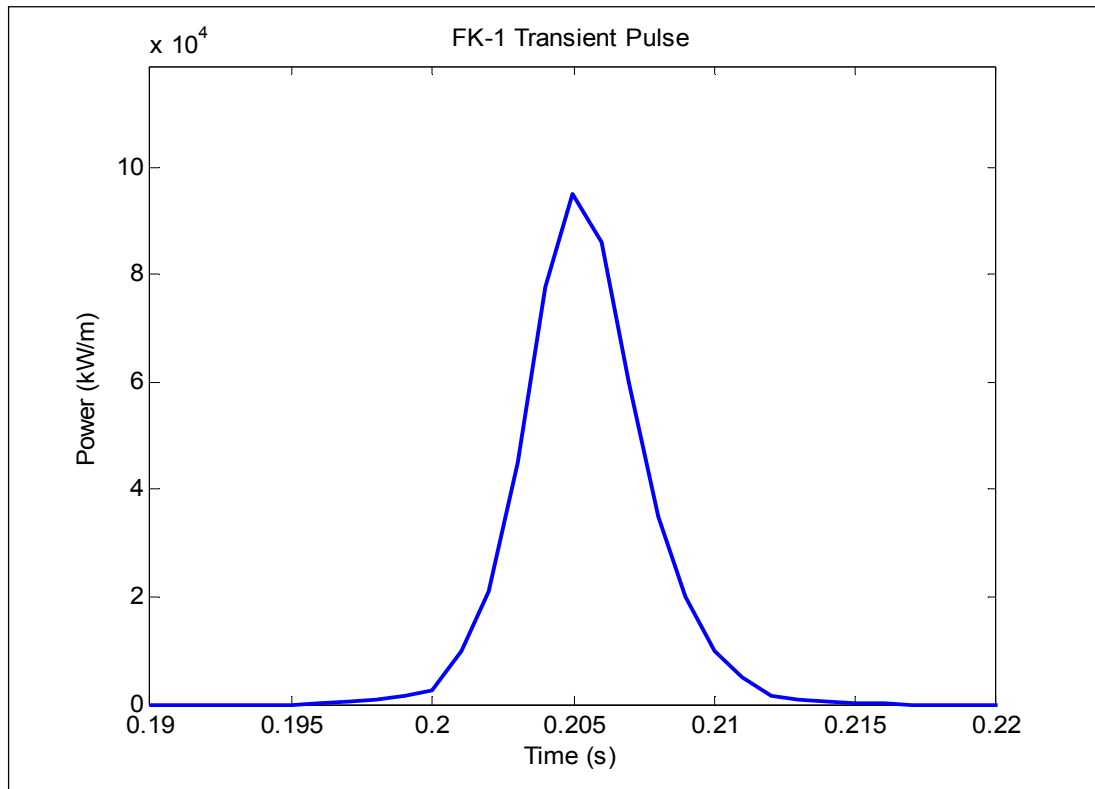
Table 2.27: FK-1 Fuel Rod Geometry

| Geometry | Value |
|--|-------------------|
| Cladding OD | 12.27 mm |
| Cladding ID | 10.43 mm |
| Cladding wall thickness | 0.92 mm |
| Fuel pellet OD | 10.31 mm |
| Pellet-cladding radial gap thickness | 0.12 mm |
| Total fuel column length | 106.0 mm |
| Fuel pellet height | 10.30 mm |
| Fuel enrichment (atom percent) | 3.9% |
| % of theoretical density (10.96 g/cc) | 95.0% |
| Pellet surface roughness | 2.0 μm |
| Cladding type | Zr-2 |
| Cladding surface roughness | 0.5 μm |
| Fill gas type | Helium |
| Fill gas pressure | 0.3 MPa |
| Fuel rod pitch | 16.26 mm |
| Coolant pressure | 0.10 MPa |
| Coolant inlet temperature | 550 K |
| Coolant mass flux around rod | |
| Heat transfer coefficient for coolant | |
| # of time steps | |
| # of axial nodes in pellet | |
| # of equal volume radial rings in pellet | |

The duration of the test is 1.000 seconds. The pulse's power history is provided in Table 2.28 and is shown in Figure 2.16.

Table 2.28: FK-1 Transient Power History

| Time (s) | Power (kW/m) |
|----------|--------------|
| 0.000 | 0.0 |
| 0.195 | 0.0 |
| 0.196 | 200.0 |
| 0.197 | 400.0 |
| 0.198 | 1000.0 |
| 0.199 | 1500.0 |
| 0.200 | 2500.0 |
| 0.201 | 10000.0 |
| 0.202 | 21000.0 |
| 0.203 | 45000.0 |
| 0.204 | 77500.0 |
| 0.205 | 95000.0 |
| 0.206 | 86000.0 |
| 0.207 | 60000.0 |
| 0.208 | 35000.0 |
| 0.209 | 20000.0 |
| 0.210 | 10000.0 |
| 0.211 | 5000.0 |
| 0.212 | 1500.0 |
| 0.213 | 1000.0 |
| 0.214 | 500.0 |
| 0.215 | 200.0 |
| 0.216 | 100.0 |
| 0.217 | 0.0 |
| 1.000 | 0.0 |

Figure 2.16: FK-1 Transient Power History Plot

The coolant temperature history can also be applied to the pulse test. The values are provided in Table 2.29. The transient time steps are shown in Table 2.30.

Table 2.29: FK-1 Transient Coolant Temperature History

| Time (s) | Coolant T (K) |
|----------|---------------|
| 0.00 | 305 |
| 0.21 | 305 |
| 0.25 | 393 |
| 0.35 | 436 |
| 0.50 | 510 |
| 0.70 | 452 |
| 0.85 | 452 |
| 1.00 | 383 |

Table 2.30: FK-1 Transient Time Step Sizes

| Step size | Time period |
|-----------|---------------|
| 0.001 s | 0.00 - 0.15 s |
| 0.00001 s | 0.15 - 0.25 s |
| 0.001 s | 0.25 - 1.00 s |

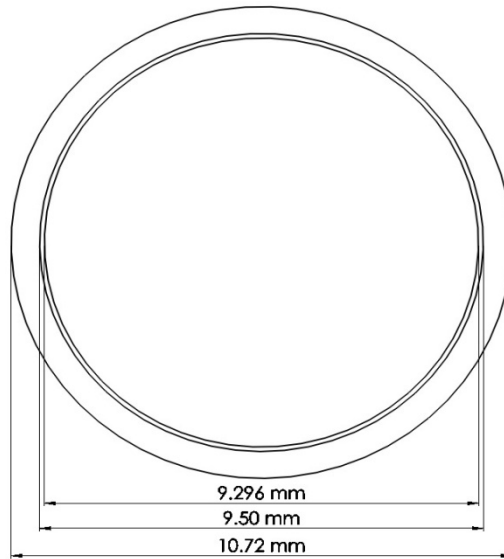
The axial power profile is assumed to be flat, due to the small axial dimension (106.0 mm). The manufacturing uncertainties are the same as in Case 4a.

Case 5a – Steady-state PWR experimental test problem

The IFA-429 experiment is also included in the IFPE Database and it has been slightly modified in order to make usable input values. The main parameters for this case are shown in Table 2.31 and Figure 2.17, which document the geometry of the fuel rod. The irradiation history of this rod is provided in Table 2.32 and is shown in Figure 2.18. The axial power is given in Table 2.33 and shown in Figure 2.19.

Table 2.31: IFA-429 Fuel Rod Geometry

| Geometry | Value |
|--|-------------------|
| Cladding OD | 10.72 mm |
| Cladding ID | 9.50 mm |
| Cladding wall thickness | 0.61 mm |
| Fuel pellet OD | 9.30 mm |
| Pellet-cladding radial gap thickness | 0.10 mm |
| Total fuel column length | 243.4 mm |
| Fuel pellet height | |
| Fuel enrichment (atom percent) | 13.0% |
| % of theoretical density (10.96 g/cc) | 95.0% |
| Pellet surface roughness | 2.0 μm |
| Cladding type | Zr-4 |
| Cladding surface roughness | 0.5 μm |
| Fill gas type | Helium |
| Fill gas pressure | 2.41 MPa |
| Fuel rod pitch | 14.3 mm |
| Coolant pressure | 15 MPa |
| Coolant inlet temperature | 510 K |
| Coolant mass flux around rod | |
| Heat transfer coefficient for coolant | |
| # of time steps | 46 |
| # of axial nodes in pellet | 11 |
| # of equal volume radial rings in pellet | 45 |

Figure 2.17: IFA-429 Fuel Rod Image**Table 2.32: IFA-429 Power History**

| Time step - | Time (days) | Power (kW/m) | Time step - | Time (days) | Power (kW/m) |
|----------------|----------------|-----------------|----------------|----------------|-----------------|
| 1 | 0.0 | 0.00 | 24 | 886.6 | 24.25 |
| 2 | 0.1 | 5.39 | 25 | 958.4 | 19.65 |
| 3 | 0.2 | 10.77 | 26 | 1011.6 | 20.31 |
| 4 | 0.3 | 16.16 | 27 | 1021.9 | 19.86 |
| 5 | 0.4 | 21.54 | 28 | 1043.5 | 22.54 |
| 6 | 29.6 | 26.93 | 29 | 1079.8 | 22.13 |
| 7 | 81.6 | 22.82 | 30 | 1115.3 | 21.41 |
| 8 | 102.2 | 24.31 | 31 | 1178.7 | 24.09 |
| 9 | 130.7 | 20.27 | 32 | 1248.3 | 21.35 |
| 10 | 186.6 | 24.35 | 33 | 1298.9 | 21.35 |
| 11 | 221.6 | 24.77 | 34 | 1340.0 | 17.55 |
| 12 | 302.8 | 20.82 | 35 | 1377.8 | 19.39 |
| 13 | 392.5 | 22.30 | 36 | 1409.9 | 19.90 |
| 14 | 422.7 | 24.42 | 37 | 1444.6 | 17.78 |
| 15 | 463.3 | 24.47 | 38 | 1482.9 | 12.43 |
| 16 | 498.2 | 25.55 | 39 | 1514.7 | 11.90 |
| 17 | 543.2 | 21.53 | 40 | 1577.1 | 15.14 |
| 18 | 644.5 | 17.98 | 41 | 1608.9 | 21.74 |
| 19 | 708.0 | 26.08 | 42 | 1641.6 | 18.43 |
| 20 | 745.2 | 23.03 | 43 | 1688.2 | 21.62 |
| 21 | 775.7 | 24.06 | 44 | 1724.6 | 19.93 |
| 22 | 800.5 | 24.11 | 45 | 1763.6 | 17.91 |
| 23 | 829.2 | 22.47 | 46 | 1784.4 | 0.00 |

Figure 2.18: IFA-429 Power History Plot

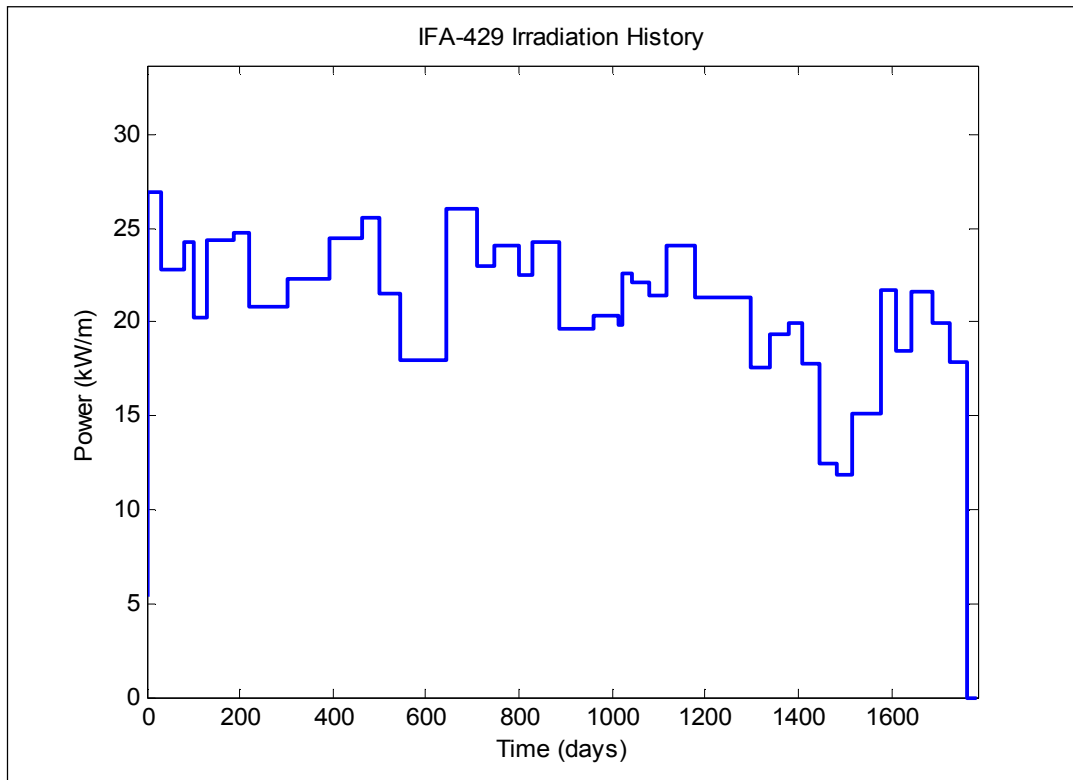
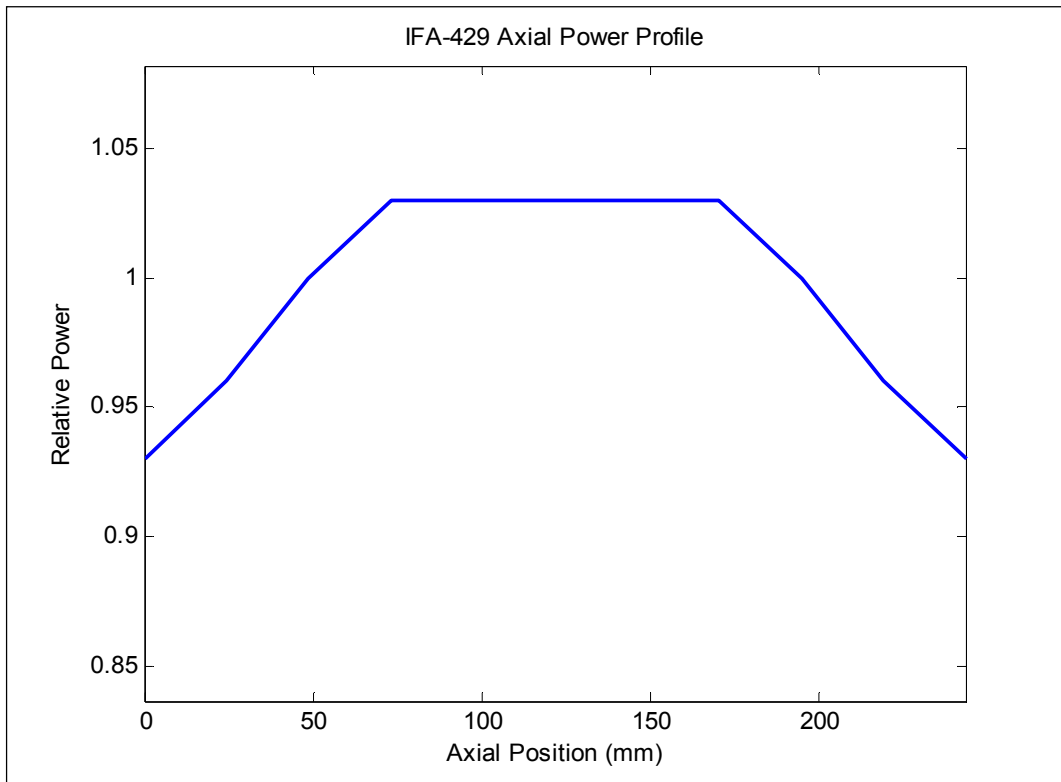


Table 2.33: IFA-429 Axial Power Profile

| Location (mm) | Relative power |
|---------------|----------------|
| 0.0 | 0.93 |
| 24.3 | 0.96 |
| 48.7 | 1.00 |
| 73.0 | 1.03 |
| 97.4 | 1.03 |
| 121.7 | 1.03 |
| 146.0 | 1.03 |
| 170.4 | 1.03 |
| 194.7 | 1.00 |
| 219.1 | 0.96 |
| 243.4 | 0.93 |

Figure 2.19: IFA-429 Axial Power Profile Plot

The manufacturing uncertainties to be applied to this case are shown in Table 2.34. These values are specific to this PWR experimental case configuration.

Table 2.34: Case 5 Manufacturing Tolerances

| Parameter | Lower limit | Upper limit | Distribution |
|-----------------------------|-------------|-------------|--------------|
| Cladding thickness | 0.58 mm | 0.64 mm | Normal |
| Fuel pellet OD | 9.28 mm | 9.32 mm | Normal |
| Fuel density | 10.3 g/cc | 10.5 g/cc | Normal |
| Gap thickness | 0.08 mm | 0.12 mm | Normal |
| U ²³⁵ enrichment | 12.95 w/o | 13.05 w/o | Normal |

The Case 5b - Transient PWR experimental test problem, the Case 6a – Steady-state VVER experimental test problem, and Case 6b - Transient VVER experimental test problems are not ready at this moment and will be provided in Version 2.0 of the Specification in Phase II.

Chapter 3: Definition of Exercise II-2: Time-dependent neutronics

This exercise introduces the time-dependence in stand-alone neutronics calculations in two time scales; short-term time phenomena described by neutron kinetics performance (mostly used for transient and accident analysis related to nuclear safety), and long-term time phenomena described by fuel assembly depletion performance (used for core design and fuel management). The neutron kinetics modelling is important component of reactor transient and accident analysis. The uncertainties in neutron kinetics calculations have an impact on evaluation of accident consequences.

Thus, the exercise is subdivided into two sub-exercises:

- a) Assembly depletion – Exercise II-2a;
- b) Neutron kinetics – Exercise II-2b.

Neutron kinetics and fuel depletion are important topics in the analysis of nuclear reactor cores due to the complexity and various sources of uncertainty in the parameters. Exercise II-2 will determine the uncertainty in predicting the relative power over time of a core after a short-term reactivity change as well as during longer-term depletion cases. These two scenarios are described as either kinetics or depletion cases. In a kinetic case, the reactivity is often changed by altering the position of control rods in the core over a relatively short period of time. The depletion cases are more typical to regular burn-up of fuel in the core, as they mimic a normal irradiation of one fuel assembly. The relative power is an important output parameter to monitor because it factors into many safety calculations as well as provides information on the operating condition of the core. Several sources of the uncertainty encountered in these types of simulations are discussed in this chapter.

This exercise will assess uncertainties in neutronics kinetics (time-dependent) predictions. PSU is developing example problems which can be used to evaluate the kinetics modelling capability of computer codes and determine the uncertainties found during these numerical simulations. The uncertainty of neutronics parameters of the initial steady state, as evaluated in Exercise I-3, will be used and propagated in each time step by adding the uncertainty of transient process calculations. These will address uncertainties in kinetics and delayed neutron data, and also the way reactivity is introduced, in techniques for space-time dependence treatment as well as other calculations.

The short-time phenomena are analysed with the time-dependent neutron kinetics models. The long-term phenomena are treated by the steady-state neutronics model coupled with depletion model (time-dependent nuclide isotopic). The time scales of these two scenarios vary by magnitudes so it is important to analyse them properly according to the main types of uncertainty parameters associated with each case.

3.1 Discussion of input, target, and output uncertainties

In Exercise II-2 the participants will propagate few-group (two-group) nodal cross-section variance and covariance matrices for both rodged and unrodged cross-sections, and:

- a) For Exercise II-2a – uncertainties of nodal fission yields, and decay constants through assembly fuel depletion to obtain uncertainties of criticality values, reactions and collapsed cross-sections, and nuclide concentrations;
- b) For Exercise II-2b – uncertainties of nodal inverse neutron group velocities, delayed neutron fractions and decay constants through a well-defined transient to obtain uncertainties in prediction

of output parameters such as total power and reactivity time evolution as well as time-dependent spatial power distributions.

For Exercise II-2 Input (I), Output (O), and propagated Uncertainty (U) parameters are identified. Guidance on assumptions for Exercise II-2a criticality values, reactions and collapsed cross-sections, and nuclide concentrations are also provided. The Input uncertainties (I) include:

- uncertainties in few-group cross-sections;
- uncertainties in burn-up and kinetics data;
- uncertainty in the reactivity introduction;
- methodological uncertainties;
- manufacturing uncertainties.

The input uncertainties for the depletion calculations (long-term) are from the cross-sections and the fission yields and decay data. The kinetics (short-term) calculation input uncertainties include the cross-sections as well as kinetics and delayed neutron data and the reactivity introduction manner. In summary, the sources of input uncertainties (noted if they are from previous exercises in the OECD LWR UAM benchmark):

- few-group nodal cross-sections;
- nodal group inverse neutron velocities, delayed neutron fractions, decay constants, and fission yields generated in Exercise I-2;
- the way reactivity is inserted/removed (speed of control rod movement, boron dilution, etc.) –added in this exercise;
- methods for space-time solution especially time integration techniques for neutronics and depletion solutions – added in this exercise.

The uncertainty in reactivity introduction covers the method in which the control rods are inserted (if it is a short-term kinetics case) and to this extent the speed at which the control rod is moved as well as the position of the rod contains some uncertainties that must be accounted for. The speed of the control rod's movement and the time at which it is inserted or removed from the assembly can have a large impact on the resulting power and reactivity experienced in the core.

Methodological uncertainties are propagated throughout the code being run by the user due to uncertainty in internal subroutines as well as approximations made while modelling and simplifying the scenario. The methods for treating space-time dependence, especially time integration techniques, are expected to propagate significant uncertainty through this exercise. The participants are responsible for performing temporal discretisation (kinetics and depletion time step sizes) convergence studies with their kinetics and depletion codes in order to remove the uncertainties associated with methodological uncertainties. The method related contribution of uncertainty can be derived from earlier benchmarks conducted within NEA/OECD. The following list details the definitions of the uncertainties as well as the sources of several of the uncertainties.

Other uncertainties carry over from previous exercises such as manufacturing tolerances for the geometry of the fuel assemblies as well as nodalisation and other modelling simplifications.

The output uncertainties for the depletion calculations are found in the nuclide concentrations, the power distribution, and the burn-up of the fuel. In the kinetics cases the uncertainties are in the reactor core power-time evolution, the reactor core inserted reactivity evolution, and the 3-D power distribution snapshots. For both cases, it is assumed that there is no feedback modelling.

The Output uncertainties (O) include:

- a) for Exercise II-2a - depletion (long-term irradiation) cases: important nuclide concentrations at the end of the irradiation;

- b) for Exercise IIb - for the kinetics (short-term control rod movement) cases: reactor core power time evolution, reactor core inserted reactivity time evolution, and 3-D power distribution snapshots.

The propagated uncertainty parameters (U) – these are the same as the output parameters, listed above. The Assumptions (A) are that there is no feedback modelling. The propagated uncertainties of this exercise are propagated to be input uncertainties in Exercise II-1 and II-3.

Some of the values used in previous PWR transient analyses are applied to this exercise as well. These values of uncertainty to propagate are:

- rod worth ($\pm 10\%$);
- individual banks ($\pm 15\%$);
- fraction of delayed neutrons ($\pm 3\%$);
- critical boron concentration at 100% Core Power (± 50 ppm);
- power distribution (at intermediate level and at 100% power) (± 0.1 x relative power density for each measured assembly power).

The users are asked to apply various uncertainties to their input values in order to measure the response of the output parameters. The changes in these outputs are an indication of how much of an effect uncertainty has on the desired results during these types of simulations.

3.2 Test problems

There are two types of test problems for this exercise: depletion cases and kinetics cases. The depletion cases are longer-term scenarios which will be calculated on the fuel assembly level, and these are single assembly cases that cover lattice depletion. The kinetics cases are calculated over a mini-core which will contain several assemblies. These scenarios cover more rapid changes in reactivity in the core and the propagation of this effect on the power level and other parameters in the mini-core. These dynamic cases are made to be representative of dynamic control rod worth, boron worth and scram conditions.

These types of cases are designed in order to address the impact of way of generating the burn-up-related and kinetics and delayed neutron data as well as the burn-up and space-time dependence treatment and corresponding uncertainties.

There will be experimental test problems that compare to experimental results and numerical test problems that simulate cores representative of the three reactors used throughout this phase: TMI-1, PB-2, and the VVER-1000. For each of these types of test cases (experimental and numerical) there will be depletion (long-term) and a kinetic (short-term) test problem, provided in this chapter. The user can use the results from the experimental test cases and compare with the actual experimental data in order to benchmark the results and study the effect of the uncertainty propagation. There are also the uncertainties in the experimental data due to measurement capabilities. For example, the SPERT III E-core data were measured with 17% uncertainty on the power measurements and ± 0.04 on the reactivity measurements. Numerical results that are outside of these measurement bounds are not very reliable results.

Some GEN-III cores may also be analysed in this chapter.

The users should run the depletion calculations and provide criticality values, reactions and collapsed cross-sections, and nuclide concentrations as well as their uncertainties for depletion in a simple assembly model. The concentrations of selected nuclides are requested at the end of the irradiation period along with associated uncertainties. These nuclides include:

^{233}U
 ^{235}U
 ^{236}U
 ^{238}U

^{239}Pu
 ^{240}Pu
 ^{241}Pu
 ^{242}Pu
 ^{241}Am
 ^{243}Am
 ^{242}Cm
 ^{244}Cm
 ^{142}Nd
 ^{143}Nd
 ^{144}Nd
 ^{145}Nd
 ^{146}Nd

Output requested for kinetics test cases: - the users are asked to run the transient cases for the given mini-core and provide a power versus time plot for the mini-core over the course of the transient together with associated uncertainties.

Case 1a – Depletion BWR numerical test problem

The first case is modelled to the parameters of PB-2 and based on an experiment performed with the Fukushima-2 reactor. It is a long-term irradiation case with no abnormal power deviations or incidents. The case will be modelled using a single fuel assembly (FA) and all of the parameters will be defined in the following tables.

The geometry of the PB-2 FA is shown in Figure 3.1.

Figure 3.1: PB-2 FA Pin Layout

| + | 1 | 2 | 3 | 4 | 5 | 6 | 7 |
|---|---|---|----|---|----|----|---|
| 1 | 4 | 3 | 3 | 2 | 2 | 2 | 3 |
| 2 | 3 | 2 | 1 | 1 | 1 | 1 | 2 |
| 3 | 3 | 1 | 5A | 1 | 1 | 5A | 1 |
| 4 | 2 | 1 | 1 | 1 | 1 | 1 | 1 |
| 5 | 2 | 1 | 1 | 1 | 6A | 1 | 1 |
| 6 | 2 | 1 | 5A | 1 | 1 | 1 | 2 |
| 7 | 3 | 2 | 1 | 1 | 1 | 2 | 2 |

The plus sign ('+') on the upper left corner of the above figure shows the location of the cruciform control rod with respect to the FA. The numbers in the above figure represent the various rods that are in the FA, and they are defined in Table 3.1.

Table 3.1: PB-2 FA Pin Descriptions

| Rod # | Enrich. | Gd ₂ O ₃ | Density |
|-------|---------|--------------------------------|-------------------|
| - | w/o | w/o | g/cm ³ |
| 1 | 2.93 | - | 10.32 |
| 2 | 1.94 | - | 10.32 |
| 3 | 1.69 | - | 10.32 |
| 4 | 1.33 | - | 10.32 |
| 5A | 2.93 | 3.00 | 10.19 |
| 6A | 2.93 | 3.00 | 10.27 |

Other details about each FA are given in Table 3.2.

Table 3.2: PB-2 FA Details

| | |
|-------------------------------|-----------|
| FA pitch | 152.4 mm |
| Active height | 3657.6 mm |
| # Water rods | 0 |
| # 3.0 w/o Gd pins | 4 |
| # 2.93% ²³⁵ U pins | 26 |
| # 1.94% ²³⁵ U pins | 12 |
| # 1.69% ²³⁵ U pins | 6 |
| # 1.33% ²³⁵ U pins | 1 |
| Total rods/FA | 49 |

The physical dimensions and parameters of the fuel rods are found in Table 3.3.

Table 3.3: PB-2 Fuel Rod Dimensions and Parameters

| | |
|--------------------|----------|
| Cladding OD | 14.30 mm |
| Cladding ID | 13.36 mm |
| Cladding thickness | 0.47 mm |
| Pin pitch | 18.75 mm |
| Fuel pellet OD | 12.12 mm |
| Fuel pellet height | 10.7 mm |
| % Density | 95.1% TD |

The PB-2 core's boundary conditions define the nominal operating conditions of the entire core. They are given in Table 3.4.

Table 3.4: PB-2 Core Boundary Conditions

| | |
|---------------------|-------------|
| Core power | 3 293 MWt |
| Coolant temperature | 464.3 K |
| Core pressure | 7.24 MPa |
| Coolant flow rate | 1680 kg/s |
| Inlet enthalpy | 1 213 kJ/kg |

The material used for the cladding in PB-2 is Zr-2, which is defined in Table 3.5.

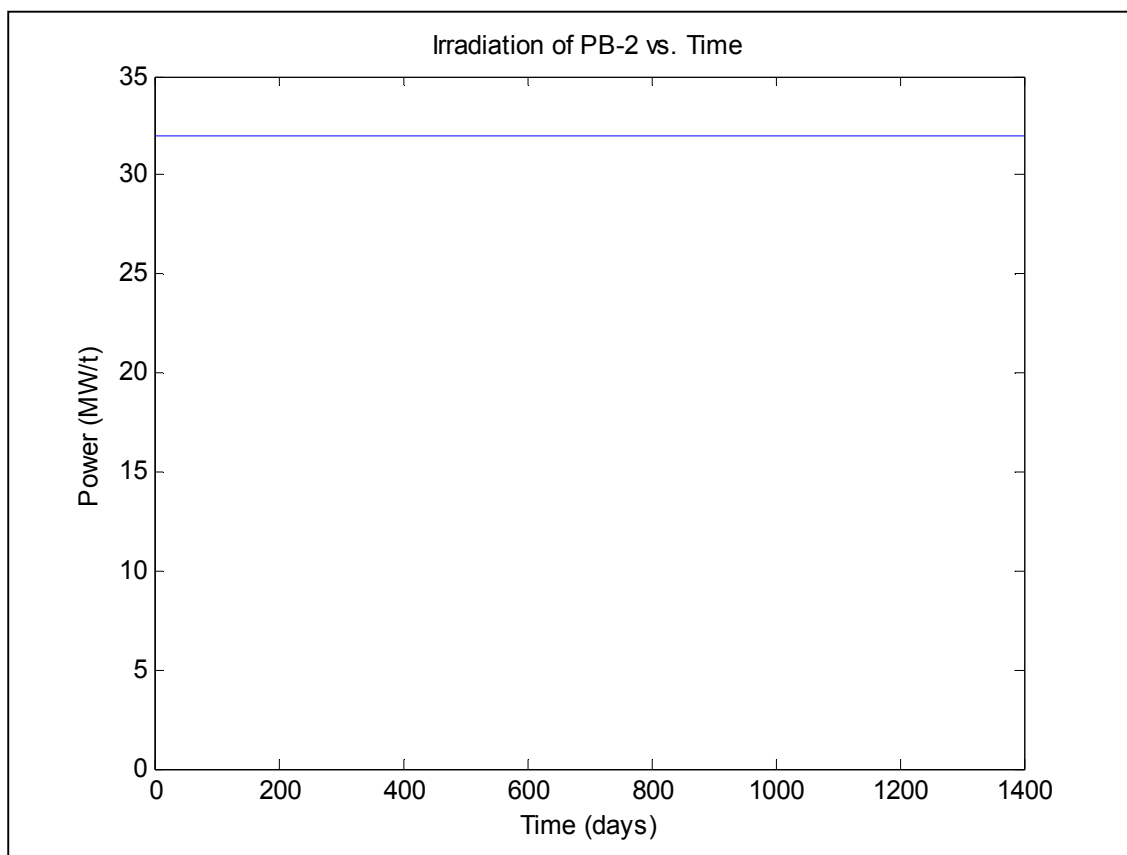
Table 3.5: PB-2 Zr-2 Cladding Composition

| Nuclide | w/o |
|---------|--------|
| O | 0.125 |
| Cr | 0.100 |
| Fe | 0.135 |
| Ni | 0.055 |
| Zr | 98.135 |
| Nb | 0.000 |
| Sn | 1.450 |

The irradiation history is defined by providing a power level of a certain axial location in the assembly. This power is assumed to be averaged over the radial profile of the Fuel Assembly (FA) at this given axial location. The axial location is defined as halfway from the bottom of the fuel rod, at 1828.8 mm. The power is assumed to be constant over the duration of the irradiation as shown in Table 3.6 and Figure 3.2.

Table 3.6: PB-2 Irradiation History

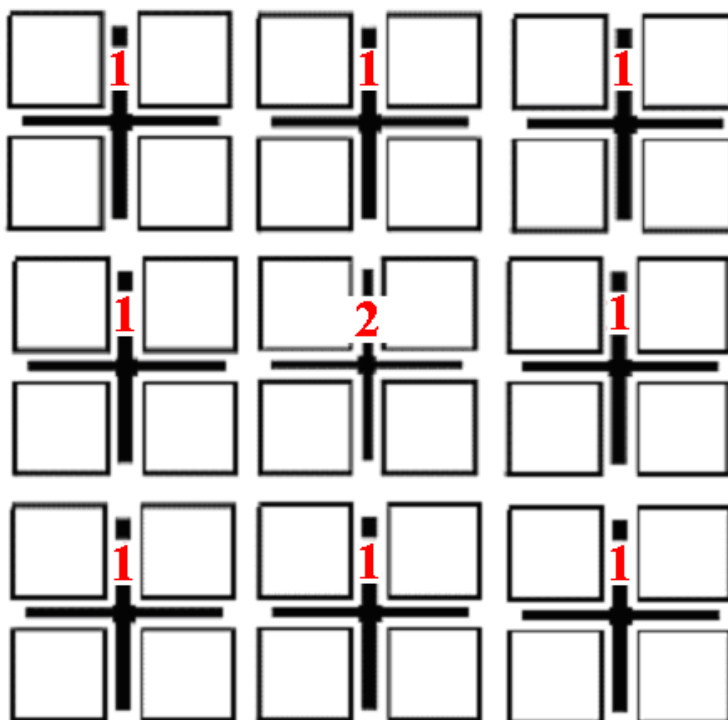
| Time | Power |
|-------|-------|
| Days | MW/t |
| 1 400 | 32.00 |

Figure 3.2: PB-2 Irradiation History Plot

Case 1b: Kinetics BWR numerical test problem

This test case involves a BWR mini-core (6x6 in FA dimensions) which has a control rod insertion and withdrawal transient. There are nine cruciform control rods included in the mini-core model. The initial core state (steady-state) is at typical hot zero power (HZP) conditions, with the central control rod fully inserted and the eight peripheral control rods fully withdrawn. Reflective radial boundary conditions and vacuum axial boundary conditions are applied to this test case. No thermal-hydraulic feedback is modelled in this test case and a reasonable power transient evolution is attained simply with control rod movement. The geometry of the mini-core is shown in Figure 3.3. The red numbers indicate peripheral (numbered 1) and central (numbered 2) control rod locations by type.

Figure 3.3: PB-2 Mini-core Geometry



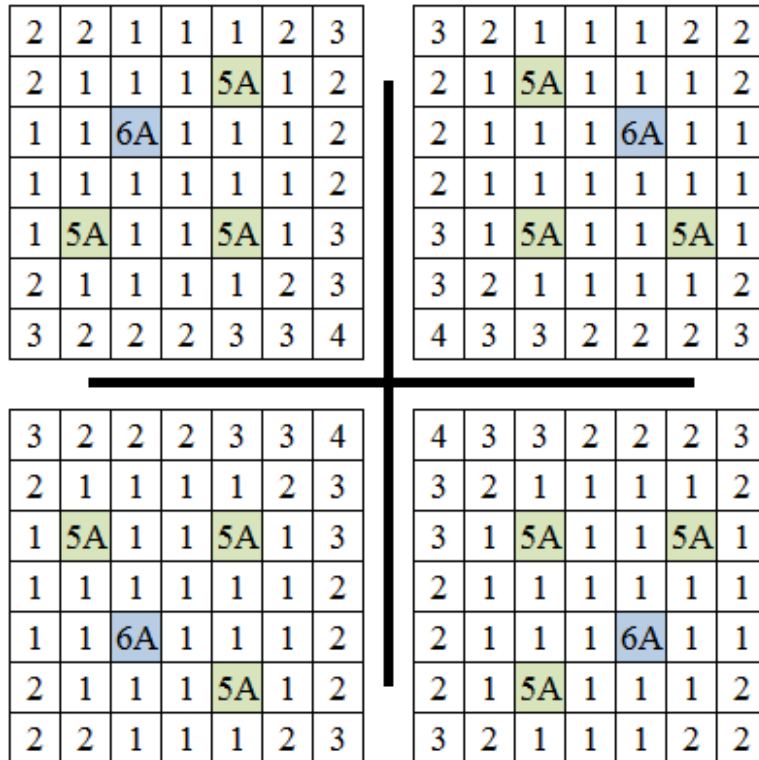
Each of the FAs (of the 36 total) is the same as in Case 1a. They are rotated with respect to the location of the cruciform control rod. This is illustrated in Figure 3.4 below. The fuel rod definitions, dimensions, and parameters are given in Tables 3.1 through 3.5.

The control rod movement transient is a basic scenario where the central control rod is initially fully inserted (corresponding to a position of 0 mm) and the eight peripheral control rods are initially fully withdrawn (corresponding to a position of 3657.8 mm). At HZP, the conditions are as found in Table 3.7.

Table 3.7: PB-2 Mini-core HZP Conditions

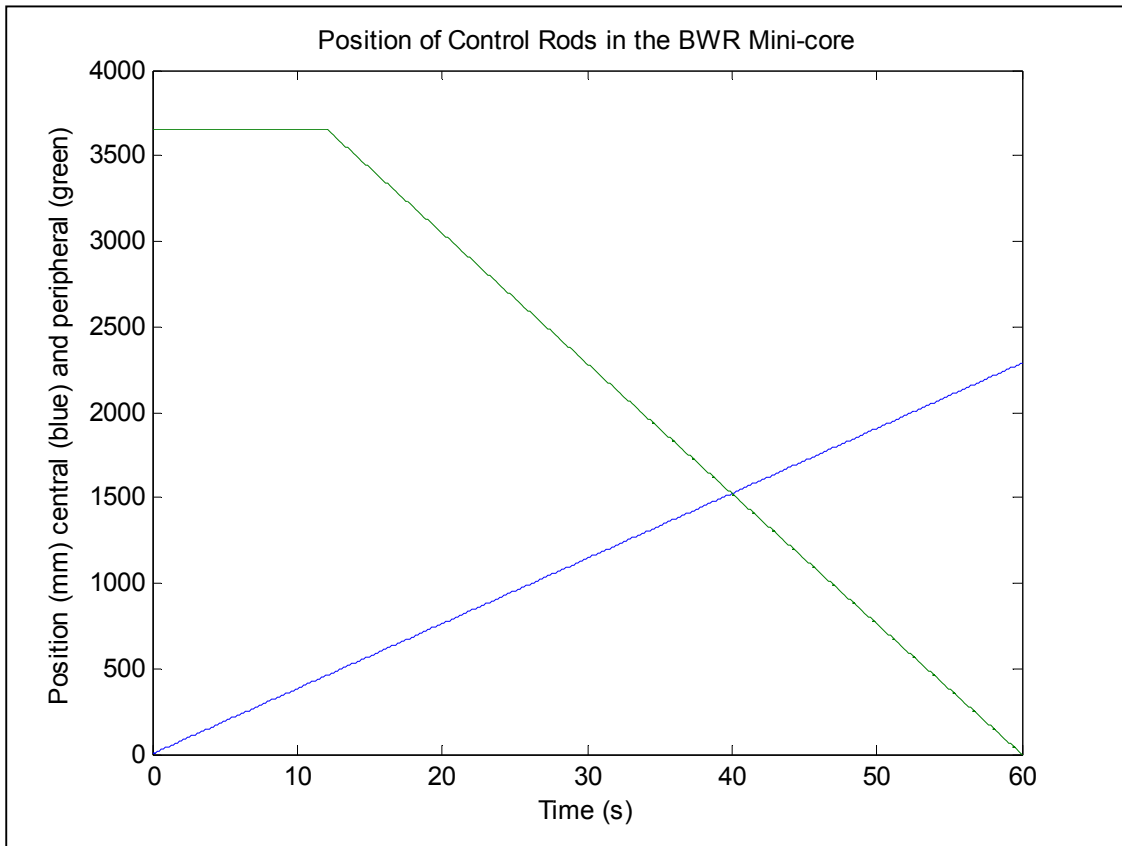
| | |
|-----------------------|-------------------------|
| Reactor conditions | HZP |
| Fuel temperature | 552.8 K |
| Cladding temperature | 552.8 K |
| Moderator temperature | 552.8 K |
| Moderator density | 754.0 kg/m ³ |
| Void fraction | 0 % |

Figure 3.4: PB-2 Fuel Assembly Geometry



The transient is initiated by withdrawing the central control rod at a speed of 3.81 cm/s. After 12.0 seconds, the eight peripheral rods are inserted at a speed of 7.62 cm/s. Figure 3.5 illustrates these control rod movements.

Figure 3.5: PB-2 Mini-core control rod movements over time



Case 2a - Depletion PWR numerical test problem

This test case is modelled to the parameters of TMI-1 and based on an experiment performed with the Takahama-3 reactor. It is a long-term irradiation case with a constant power level at all times. The case will be modelled using a single fuel assembly and all of the parameters will be defined in the following tables.

The numbers in the above figure represent the various rods that are in the FA, and they are defined in Table 3.8.

Table 3.8: TMI-1 FA Pin Descriptions

| Marker | Rod type |
|--------|---------------------------------------|
| g | 2.0 w/o Gd 4.12% ²³⁵ U pin |
| G | Guide tube |
| I | Instrumentation tube |
| - | 4.12% ²³⁵ U fuel pin |

Other details about each FA are given in Table 3.9.

The geometry of the TMI-1 FA is defined by:

Figure 3.6: TMI-1 FA Pin Layout

| | 1 | 2 | 3 | 4 | 5 | 6 | 7 | 8 | 9 | 10 | 11 | 12 | 13 | 14 | 15 |
|----|---|---|---|---|---|---|---|---|---|----|----|----|----|----|----|
| 1 | - | - | - | - | - | - | - | - | - | - | - | - | - | - | - |
| 2 | - | g | - | - | - | - | - | - | - | - | - | - | - | g | - |
| 3 | - | - | - | - | - | G | - | - | - | G | - | - | - | - | - |
| 4 | - | - | - | G | - | - | - | - | - | - | - | G | - | - | - |
| 5 | - | - | - | - | - | - | - | - | - | - | - | - | - | - | - |
| 6 | - | - | G | - | - | G | - | - | - | G | - | - | G | - | - |
| 7 | - | - | - | - | - | - | - | - | - | - | - | - | - | - | - |
| 8 | - | - | - | - | - | - | - | I | - | - | - | - | - | - | - |
| 9 | - | - | - | - | - | - | - | - | - | - | - | - | - | - | - |
| 10 | - | - | G | - | - | G | - | - | - | G | - | - | G | - | - |
| 11 | - | - | - | - | - | - | - | - | - | - | - | - | - | - | - |
| 12 | - | - | - | G | - | - | - | - | - | - | - | G | - | - | - |
| 13 | - | - | - | - | - | G | - | - | - | G | - | - | - | - | - |
| 14 | - | g | - | - | - | - | - | - | - | - | - | - | - | g | - |
| 15 | - | - | - | - | - | - | - | - | - | - | - | - | - | - | - |

Table 3.9: TMI-1 FA Details

| | |
|-------------------------------|-----------|
| FA pitch | 218.1 mm |
| Active height | 3657.6 mm |
| # Guide tubes | 16 |
| # Instrumentation tubes | 1 |
| # 2.0 w/o Gd pins | 4 |
| # 4.12% ²³⁵ U pins | 204 |
| Total rods/FA | 225 |

The physical dimensions and parameters of the fuel rods are found in Table 3.10.

Table 3.10: TMI-1 Fuel, Guide, and Instrumentation Rod Dimensions and Parameters

| | |
|-------------------------|-----------|
| Cladding OD | 10.922 mm |
| Cladding ID | 9.58 mm |
| Cladding thickness | 0.673 mm |
| Pin pitch | 14.427 mm |
| Fuel pellet OD | 9.390 mm |
| Fuel pellet height | 11.4 mm |
| % Density | 93.8% TD |
| Guide tube OD | 13.462 mm |
| Guide tube ID | 12.649 mm |
| Instrumentation tube OD | 12.522 mm |
| Instrumentation tube ID | 11.201 mm |

The TMI-1 core's boundary conditions define the nominal operating conditions of the entire core. They are given in Table 3.11.

Table 3.11: TMI-1 Core Boundary Conditions

| | |
|---------------------|-----------|
| Core power | 2 772 MWt |
| Coolant temperature | 562 K |
| Core pressure | 15.51 MPa |
| Coolant flow rate | |

The material used for the cladding in TMI-1 is Zr-4, which is defined in Table 3.12.

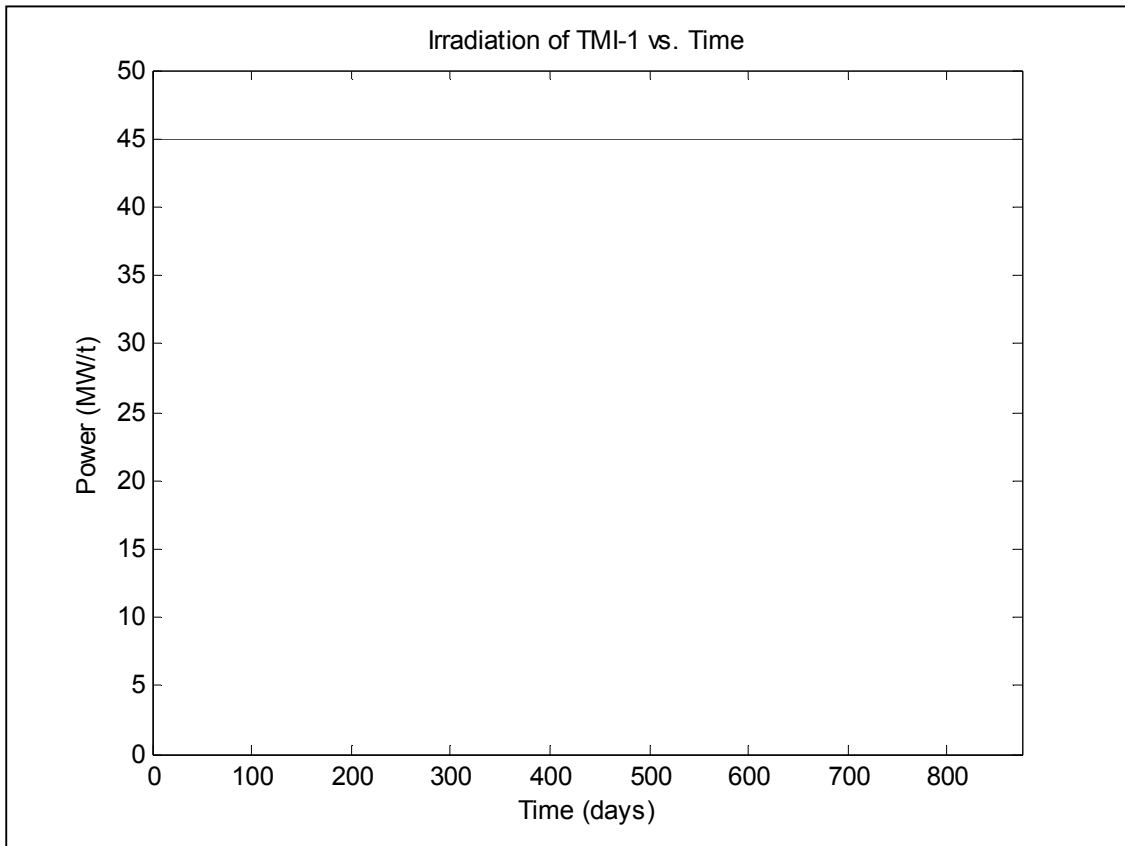
Table 3.12: TMI-1 Zr-4 Cladding Composition

| Nuclide | w/o |
|---------|--------|
| O | 0.125 |
| Cr | 0.100 |
| Fe | 0.210 |
| Ni | 0.000 |
| Zr | 98.115 |
| Nb | 0.000 |
| Sn | 1.450 |

The irradiation history is defined by providing a power level of a certain axial location in the assembly. This power is assumed to be averaged over the radial profile of the FA at this given axial location. The axial location is defined as halfway from the bottom of the fuel rod, at 1828.8 mm. The power is assumed to be constant over the duration of the irradiation as shown in Table 3.13 and Figure 3.7.

Table 3.13: TMI-1 Irradiation History

| Time | Power |
|------|-------|
| Days | MW/t |
| 875 | 45.00 |

Figure 3.7: TMI-1 Irradiation History Plot**Case 2b: Kinetics PWR numerical test problem**

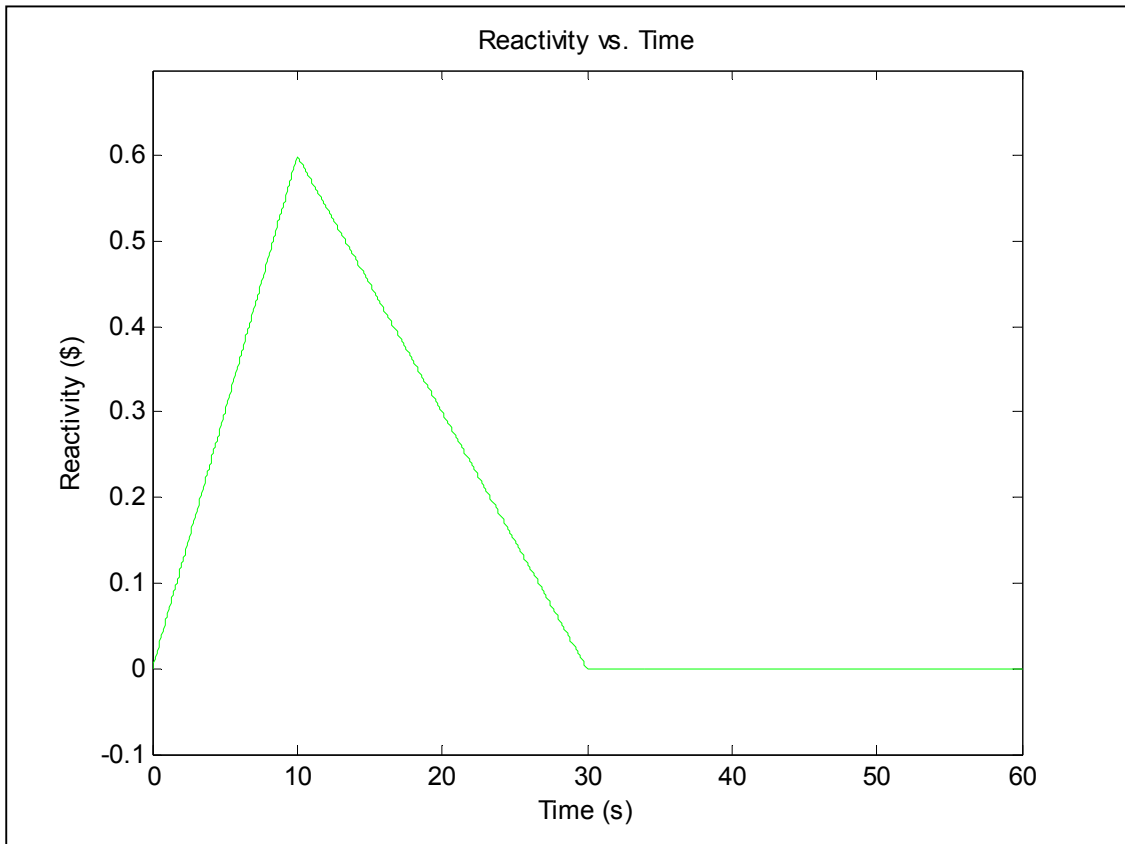
This test case involves a PWR mini-core (3x3 in FA dimensions) which has a control rod movement scenario. These nine FAs are surrounded by reflector assemblies. Only the central FA contains control rods, the others are unrodded. This is shown in the following figure, where the assemblies are marked with 'R' for rodded and 'U' for unrodded.

Figure 3.8: TMI-1 Mini-core Geometry

| | | | | |
|------------------|------------------|------------------|------------------|------------------|
| Reflector | Reflector | Reflector | Reflector | Reflector |
| Reflector | U | U | U | Reflector |
| Reflector | U | R | U | Reflector |
| Reflector | U | U | U | Reflector |
| Reflector | Reflector | Reflector | Reflector | Reflector |

Each of the FAs (of the 36 total) is the same as in Case 2a. The fuel rod definitions, dimensions, and parameters are given in Tables 3.8 through 3.12 of the previous section.

The central assembly control rods are withdrawn (from their initial, fully inserted positions) a distance of 5.0 cm in 10 seconds. They are then reinserted into the assembly a distance of 5.0 cm over the course of 20 seconds. A reactivity versus time plot shows the relative times of these movements in Figure 3.9.

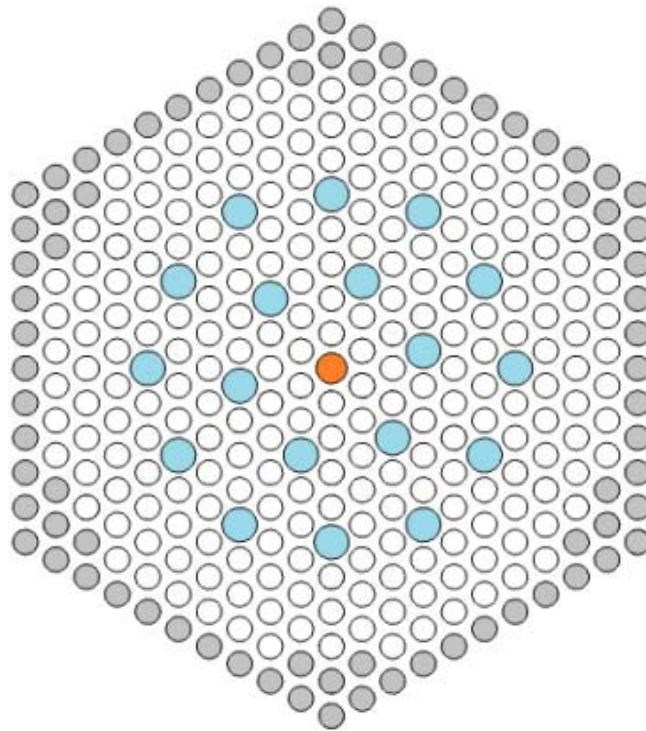
Figure 3.9: TMI-1 mini-core reactivity versus time plot

Case 3a.-Depletion VVER numerical test problem

This is a depletion case modelled for the VVER-1000 reactor such as the one at Kozloduy-6. It is a long-term irradiation case with no abnormal power deviations or incidents. The case will be modelled using a single fuel assembly (FA) and all of the parameters will be defined in the following tables.

The geometry of the VVER-1000 FA is shown in Figure 3.10.

Figure 3.10: VVER-1000 FA Pin Layout



| |
|--|
| Guide tubes (18) |
| Instrumentation rod (1) |
| 3.0 w/o ²³⁵ U fuel pins (78) |
| 3.3 w/o ²³⁵ U fuel pins (234) |

Other details about each FA are given in Table 3.14.

Table 3.14: VVER-1000 FA Details

| | |
|---------------------------------|----------|
| FA pitch | 236.0 mm |
| Active height | 3 837 mm |
| # Water rods | 1 |
| # Guide tubes | 18 |
| # 3.0 w/o ²³⁵ U pins | 78 |
| # 3.3 w/o ²³⁵ U pins | 234 |
| Total rods/FA | 331 |

The physical dimensions and parameters of the fuel rods are found in Table 3.15.

Table 3.15: VVER-1000 Fuel Rod Dimensions and Parameters

| | |
|------------------------|----------|
| Cladding OD | 9.10 mm |
| Cladding ID | 7.72 mm |
| Cladding thickness | 0.69 mm |
| Pin pitch | 12.75 mm |
| Fuel pellet OD | 7.53 mm |
| Fuel pellet ID | 1.40 mm |
| Fuel pellet height | 9.1 mm |
| % Density | 94.9% TD |
| Guide tube OD | 12.60 mm |
| Guide tube ID | 11.00 mm |
| Instrumentation rod OD | 11.20 mm |
| Instrumentation rod ID | 9.60 mm |

The VVER-1000 core's boundary conditions define the nominal operating conditions of the entire core, which are given in Table 3.16.

Table 3.16: VVER-1000 Core Boundary Conditions

| | |
|---------------------|-------------|
| Core power | 3 000 MWt |
| Coolant temperature | 560 K |
| Core pressure | 15.7 MPa |
| Coolant flow rate | 1 7611 kg/s |

The material used for the cladding in VVER-1000 is Zr+1% Nb, which is defined in Table 3.17.

Table 3.17: VVER-1000 Zr+1% Nb Cladding Composition

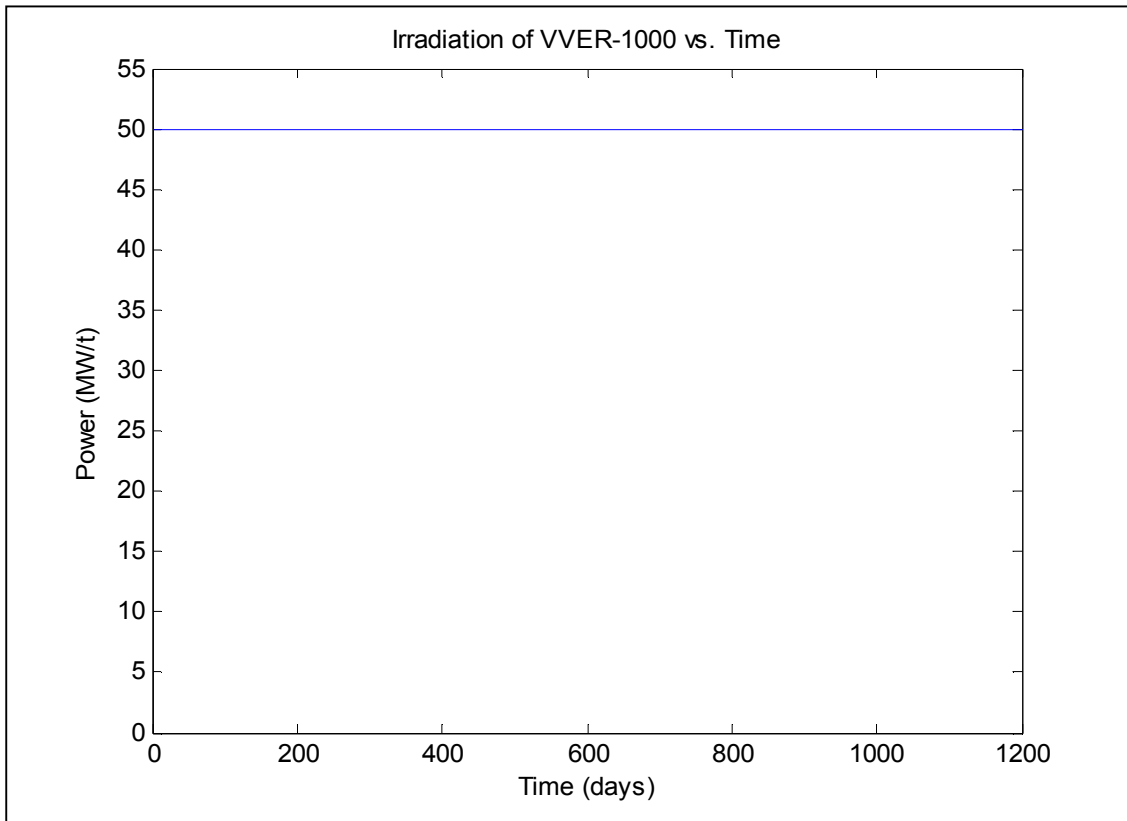
| Nuclide | w/o |
|---------|--------|
| Zr | 98.991 |
| Fe | 0.009 |
| Nb | 1.000 |

The irradiation history is defined by providing a power level of a certain axial location in the assembly. This power is assumed to be averaged over the radial profile of the FA at this given axial location. The axial location is defined as halfway from the bottom of the fuel rod, at 1918.5 mm. The power is assumed to be constant over the duration of the irradiation as shown in Table 3.18 and Figure 3.11.

Table 3.18: VVER-1000 Irradiation History

| Time | Power |
|-------|-------|
| Days | MW/t |
| 1 200 | 50.0 |

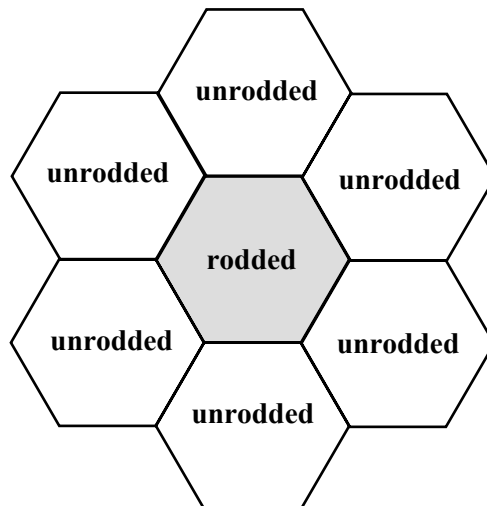
Figure 3.11: VVER-1000 Irradiation History Plot



Case 3b – Kinetics VVER numerical test problem

This test case uses Kozloduy-6 VVER-1000 mini-core as shown in Figure 3.12.

Figure 3.12: Color-set configuration for Kozloduy-6



The assembly specification is provided in Case 3a. The radial boundary conditions are reflective. The assembly in the middle indicated as “rodded” is the assembly where the control rods are moved. The

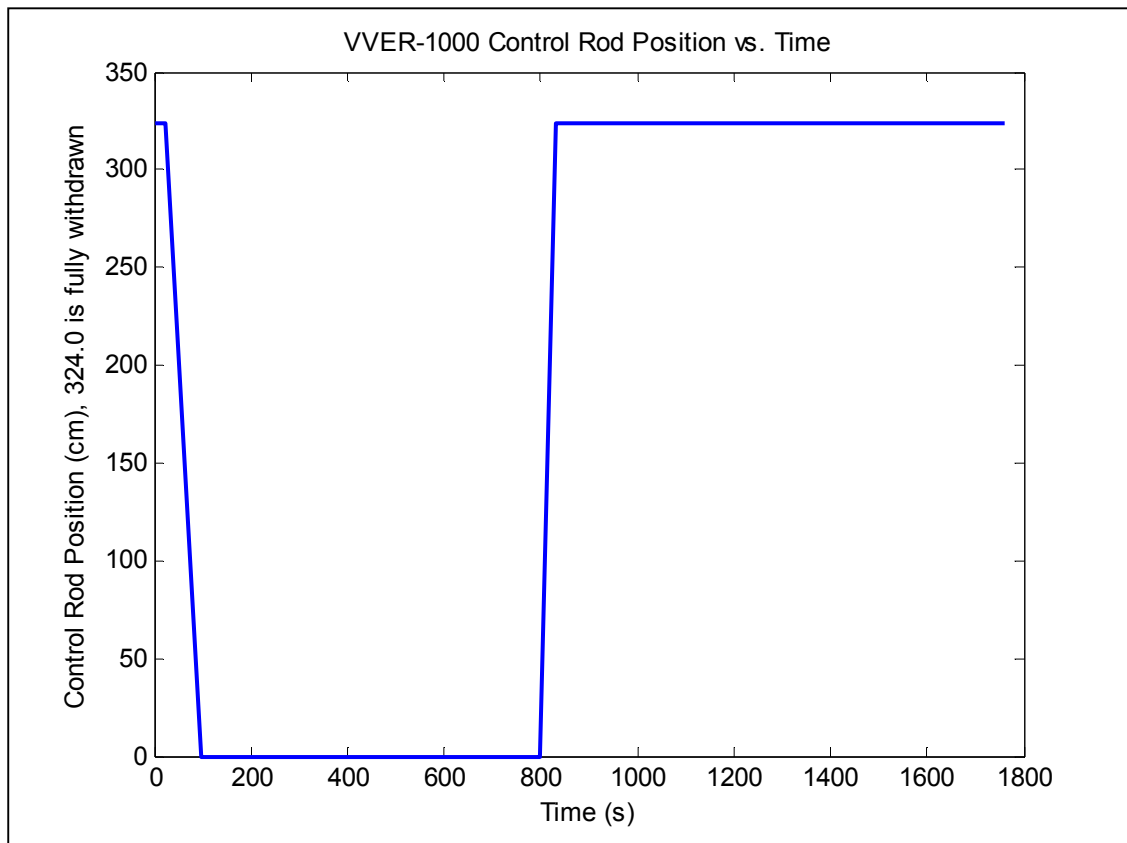
control rods from this single assembly are inserted and then withdrawn at a later time. These movements are defined in Table 3.19 and shown in Figure 3.13.

Table 3.19: VVER-1000 Control Rod Movement

| Time | Position (cm) |
|--------|---------------|
| 0.0 | 324.0 |
| 21.8 | 324.0 |
| 95.5 | 0.0 |
| 798.1 | 0.0 |
| 831.0 | 324.0 |
| 1760.0 | 324.0 |

The motion of the control rods is equal to 4.40 cm/s while being inserted and 9.85 cm/s while being withdrawn.

Figure 3.13: VVER-1000 Control Rod Position vs. Time Plot



Case 4a - Depletion BWR experimental test problem

This test case is an experimental case designed on the Fukushima Daina-2 (FK-2) irradiation and subsequent post-irradiation examination (PIE) performed at the Tokyo Electric Company's plant by the Japan Atomic Energy Research Institute (JAERI). The modelled fuel assembly was irradiated in this reactor where its power levels were monitored and recorded. After the irradiation, several fuel rods were examined to determine the concentrations of several important nuclides. The fuel assembly is an 8x8 BWR assembly with several gadolinium pins as well as two water rods. These are marked and located in the figure below.

The geometry of the FK-2 FA is shown in Figure 3.14:

Figure 3.14: FK-2 FA Pin Layout

| | 1 | 2 | 3 | 4 | 5 | 6 | 7 | 8 |
|---|---|---|---|---|---|---|---|---|
| 1 | 5 | 4 | 3 | 3 | 3 | 3 | 4 | 5 |
| 2 | 4 | 1 | G | 2 | 2 | G | 1 | 4 |
| 3 | 3 | G | 2 | 4 | 4 | 2 | G | 3 |
| 4 | 3 | 2 | 4 | 3 | W | 4 | 2 | 3 |
| 5 | 3 | 2 | 4 | W | 3 | 4 | 2 | 3 |
| 6 | 3 | G | 2 | 4 | 4 | 2 | G | 3 |
| 7 | 4 | 1 | G | 2 | 2 | G | 1 | 4 |
| 8 | 5 | 4 | 3 | 3 | 3 | 3 | 4 | 5 |

The numbers in Figure 3.14 represent the various rods that are in the FA, and they are defined in Table 3.20.

Table 3.20: FK-2 FA Pin Descriptions

| | |
|---|---|
| G | Gd ₂ O ₃ +UO ₂ pin |
| W | water rod |
| 1 | 3.63% ²³⁵ U pin |
| 2 | 3.22% ²³⁵ U pin |
| 3 | 3.18% ²³⁵ U pin |
| 4 | 2.72% ²³⁵ U pin |
| 5 | 1.89% ²³⁵ U pin |
| 1 | SF-98 Location |
| G | SF-99 Location |

SF-98 and SF-99 are the two fuel pins that were analysed in the PIE. The nuclides found in these two pins are available as experimental data with which to compare the calculated results. Other details about the FA are given in Table 3.21.

Table 3.21: FK-2 FA Details

| | |
|-------------------------------|----------|
| FA pitch | 152 mm |
| Active height | 3 710 mm |
| # Water rods | 2 |
| # 6.0 w/o Gd pins | 8 |
| # 3.63% ²³⁵ U pins | 4 |
| # 3.22% ²³⁵ U pins | 12 |
| # 3.18% ²³⁵ U pins | 18 |
| # 2.72% ²³⁵ U pins | 16 |
| # 1.89% ²³⁵ U pins | 4 |
| Total rods/FA | 64 |

The physical dimensions and parameters of the fuel rods are found in Table 3.22.

Table 3.22: FK-2 Fuel Rod Dimensions and Parameters

| | |
|--------------------|---------|
| Cladding OD | 12.3 mm |
| Cladding ID | 10.6 mm |
| Cladding thickness | 0.86 mm |
| Pin pitch | 16.3 mm |
| Fuel pellet OD | 10.3 mm |
| Fuel pellet height | 10.0 mm |
| % Density | 95% TD |
| Water rod OD | 15.0 mm |

The FK-2 core's boundary conditions define the nominal operating conditions of the entire core. They are given in Table 3.23.

Table 3.23: FK-2 Core Boundary Conditions

| | |
|---------------------|--------------|
| Core power | 3 293 MWt |
| Coolant temperature | 560 K |
| Core pressure | 6.93 MPa |
| Coolant flow rate | 48.3 kT/hr |
| Inlet subcooling | 11.4 kcal/kg |

The material used for the cladding in FK-2 is Zr-2, which is defined in Table 3.24.

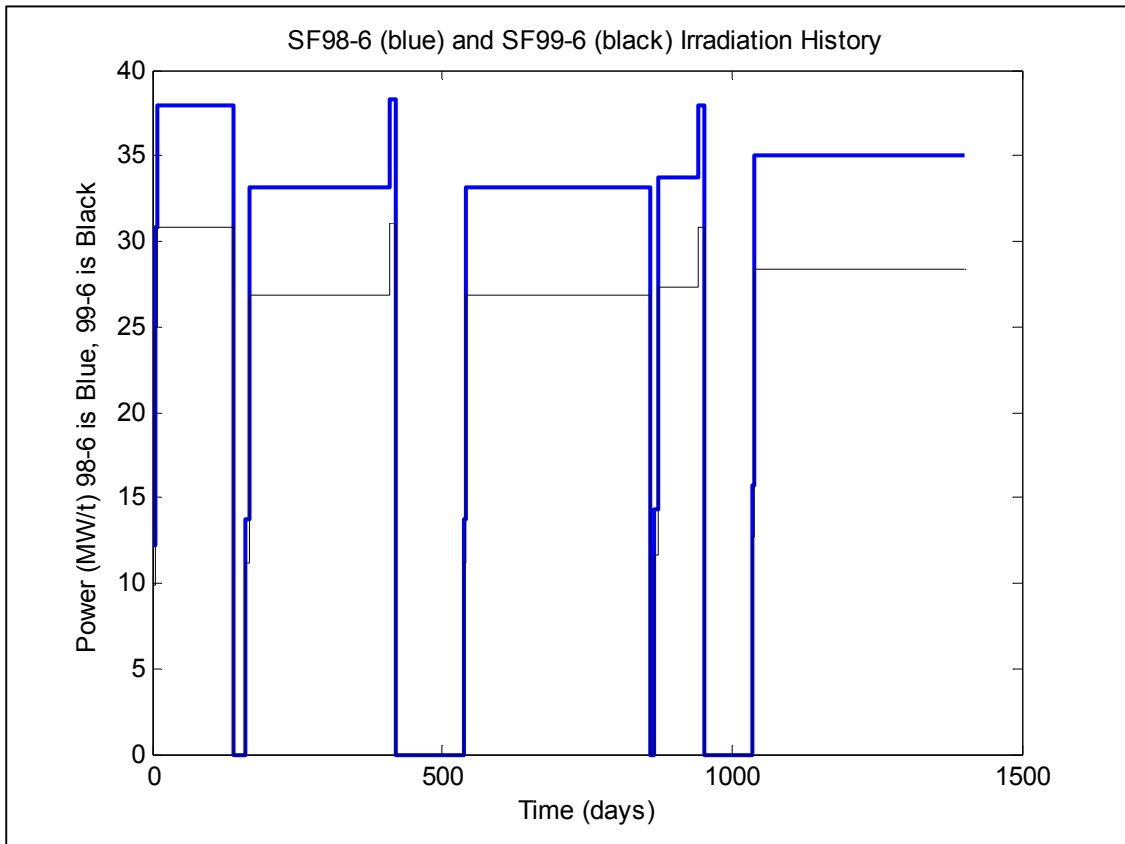
Table 3.24: FK-2 Zr-2 Cladding Composition

| Nuclide | w/o |
|---------|--------|
| O | 0.125 |
| Cr | 0.100 |
| Fe | 0.135 |
| Ni | 0.055 |
| Zr | 98.135 |
| Nb | 0.000 |
| Sn | 1.450 |

The irradiation histories for both the SF-98 and SF-99 fuel rods are provided in Table 3.25. The samples were taken at a certain axial location along the rod, and this distance is specified in Table 3.25 as the ‘mm from bottom’ of the fuel rod. There are two different values for the power given (at very similar axial locations) because they are found in two different types of fuel rods, as shown in Figure 3.14.

Table 3.25: FK-2 Irradiation History

| For PIE Sample: | | SF98-6 | SF99-6 |
|-----------------|-----------------|--------------|--------------|
| mm from bottom: | | 2050 | 2061 |
| Time (days) | Cumulative days | Power (MW/t) | Power (MW/t) |
| 0 | 0 | 0.00 | 0.00 |
| 6 | 6 | 12.21 | 9.89 |
| 3 | 9 | 30.81 | 24.97 |
| 132 | 141 | 37.98 | 30.78 |
| 21 | 162 | 0.00 | 0.00 |
| 5 | 167 | 13.76 | 11.15 |
| 244 | 411 | 33.13 | 26.85 |
| 8 | 419 | 38.36 | 31.09 |
| 117 | 536 | 0.00 | 0.00 |
| 5 | 541 | 13.76 | 11.15 |
| 317 | 858 | 33.13 | 26.85 |
| 9 | 867 | 0.00 | 0.00 |
| 4 | 871 | 14.34 | 11.62 |
| 72 | 943 | 33.71 | 27.33 |
| 10 | 953 | 37.98 | 30.78 |
| 81 | 1 034 | 0.00 | 0.00 |
| 3 | 1 037 | 15.69 | 12.72 |
| 365 | 1 402 | 35.07 | 28.42 |

Figure 3.15: FK-2 Irradiation History PlotCase 4b – Kinetics BWR experimental test problem

The case is not ready at this time and will be provided in Version 2.0 of the Specification.

Case 5a - Depletion PWR experimental test problem

Similar to the previous test case (from FK-2), this case was also a PIE performed by JAERI on an irradiated fuel assembly from the Takahama-3 (TK-3) PWR reactor.

The geometry of the TK-3 FA is shown in Figure 3.16.

Figure 3.16: TK-3 FA Pin Layout

| | | | | | | | | | | | | | | | | | |
|-----------|----------|----------|----------|----------|----------|----------|----------|----------|----------|-----------|-----------|-----------|-----------|-----------|-----------|-----------|-----------|
| | 1 | 2 | 3 | 4 | 5 | 6 | 7 | 8 | 9 | 10 | 11 | 12 | 13 | 14 | 15 | 16 | 17 |
| 1 | - | - | - | - | - | - | - | - | - | - | - | - | - | - | - | - | - |
| 2 | - | - | - | - | - | - | - | - | - | - | - | - | - | - | - | - | - |
| 3 | - | - | - | - | G | W | - | - | W | - | - | W | G | - | - | - | - |
| 4 | - | - | - | W | - | - | - | - | G | - | - | - | - | W | - | - | - |
| 5 | - | - | G | - | - | - | - | - | - | - | - | - | - | - | G | - | - |
| 6 | - | - | W | - | - | W | - | - | W | - | - | W | - | - | W | - | - |
| 7 | - | - | - | - | - | - | G | - | - | - | G | - | - | - | - | - | - |
| 8 | - | - | - | - | - | - | - | - | - | - | - | - | - | - | - | - | - |
| 9 | - | - | W | G | - | W | - | - | W | - | - | W | - | G | W | - | - |
| 10 | - | - | - | - | - | - | - | - | - | - | - | - | - | - | - | - | - |
| 11 | - | - | - | - | - | - | G | - | - | - | G | - | - | - | - | - | - |
| 12 | - | - | W | - | - | W | - | - | W | - | - | W | - | - | W | - | - |
| 13 | - | - | G | - | - | - | - | - | - | - | - | - | - | - | G | - | - |
| 14 | - | - | - | W | - | - | - | - | G | - | - | - | - | W | - | - | - |
| 15 | - | - | - | - | G | W | - | - | W | - | - | W | G | - | - | - | - |
| 16 | - | - | - | - | - | - | - | - | - | - | - | - | - | - | - | - | - |
| 17 | - | - | - | - | - | - | - | - | - | - | - | - | - | - | - | - | - |

The numbers in Figure 3.16 represent the various rods that are in the FA, and they are defined in Table 3.26.

Table 3.26: TK-3 FA Pin Descriptions

| Marker | Rod type |
|--------|---------------------------------------|
| G | 6.0 w/o Gd 2.63% ²³⁵ U pin |
| W | Control rod (water filled) |
| - | 4.11% ²³⁵ U fuel pin |
| - | SF-95 Location (NT3G23 FA) |
| G | SF-96 Location (NT3G23 FA) |

Other details about each FA are given in Table 3.27.

Table 3.27: TMI-1 FA Details

| | |
|-------------------------------|----------|
| FA pitch | 214 mm |
| Active height | 3 660 mm |
| # Water rods | 25 |
| # 6.0 w/o Gd pins | 16 |
| # 4.11% ²³⁵ U pins | 248 |
| Total rods/FA | 289 |

The physical dimensions and parameters of the fuel rods are found in Table 3.28.

Table 3.28: TK-3 Fuel, Guide, and Instrumentation Rod Dimensions and Parameters

| | |
|--------------------|----------|
| Cladding OD | 9.5 mm |
| Cladding ID | 8.2 mm |
| Cladding thickness | 0.64 mm |
| Pin pitch | 12.65 mm |
| Fuel pellet OD | 8.05 mm |
| Fuel pellet height | 9.0 mm |
| % Density | 95% TD |
| Water rod OD | 12.26 mm |
| Water rod ID | 11.46 mm |

The TK-3 core's boundary conditions define the nominal operating conditions of the entire core. They are given in Table 3.29.

Table 3.29: TK-3 Core Boundary Conditions

| | |
|---------------------|-----------|
| Core power | 2 652 MWt |
| Coolant temperature | 576 K |
| Core pressure | 16.0 MPa |
| Coolant flow rate | |

The material used for the cladding in TK-3 is Zr-4, which is defined in Table 3.29.

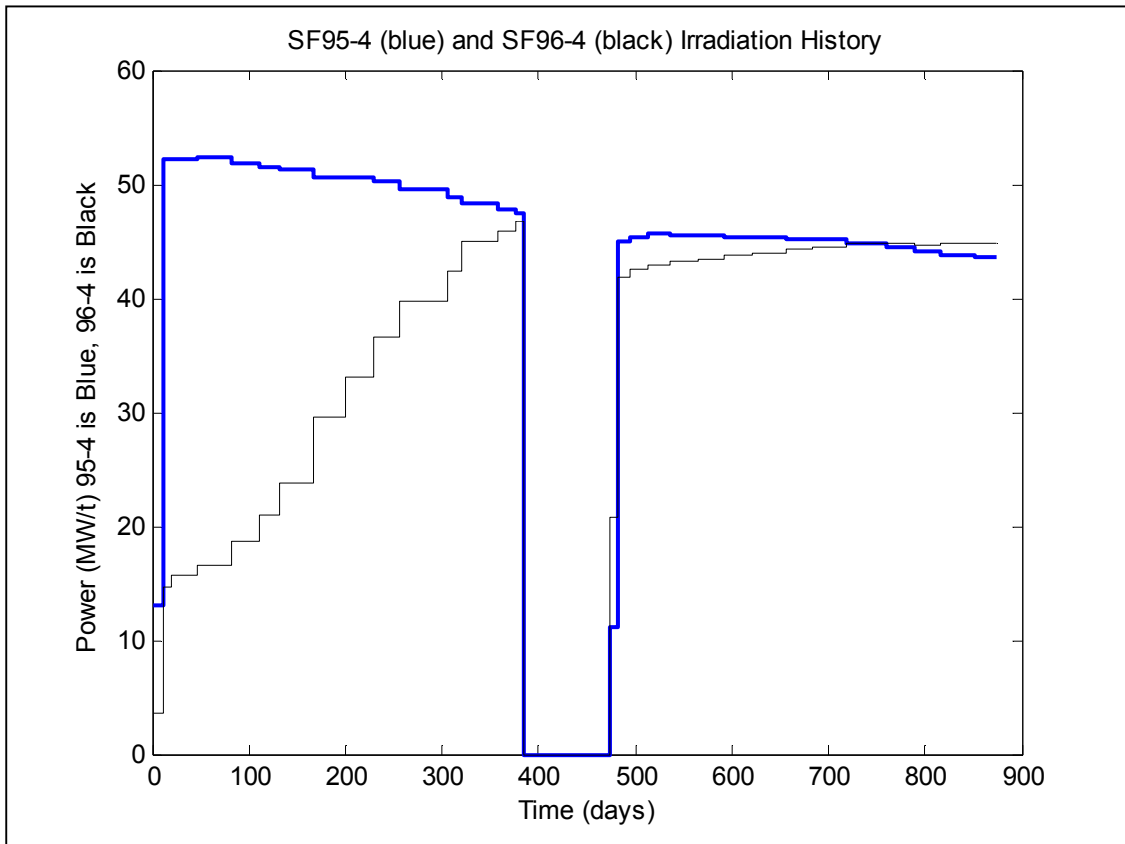
Table 3.30: TK-3 Zr-4 Cladding Composition

| Nuclide | Concentration |
|----------|---------------|
| Cr (nat) | 7.5891E-05 |
| Fe (nat) | 1.4838E-04 |
| Zr (nat) | 4.2982E-02 |

The irradiation history, shown in Table 3.31 below, gives the power experienced at specific axial locations of the two rods that were examined during the PIE. The locations of these two rods were shown previously in Figure 3.16. The two power profiles are markedly different due to the fact that sample SF95-4 (the blue line in Figure 3.17) is part of a standard fuel rod with no burnable poisons, while SF96-4 (the black line in Figure 3.17) is part of a fuel rod that contains 6.0 w/o Gd₂O₃ as well as 2.63% ²³⁵U. The BP holds the power down initially as the gadolinium slowly loses its effectiveness and then the power becomes flatter, as expected during a normal fuel rod's irradiation history.

Table 3.31: TK-3 Irradiation History

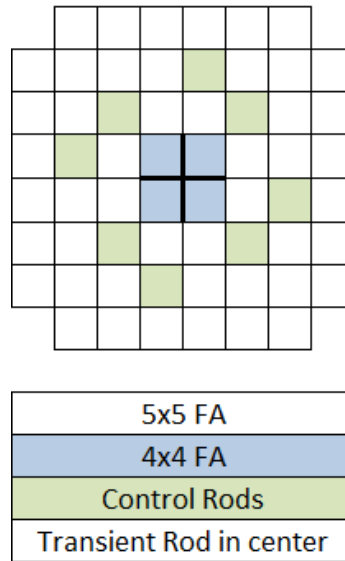
| For PIE Sample: | | SF95-4 | SF96-4 |
|-----------------|-----------------|--------------|--------------|
| mm from bottom: | | 1646 | 1671 |
| Time (days) | Cumulative days | Power (MW/t) | Power (MW/t) |
| 0 | 0 | 0.00 | 0.00 |
| 12 | 12 | 13.04 | 3.68 |
| 8 | 20 | 52.15 | 14.73 |
| 27 | 47 | 52.17 | 15.62 |
| 35 | 82 | 52.40 | 16.60 |
| 28 | 110 | 51.89 | 18.70 |
| 21 | 131 | 51.57 | 20.93 |
| 35 | 166 | 51.37 | 23.71 |
| 35 | 201 | 50.58 | 29.57 |
| 28 | 229 | 50.61 | 33.02 |
| 27 | 256 | 50.31 | 36.50 |
| 49 | 305 | 49.60 | 39.72 |
| 15 | 320 | 48.93 | 42.37 |
| 37 | 357 | 48.26 | 44.99 |
| 19 | 376 | 47.77 | 45.79 |
| 9 | 385 | 47.48 | 46.76 |
| 88 | 473 | 0.00 | 0.00 |
| 10 | 483 | 11.19 | 20.83 |
| 11 | 494 | 44.97 | 41.92 |
| 20 | 514 | 45.41 | 42.48 |
| 23 | 537 | 45.62 | 42.93 |
| 28 | 565 | 45.55 | 43.18 |
| 28 | 593 | 45.46 | 43.43 |
| 28 | 621 | 45.37 | 43.71 |
| 35 | 656 | 45.29 | 43.99 |
| 28 | 684 | 45.20 | 44.24 |
| 34 | 718 | 45.09 | 44.46 |
| 43 | 761 | 44.91 | 44.74 |
| 28 | 789 | 44.49 | 44.74 |
| 28 | 817 | 44.06 | 44.66 |
| 35 | 852 | 43.82 | 44.76 |
| 15 | 867 | 43.63 | 44.81 |
| 8 | 875 | 43.56 | 44.83 |

Figure 3.17: TK-3 Irradiation History PlotCase 5b – Kinetics PWR experimental test problem

This case comes from the SPERT III Reactor with the E-core revision, which contains 60 fuel assemblies in PWR-like conditions. The experiments performed at this reactor were reactivity insertions and then the peak power and energy released were measured. The reactivity is controlled with a central, cruciform transient rod that contains boron. There are also 4 linked sets of control rods (which take up the place of 8 fuel assemblies) in the core.

Experimental errors for this reactor are 17% for the power and energy measurements, and \$0.04 for the reactivity of the core.

The geometry of the SPERT III E-core is shown in Figure 3.18.

Figure 3.18: SPERT III E-core Geometry

There are 48 of the 5x5 FAs in the core, each is 76.2 mm wide. There are 4 of the 4x4 FAs in the core, each is 63.5 mm wide. There are 8 control rod FAs in the core, and each has two sections. The upper section is 1.35 w/o B10 in a box shape. This box is 63.40 mm wide with a wall thickness of 4.72 mm. The height of the upper poison section is 1168.4 mm. The lower section is the same as the fuel found in the 4x4 assembly, and with a height of 1159.3 mm. The dimensions of the various parameters needed to define the geometry of the fuel assemblies are given below in Table 3.32.

Table 3.32: SPERT III E-core Dimensions

| | |
|--------------------|------------------------|
| Cladding OD | 11.84 mm |
| Cladding ID | 10.82 mm |
| Cladding thickness | 0.508 mm |
| Pin pitch | 14.86 mm |
| Fuel pellet OD | 10.67 mm |
| Fuel pellet height | 12.98 mm |
| Pellet density | 10.5 g/cm ³ |

The central transient rod is also split into two sections; the upper section is made of 18-8 SS and is 1422.4 mm in length. The lower section, or the absorber section, is 965.2 mm long and made of 1.35 w/o B10. The cruciform blade has a thickness of 4.76 mm and the total width is 130.175 mm.

The initial conditions of the core under which the experiments were originally performed are shown in Table 3.33. The core was at 'cold startup' for this case, which means that the initial power was low and so was the inlet temperature.

Table 3.33: SPERT III E-core Initial Conditions

| | |
|---------------------|-----------|
| Core power | 50 W |
| Coolant temperature | 299 K |
| Core pressure | 0.101 MPa |
| Coolant flow rate | 0 kg/s |

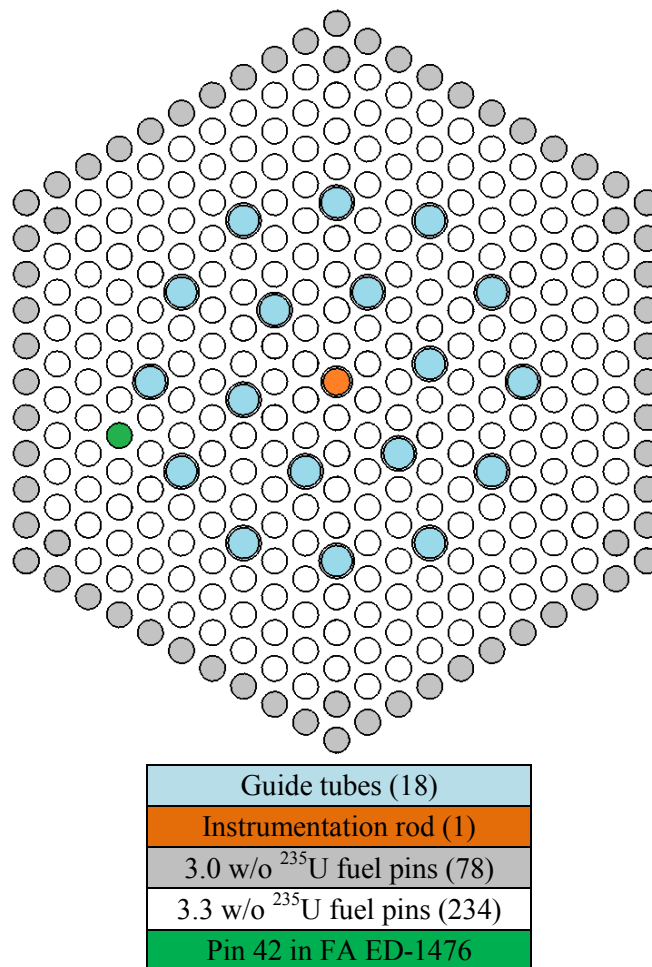
The reactivity incident in this case is modelled on case #43 which was run at the SPERT facility in the 1960s. For this case, the reactor is set to have a period of 10.0 ms and the inserted reactivity is equal to β . The peak power occurs in a relatively short time after this reactivity is initiated.

Case 6a – Depletion VVER experimental test problem

This test case is based on data from an ORNL PIE performed on an irradiated VVER-1000 reactor, using fuel assembly ED-1476 as the experimental data source. The irradiation occurred over three cycles, each about 10-12 months in duration.

The geometry of the VVER-1000 FA is shown in Figure 3.19:

Figure 3.19: VVER-1000 FA Pin Layout



Pin 42 is marked (in green) because it is the location of the PIE analysis. It is the only pin for which the nuclide concentrations were reported and therefore it will be used in comparison with the calculated results. Other details about each FA are given in Table 3.34.

Table 3.34: VVER-1000 FA Details

| | |
|---------------------|----------|
| FA pitch | 236.0 mm |
| Active height | 3 550 mm |
| # Water rods | 1 |
| # Guide tubes | 18 |
| # 3.6 w/o fuel pins | 66 |
| # 4.4 w/o fuel pins | 246 |
| Total rods/FA | 331 |

The physical dimensions and parameters of the fuel rods are found in Table 3.35.

Table 3.35: VVER-1000 Fuel Rod Dimensions and Parameters

| | |
|------------------------|----------|
| Cladding OD | 9.16 mm |
| Cladding ID | 7.72 mm |
| Cladding thickness | 0.72 mm |
| Pin pitch | 12.75 mm |
| Fuel pellet OD | 7.55 mm |
| Fuel pellet ID | 2.30 mm |
| Fuel pellet height | 9.1 mm |
| % Density | 95% TD |
| Guide tube OD | 12.65 mm |
| Guide tube ID | 10.90 mm |
| Instrumentation rod OD | 11.25 mm |
| Instrumentation rod ID | 9.60 mm |

The VVER-1000 core's boundary conditions define the nominal operating conditions of the entire core. They are given in Table 3.36.

Table 3.36: VVER-1000 Core Boundary Conditions

| | |
|---------------------|-------------|
| Core power | 3 000 MWt |
| Coolant temperature | 575 K |
| Core pressure | 15.7 MPa |
| Coolant flow rate | 17 611 kg/s |

The material used for the cladding in VVER-1000 is Zr+1% Nb, which is defined in Table 3.37.

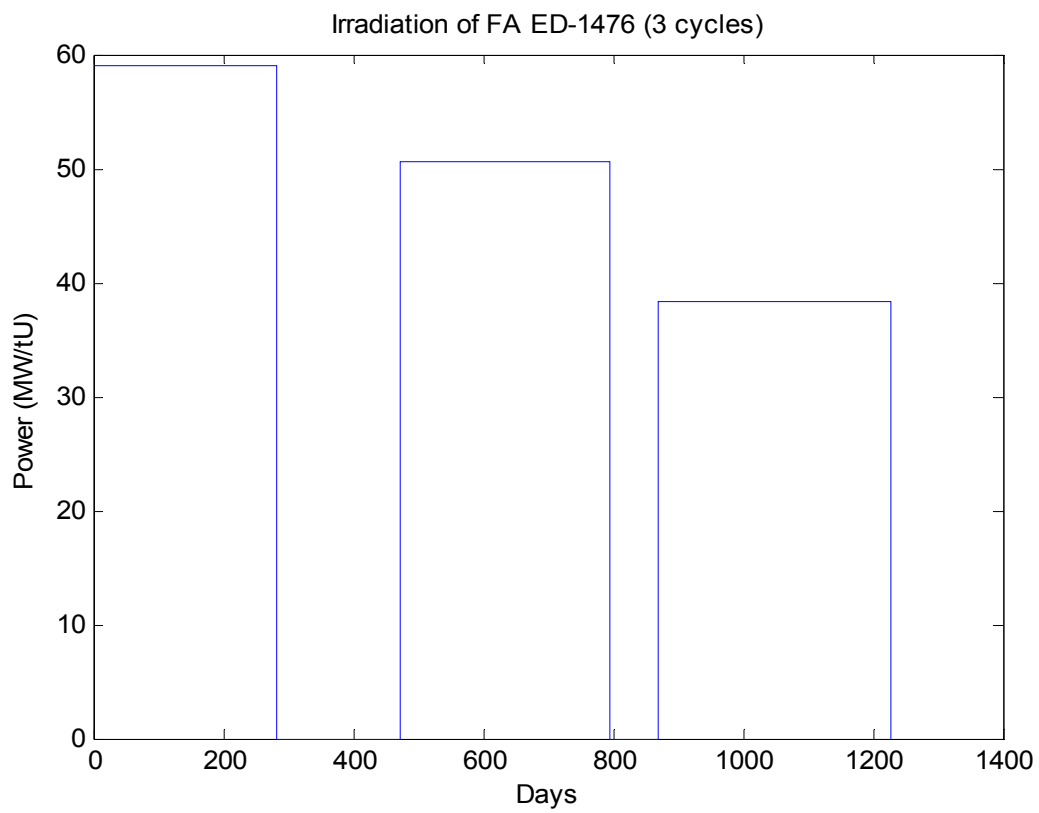
Table 3.37: VVER-1000 Zr+1% Nb Cladding Composition

| Nuclide | w/o |
|---------|--------|
| Zr | 98.991 |
| Fe | 0.009 |
| Nb | 1.000 |

The irradiation is assumed to be three cycles of constant power with two periods of decay in between. This is illustrated in Table 3.38 and Figure 3.20. The power is assumed to be the average power of the fuel assembly over the time period of depletion.

Table 3.38: VVER-1000 Irradiation History

| Time (days) | Cumulative days | Power (MW/t) |
|-------------|-----------------|--------------|
| 283 | 283 | 58.96 |
| 189 | 472 | 0.00 |
| 322 | 794 | 50.53 |
| 79 | 873 | 0.00 |
| 359 | 1 232 | 38.28 |

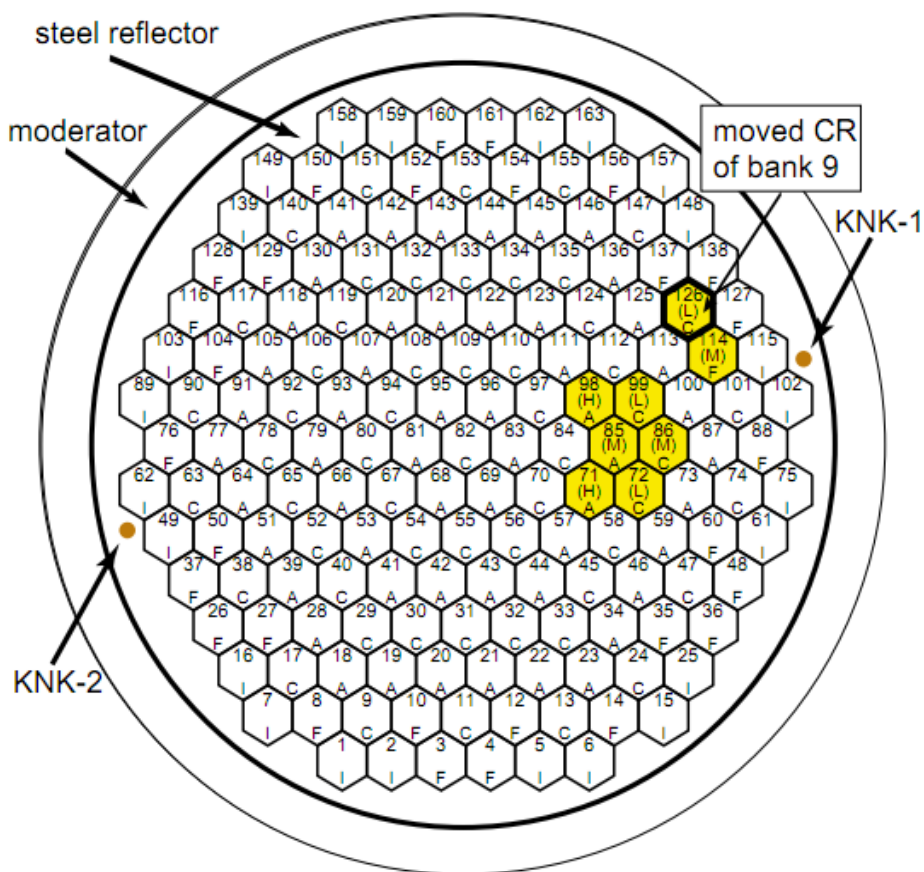
Figure 3.20: VVER-1000 Irradiation History Plot

Case 6b: Kinetic VVER experimental test problem

This test case, performed with a VVER-1000 fuel assembly, is based on an experiment at the V-1000 facility in Moscow. The core is a full-sized VVER-1000 core with 163 assemblies at a 236.0 mm pitch. The core and the fuel assembly in which the control rod transient occurs are shown in Figure 3.21. There is one fuel assembly in which the control rods will be inserted and then withdrawn over a short period of time. This causes a large change in the reactivity and this scenario will be analysed in this test case.

This particular core contains several profiled FAs which contain fuel rods of two different enrichments, as well as flat FAs in which all the fuel rods are of the same enrichment. The geometry of the entire core is shown in Figure 3.22, with the different types of FAs distinguished by the letters ‘A’ through ‘I’, and the control rod groups specified by roman numerals I through X underneath the FA type (if there are control rods for that particular assembly).

Figure 3.21: VVER-1000 Core Based on the V-1000 Facility



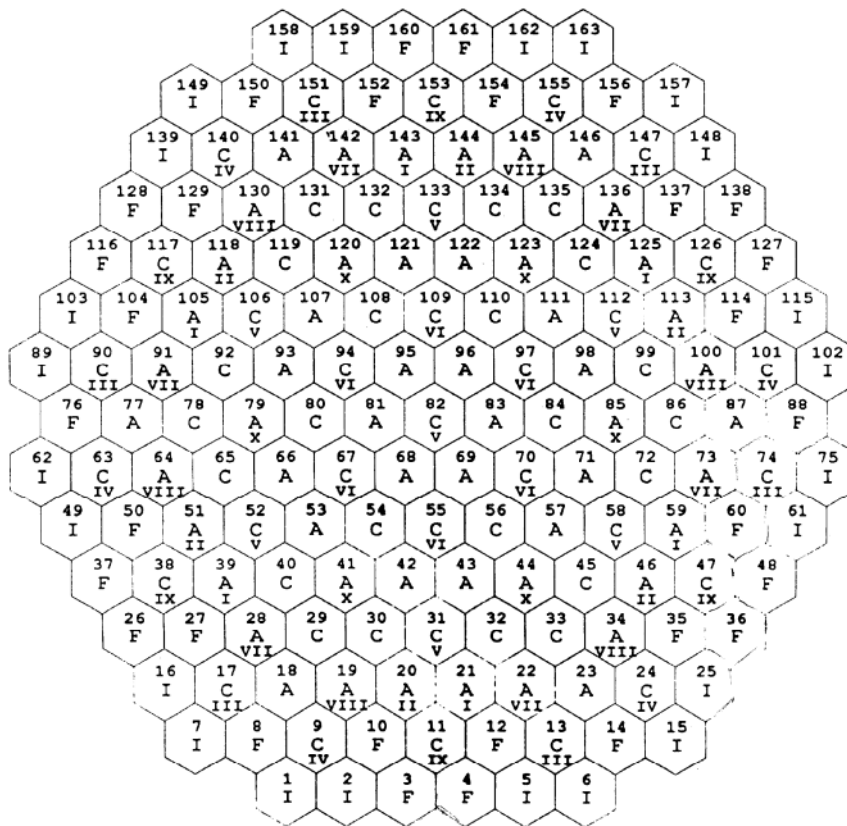
Enrichments of U-235:

A - 1.6 %

F - 4.4% + 3.3%

C - 3.0%

I - 4.4%

Figure 3.22: V-1000 Core Fuel Assemblies

The fuel assemblies shown in Figure 3.23 are defined by Table 3.39, which gives the enrichments of the fuel rods based on the indicator shown in the above figure.

Table 3.39: V-1000 Core Fuel Assemblies Defined

| Indicator | Type | Enrichment | #/Core |
|-----------|----------|------------|--------|
| A | Flat | 1.6/1.6 | 54 |
| C | Flat | 3.0/3.0 | 55 |
| F | Profiled | 4.4/3.6 | 30 |
| I | Flat | 4.4/4.4 | 24 |

If the assembly is profiled (such as assembly type F in Table 3.39) then there are 78 fuel pins that mostly line the outside of the FA of the lower enrichment, and then the remaining fuel pins (234 of them) are of the higher enrichment, as shown in Figure 3.24. These are shown as either gray (the lower enrichment of the profiled assembly) or white (the higher enrichment) below. All of the fuel assemblies in this core have the same geometry for the 18 guide tubes and the central rod.

Figure 3.23: VVER-1000 Profiled Fuel Assembly

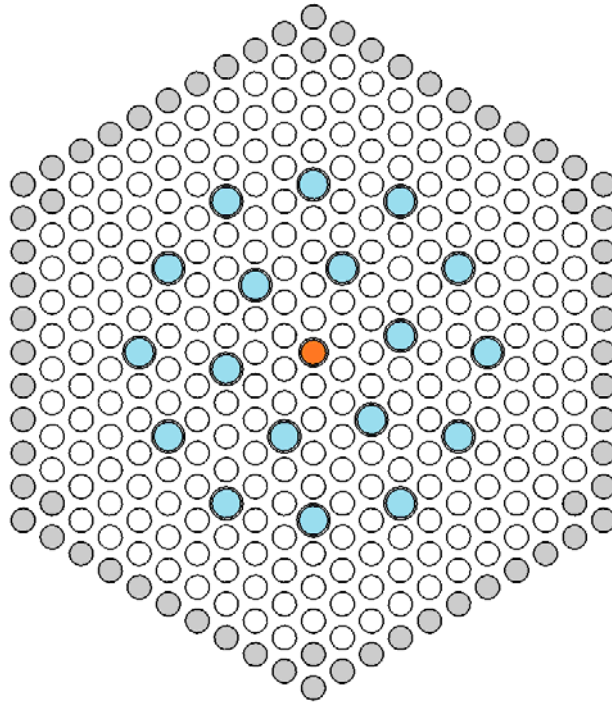
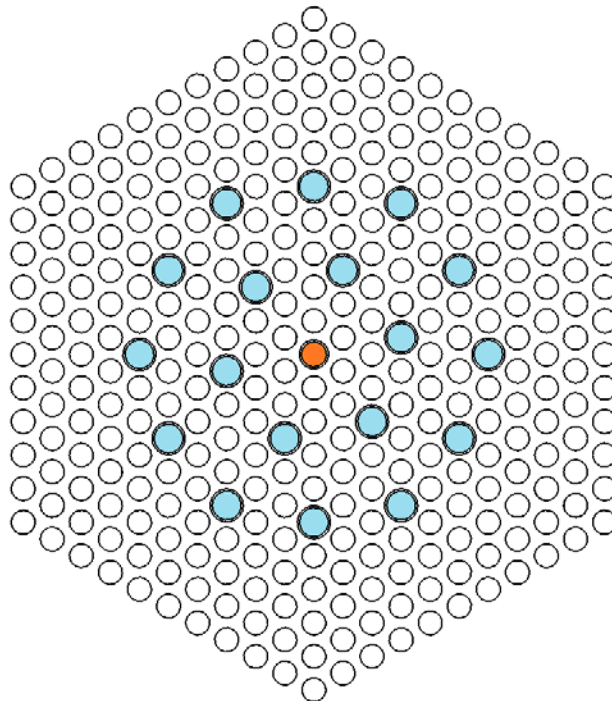


Figure 3.24: VVER-1000 Flat Fuel Assembly



The fuel assemblies are all set at a pitch of 236 mm within the core. The other dimensions important to this case are given in Tables 3.40 and 3.41.

Table 3.40: V-1000 Fuel Assembly Specifications

| | |
|---------------|----------|
| FA pitch | 236.0 mm |
| Active height | 3 530 mm |
| # Water rods | 1 |
| # Guide tubes | 18 |
| # Fuel pins | 312 |
| Total rods/FA | 331 |

Table 3.41: V-1000 Fuel Rod Dimensions and Parameters

| | |
|--------------------|----------|
| Cladding OD | 9.17 mm |
| Cladding ID | 7.79 mm |
| Cladding thickness | 0.69 mm |
| Pin pitch | 12.75 mm |
| Fuel pellet OD | 7.55 mm |
| Fuel pellet ID | 2.30 mm |
| Fuel pellet height | 9.1 mm |
| % Density | 95% TD |
| Guide tube OD | 12.65 mm |
| Guide tube ID | 10.90 mm |
| Central rod OD | 10.30 mm |
| Central rod ID | 9.00 mm |

There are 14 spacer grids evenly spaced axially every 235 mm along the fuel assemblies. Each has a height of 200 mm and a mass of 654 grams. The guide tubes as well as the spacer grids are made of stainless steel as defined in Table 3.43. The fuel rod cladding is made of zircalloy, as defined below in Table 3.42.

Table 3.42: V-1000 Zircalloy Composition

| Nuclide | w/o |
|---------|-------|
| Zr | 98.97 |
| Nb | 1.00 |
| Hf | 0.03 |

Table 3.43: V-1000 Stainless Steel Composition

| Nuclide | w/o |
|---------|-------|
| C | 0.12 |
| Cr | 18.50 |
| Ni | 10.50 |
| Ti | 1.00 |
| Fe | 69.88 |

The moderator of the V-1000 is boric acid in water, at a concentration of 8.74 grams per liter. The critical level of the moderator in the core is provided as 324 cm. The moderator temperature is 291.8 K. There is also an initial excess reactivity of $0.035 \beta_{\text{eff}}$.

The control rod movement transient consists of two motions. The control rods are inserted and then held in place for some time until they are withdrawn completely. The control rod positions are given in centimeters, where the fully withdrawn position is equal to 324.0 cm and the fully inserted position is equal to 0.0 cm. The positions and velocities of the control rods for the insertion portion (time from 0 to 100 seconds) are shown in Table 3.44. The period of time from $t = 100$ seconds until the rods are withdrawn from the core (at approximately $t = 800$ seconds) involves no motion of the control rods. The data are broken down into two tables in order to remove the trivial time steps.

Table 3.44: Control Rod Positions and Velocities for the insertion portion

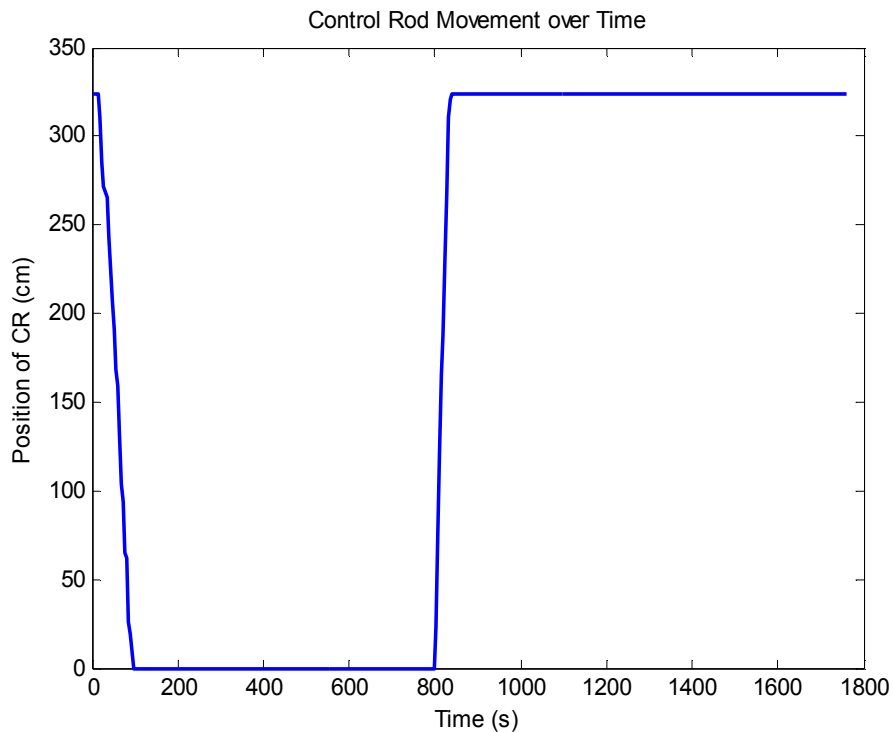
| Time (s) | CR Position (cm) | CR Velocity (cm/s) |
|----------|------------------|--------------------|
| 2.03 | 324.00 | 0.000 |
| 6.52 | 324.00 | 0.000 |
| 10.99 | 324.00 | 0.000 |
| 15.46 | 324.00 | -2.912 |
| 19.91 | 311.04 | -5.799 |
| 24.38 | 285.12 | -2.906 |
| 28.84 | 272.16 | -1.453 |
| 33.30 | 265.68 | -5.097 |
| 37.75 | 243.00 | -4.359 |
| 42.21 | 223.56 | -3.632 |
| 46.67 | 207.36 | -3.640 |
| 51.12 | 191.16 | -5.085 |
| 55.58 | 168.48 | -2.175 |
| 60.05 | 158.76 | -5.799 |
| 64.52 | 132.84 | -6.553 |
| 68.97 | 103.68 | -2.179 |
| 73.43 | 93.96 | -6.582 |
| 77.86 | 64.80 | -0.728 |
| 82.31 | 61.56 | -8.063 |
| 86.73 | 25.92 | -1.476 |
| 91.12 | 19.44 | -4.418 |
| 95.52 | 0.00 | 0.000 |
| 99.91 | 0.00 | 0.000 |

The time from 100 to 800 seconds involves no motion; the control rods are stationary at the 0.00 cm position. The remaining transient time steps are shown in Table 3.45.

Table 3.45: Control Rod Positions and Velocities for times of the withdrawal portion

| Time (s) | CR Position (cm) | CR Velocity (cm/s) |
|----------|------------------|--------------------|
| 793.92 | 0.00 | 0.000 |
| 798.15 | 0.00 | 5.362 |
| 802.38 | 22.68 | 13.052 |
| 806.60 | 77.76 | 9.934 |
| 810.84 | 119.88 | 10.749 |
| 815.06 | 165.24 | 5.324 |
| 819.32 | 187.92 | 9.981 |
| 823.54 | 230.04 | 9.084 |
| 827.82 | 268.92 | 9.773 |
| 832.13 | 311.04 | 2.266 |
| 836.42 | 320.76 | 0.757 |
| 840.70 | 324.00 | 0.000 |
| 844.99 | 324.00 | 0.000 |
| 849.27 | 324.00 | 0.000 |
| 853.56 | 324.00 | 0.000 |

These control rod positions are more easily visualised in Figure 3.25

Figure 3.25: V-1000 Transient Control Rod Movement versus Time

Chapter 4: Definition of Exercise II-3: Bundle thermal-hydraulics

This exercise will address the uncertainties in fuel bundle thermal-hydraulic analysis and safety evaluation. While Exercise II-1 determines the uncertainty in fuel temperature prediction (which is related to the Doppler feedback prediction), Exercise II-3 determines uncertainty in predicting moderator parameters, which are related to moderator feedback prediction. This exercise will model a fuel assembly bundle under either steady-state or transient conditions, instead of just a single fuel pin as found in Exercise II-1. These parameters cover values such as the moderator temperature, moderator density, and the void fraction. Uncertainty in this exercise can arise from:

- operational uncertainties;
- geometry uncertainties;
- modelling uncertainties;
- code uncertainties.

There is a complex two-phase flow across the bundle that requires special attention to correlations and other equations used by the codes. Accurate representations of the thermal hydraulics and moderator parameters are important because they provide a basis for the safety analysis of this section of the reactor.

The thermal-hydraulic uncertainties are important in reactor modelling because they can strongly affect many parameters that are included in the design and safety analysis such as fuel temperature and the coolant void fraction. Some of these input parameters will have more of an effect on the propagated parameters than others and this exercise will provide a way to quantise these amounts. Codes can then be fine-tuned in order to reduce the error in modelling with respect to the thermal-hydraulic aspect of the calculations.

To determine the effects of the input uncertainties on the moderator parameters the users are advised to run through the exercise using their own thermal-hydraulic codes and analyses. The importance and propagation of these effects can be measured and ranked as a benchmark for accuracy in thermal-hydraulic modelling. Details of how the input uncertainties can affect the output and propagated uncertainties are explained below.

These effects differ greatly from the various types of reactors due to geometry changes such as the types of spacer grids in a BWR versus those in a PWR as well as the fact that the core operating conditions of each are very different. The best way to analyse this is to utilise test cases that are adapted to each type of reactor as well as representative of various types of thermal-hydraulic scenarios. This leads to the 12 test cases found later in this chapter. The exercises in this chapter include both steady-state and transient scenarios that cover BWR, PWR, and VVER bundle thermal-hydraulics. The cases will provide a method for measuring the associated uncertainty with the numerous inputs and calculations required to simulate the tests. There will be numerical cases representative of the Peach Bottom Unit 2 (BWR), Three Mile Island Unit 1 (PWR), and Kozloduy Unit 6 (VVER-1000) reactors as well as experimental cases that are similar in geometry to the fuel assemblies of these reactors. The experimental cases come from previously performed experiments with detailed results such as the measured void fraction and DNBR under various core conditions. These experiments often occurred at integral facilities which may be scaled-down versions of normal fuel assemblies in order to facilitate experimental procedures, but the properties can still be adapted to fit the reactors of interest.

4.1 Discussion of input, target and output uncertainties

There are many Input (I) uncertainties in this exercise due to the complex geometry of the components and materials in the fuel assembly bundles and the potential uncertainties in all of its dimensions and also due to other factors that arise during the code's calculations. The main sources of uncertainty are grouped into the following categories: operational, geometry, modelling, and code uncertainties.

The propagated (U) and Output (O) uncertainties for this exercise are the void fraction and DNB measurements at various locations along the bundle. If it is a transient case with multiple time steps, then these values will be tracked at certain axial locations for the time steps. For experimental test problems the measurement errors are also provided.

The sources input uncertainties for Exercise II-3 are discussed below along with values and PDFs to be used in uncertainty analysis. The operating conditions, such as the reactor power and coolant flow rate, vary over time and thus, have associated uncertainties. These boundary conditions often depend on each other so monitoring them during experimental procedures becomes important. Deviations in these values come from inaccuracies in measurements as well as natural cycles in the reactor. These can also be called the boundary condition effects, as they are used to define the main operating conditions of the core. These variations are small during steady-state conditions but still carry some uncertainties that will propagate to the output and propagated parameters. The values given in Table 4.1 are to be used as the estimated accuracy of the operational parameters, as found in the BFBT and PSBT specifications. The PDF is the assumed distribution function for each parameter.

Table 4.1: Exercise II-3 Core Boundary Condition Uncertainties

| Parameter | BWR | PWR | VVER | PDF |
|-------------------------|-------------|-------------|-------------|------------|
| System pressure | $\pm 1.0\%$ | $\pm 1.0\%$ | $\pm 2.0\%$ | Normal |
| Flow | $\pm 1.0\%$ | $\pm 1.5\%$ | $\pm 4.5\%$ | Normal |
| Power | $\pm 1.5\%$ | $\pm 1.0\%$ | $\pm 0.3\%$ | Normal |
| Inlet fluid temperature | ± 1.5 K | ± 1.0 K | ± 2.0 K | Uniform |

The geometry, which includes the various dimensions and the layout of the bundle and core, affects the way coolant flows as well as other parameters pertinent to this exercise. The components of the bundle, such as the fuel rods and channel spacers, carry some uncertainties in their manufactured tolerances, which were studied in Chapter 2. The outer cladding diameters as well as the surface roughness of the cladding are some of the tolerances from the fuel rod that should be considered since the coolant flow is exposed to this portion of the rod. The rod pitch and the spacer grid locations can also cause differences in calculations. Variations in the dimensions of the spacer grids can have an effect on the loss coefficient of the grid as well as an effect on the flow of the fluid along the bundle. It is important to take the dimensions of the grids into account when performing a thermal-hydraulic analysis of the fuel assembly in the reactor core. For the three types of reactors examined in this bundle, the geometry (manufacturing) tolerances for the bundle are shown in Table 4.2. The heated rods correspond to fuel rods (electrically heated rods are commonly used at bundle test facilities).

The effects of these tolerances are important to quantify because tolerances are built into everything that is manufactured and there is almost no way to eliminate this uncertainty from a nuclear reactor. Other uncertainties can actually be improved but the manufacturing uncertainties are accepted as inherent and fixed.

There is also the physical distortion of the bundle or the test assembly that occurs when the system is in operation due to heat that causes thermal expansion of the various components. This distortion can also be affected by the geometry and dimension of the spacer grids which makes for a complex arrangement in determining the magnitude of the distortion. The distortion will not be analysed in this exercise.

Table 4.2: Exercise II-3 Geometry Uncertainties

| Parameter | BWR | PDF/BWR | PWR | PDF/PWR | VVER | PDF/VVER |
|---------------------------|----------|---------|----------|---------|----------|----------|
| Heated rod diameter | ±0.04 mm | Normal | ±0.02 mm | Normal | ±0.10 mm | Uniform |
| Heated rod displacement | ±0.45 mm | Normal | ±0.45 mm | Normal | ±0.45 mm | Uniform |
| Flow channel inner width | ±0.05 mm | Normal | - | - | - | - |
| Flow channel displacement | ±0.20 mm | Normal | ±0.20 mm | Normal | ±0.20 mm | Uniform |
| Power distribution | ±3 % | Normal | ±3 % | Normal | ±3 % | Normal |

The system will lose some accuracies as it is simplified in order to be used as code input, since it is difficult and impractical to exactly model every detail of the reactor or bundle exactly as it is. In transient scenarios the time history of the various input parameters (such as inlet temperature and pressure) must be discretised to various time steps and the number of time steps selected can have a large impact on the overall accuracy of the model. Even in steady-state cases, some homogenisation is assumed in order to make the bundle easier to simulate using a computer code.

The axial power distribution of the fuel rods must be nodalised in order to be represented in the code and this means truncating the actual power distribution down to a smaller number of nodes. If more nodes are used, the accuracy can be increased up to a certain limit where the small distance between nodes will not be valid for calculations and thus will increase error in the calculations. Often a cosine shape is assumed for the power distribution when in an actual reactor the shape is not so simple. This has an effect on the propagated parameters but it is difficult to measure because accurate representations of the axial power shape are difficult to use as input.

The radial power distribution of the pins within the assembly is also difficult to determine since there are many pins for some assemblies such as the TMI-1 fuel assemblies and the relative power of these pins is not a simple pattern. These pin powers are also strongly affected by the burn-up of the assembly as well as the location of gadolinium or other BP pins in the assembly.

Also of importance is measurement accuracy especially for comparisons in the experimental test cases. The void fraction and DNB are measured with equipment that has some inherent uncertainty. The estimated values for the void fraction measurements are shown for PWR in Table 4.3a (as found in the PSBT Specification) and for BWR in Table 3.4b (as found in the PSBT Specification).

Table 4.3a: Estimated Accuracy for Void Fraction Measurements in PWR

| Quantity | Accuracy |
|------------------------------------|----------|
| Void fraction measurement | |
| CT measurement | |
| Gamma-ray beam width | 1 mm |
| Subchannel averaged (steady-state) | 3% void |
| Spatial resolution of one pixel | 0.5 mm |
| Chordal measurement | |
| Gamma-ray beam width (center) | 3 mm |
| Gamma-ray beam width (side) | 2 mm |
| Subchannel averaged (steady-state) | 4% void |
| Subchannel averaged (transient) | 5% void |

Table 4.3b: Estimated Accuracy for Void Fraction Measurements in BWR

| Quantity | Accuracy |
|-------------------------------|-----------------|
| X-ray CT scanner | |
| Local void fraction | 8% |
| Sub-channel void fraction | 3% |
| Cross-sectional void fraction | 2% |
| Spatial resolution | 0.3 mm × 0.3 mm |
| Scanning time | 15 seconds |
| X-ray densitometer | |
| Sampling time | Max. 60 seconds |

The accuracy of the measurement varies with the type of scenario (steady-state or transient) as well as the type of measurement. Since these are not input uncertainties they will not be used to determine the effect on the propagated parameters, rather they are used directly to compare the output and propagated uncertainties in void fraction and DNB predictions with the measurement uncertainties for the experimental test cases. Measurements are also made at certain locations so the axial distribution of the void fraction, for example, may be an interpolated plot that relies on upper and lower measurements. This is very difficult to improve without the installation of a continuous way to measure void and DNB along a bundle. Comparing computed code results to inaccurate experimental results is not the most desirable objective, but given the limited availability of measured data and results, they are still close enough to help benchmark the codes.

The use of computer codes for analysis of the thermal-hydraulics of a reactor requires a very complex code that is capable of generating many different intermediate values used in the calculations. These values are almost always based on approximations that are determined from interpolations of known data. The correlations are mostly valid over a range of temperatures but lose accuracy near either side of these ranges. The time steps used by the code are another important factor, since too large steps during a transient scenario can leave out lots of information while too small steps can challenge the code computationally. The subroutines that calculate the intermediate parameters such as temperature in the fluid have some rounding errors that propagate through following calculations. The time steps are not altered during this exercise, but they would make a good extra project based on the test cases here.

The code uncertainties should be determined by the users to change in their own codes. For example, uncertainties in fluid conductivity correlation could be assumed to follow normal distribution within + or – 2% from its typical value. The users should be able to modify their own codes in order to reflect these changes and then run each case with the modified values. The changes made by the users should be noted in the results.

As has been previously discussed, there are various groups of uncertainties that can affect the desired output values of the void and DNB distribution. The parameters that have the largest effect are the most important to study due to their significance on the results of the test cases. The boundary condition effects are expected to be important with variations in the coolant mass flow rate and the power. Of the geometry effects, those with the largest anticipated importance are the Sub-channel area and the heated perimeter. The model parameters are built into the codes and are grouped under code uncertainties; the important ones are the mixing coefficient and the equilibrium distribution weighting factor in the void drift. Another code uncertainty with large expected effects on the void and DNB distribution is the interfacial friction factor. The uncertainty in these parameters can vary with manufacturing tolerances so it is important to take into account the effects on each of the propagated and output parameters by performing the selected test cases.

4.2 Test Problems

For this chapter the test cases are selected to provide exercises that cover both steady-state and transient scenarios for each of the LWR types - BWR, PWR, and VVER. For Exercise II-3 (Fuel bundle thermal-hydraulics), measured data are available for the BWR bundle type (from the OECD/NRC BFBT benchmark), and for the PWR bundle (from the OECD/NRC PSBT benchmark). Some of the VVER-1000 data will be taken from the VVER-1000 Coolant Transient Benchmark (OECD V1000CT benchmark).

There will be numerical cases which are adapted to match the dimensions and conditions of PB-2, TMI-1, and Kozloduy-6, as well as experimental cases, which give a benchmark for actual data that have been taken during bundle tests performed at research facilities and operational reactors. These thermal-hydraulic bundle tests can be performed on a variety of codes and the users are asked to model each case using the parameters defined in the following sections.

Each test case will ask for the user to adjust certain parameters in order to complete a sensitivity analysis. The input parameters to be varied are the core boundary conditions, which include:

- core power;
- core pressure;
- coolant flow rate;
- coolant inlet temperature.

The geometry parameters that are varied are:

- fuel rod outer diameter;
- fuel rod displacement;
- flow channel inner width (if applicable);
- flow channel displacement (if applicable);
- power distribution (of pins).

The transient cases will request results at various time steps during the scenario, while the steady-state cases will have their calculations performed at a single time.

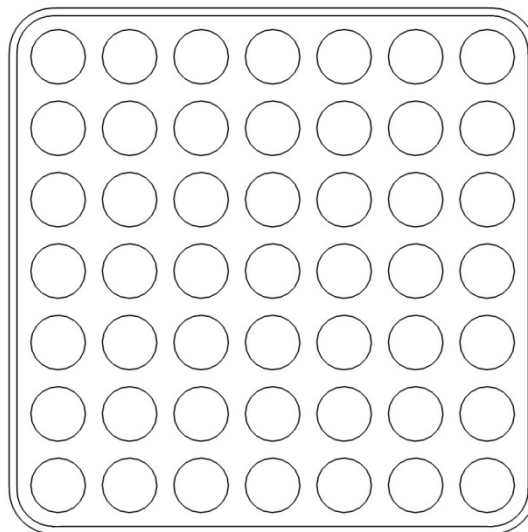
The code parameters to be varied by the user are left up to the user to decide; some suggestions would be thermal conductivities and parameters within heat transfer correlations. For the steady-state cases (Cases 1a-6a) the users are asked to report the void fraction and its associated uncertainty at each node. For the transient cases (Cases 1b-6b) the users are asked to provide the void fraction at various time steps during the scenario. The templates for these results are provided in Chapter 5 of this report.

Case 1a – Steady-state BWR numerical test problem

This numerical case is partially modelled on the BTBT Benchmark cases and modified in order to fit the dimensions of a fuel assembly bundle from the Peach Bottom Unit 2 plant. Each of the steady-state cases in this exercise is a single bundle with given boundary conditions to be used as input in the users' codes. The geometry of this BWR case is specified below, starting with the important dimensions of Table 4.4 and Figure 4.1.

Table 4.4: PB-2 Bundle Geometry

| Geometry | Value |
|--|--------------|
| Rod array | 7 x7 |
| Number of fuel rods | 49 |
| Number of fuel rods with 3.0 w/o Gd2O3 | 4 |
| Number of thimble rods | 0 |
| Fuel rod OD | 14.30 mm |
| Fuel rod pitch | 18.75 mm |
| Fuel rod length | 3657.6 mm |
| Flow channel inner width | 134.09 mm |
| Number of MV spacers | 7 |
| Number of NMV spacers | 0 |

Figure 4.1: PB-2 Bundle Image

The core boundary conditions are provided in Table 4.5.

Table 4.5: PB-2 Bundle Boundary Conditions

| Core conditions | Value |
|---------------------------|-------------|
| Reactor power | 3 293 MWt |
| Core pressure | 7.0 MPa |
| Coolant inlet temperature | 543 K |
| Coolant flow rate | 12 900 kg/s |

The locations of the spacer grids along the bundle are provided below. The types are also indicated in Table 4.6. MV stands for ‘mixing vane’ and NMV is ‘non-mixing vane’ in reference to the type of grids used in the bundle. All locations are measured from the bottom of the bundle.

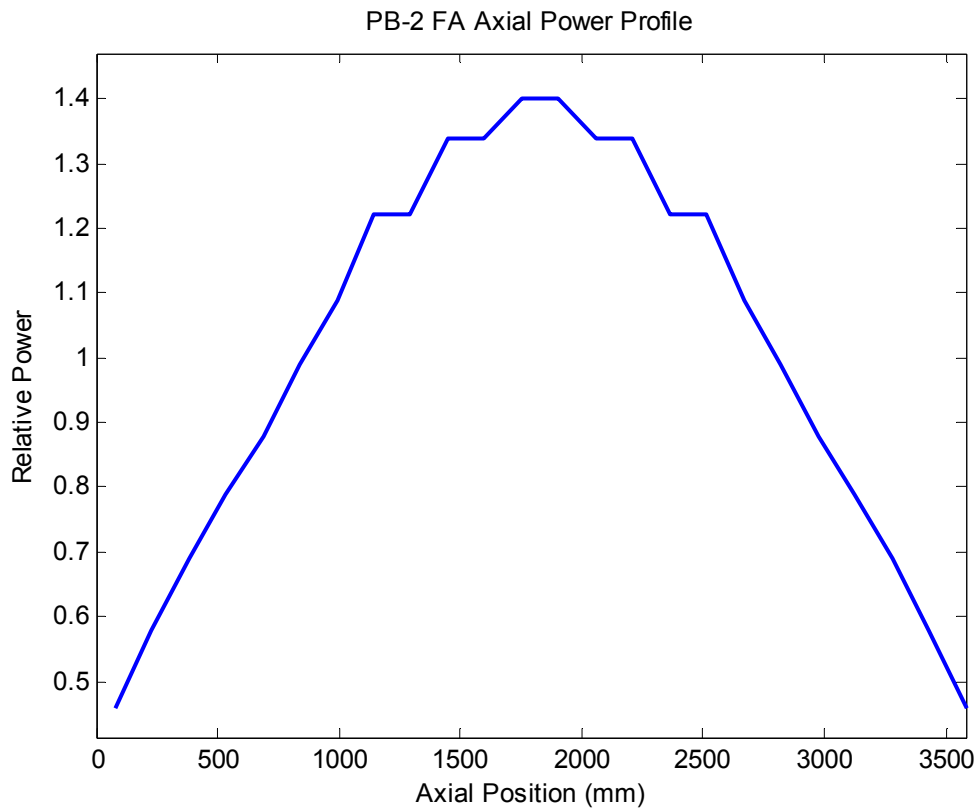
Table 4.6: PB-2 Spacer Grid Locations

| Type | Location (mm) |
|------|---------------|
| - | |
| MV | 480.0 |
| MV | 990.6 |
| MV | 1503.7 |
| MV | 2014.2 |
| MV | 2527.3 |
| MV | 3037.8 |
| MV | 3548.4 |

More detailed information on the spacer grids can be obtained from the authors as needed. The axial power profile of the bundle is from the BFBT benchmark, and is shown in Table 4.7 and Figure 4.2. The values are measured from the bottom of the bundle.

Table 4.7: PB-2 Bundle Axial Power Profile

| Location (mm) | Relative power - | Location (mm) | Relative power - |
|---------------|------------------|---------------|------------------|
| 76.2 | 0.46 | 1905.0 | 1.40 |
| 228.6 | 0.58 | 2057.4 | 1.34 |
| 381.0 | 0.69 | 2209.8 | 1.34 |
| 533.4 | 0.79 | 2362.2 | 1.22 |
| 685.8 | 0.88 | 2514.6 | 1.22 |
| 838.2 | 0.99 | 2667.0 | 1.09 |
| 990.6 | 1.09 | 2819.4 | 0.99 |
| 1143.0 | 1.22 | 2971.8 | 0.88 |
| 1295.4 | 1.22 | 3124.2 | 0.79 |
| 1447.8 | 1.34 | 3276.6 | 0.69 |
| 1600.2 | 1.34 | 3429.0 | 0.58 |
| 1752.6 | 1.40 | 3581.4 | 0.46 |

Figure 4.2: PB-2 Bundle Axial Power Profile Plot

Another important aspect of modelling these test cases is the radial power distribution of the fuel rods. The values in this case were obtained from running the assembly in Studsvik's CASMO-4 code. The details for the fuel pin types and locations are found in Table 3.1 of Chapter 3, as these have an effect on the power distribution. In the following table, the '+' sign refers to the relative location of the control rod, which is not included in this thermal-hydraulic model. The cells highlighted in green in Table 4.8 show the locations of the fuel rods which contain gadolinium poison, which is the explanation to their lower relative values. These values have been normalised to 1.000.

Table 4.8: PB-2 Bundle Radial Power Profile

| + | 1 | 2 | 3 | 4 | 5 | 6 | 7 |
|---|-------|-------|-------|-------|-------|-------|-------|
| 1 | 1.111 | 1.158 | 1.044 | 1.108 | 1.103 | 1.149 | 1.142 |
| 2 | 1.158 | 1.028 | 1.171 | 1.124 | 1.122 | 1.163 | 1.026 |
| 3 | 1.044 | 1.171 | 0.335 | 0.884 | 0.882 | 0.335 | 1.171 |
| 4 | 1.108 | 1.124 | 0.884 | 0.841 | 0.814 | 0.89 | 1.144 |
| 5 | 1.103 | 1.122 | 0.882 | 0.814 | 0.325 | 0.947 | 1.206 |
| 6 | 1.149 | 1.163 | 0.335 | 0.89 | 0.947 | 1.108 | 0.98 |
| 7 | 1.142 | 1.026 | 1.171 | 1.144 | 1.206 | 0.98 | 1.123 |

Case 1b - Transient BWR numerical test problem

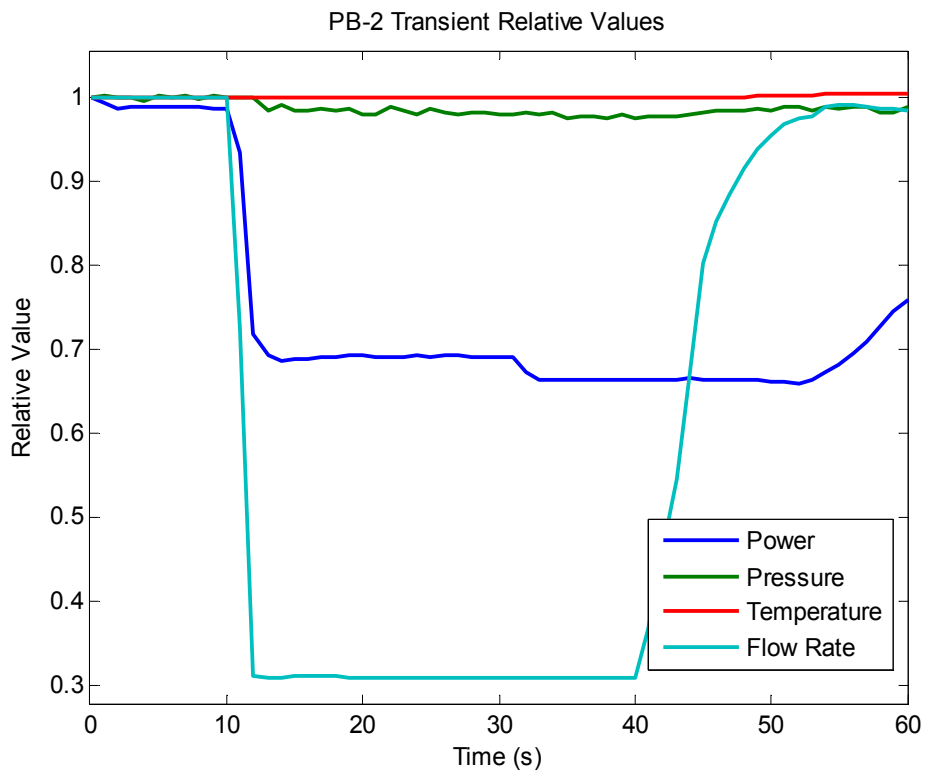
The transient case for PB-2 is based on the same bundle geometry and power profiles, but now the boundary conditions are changed over time to simulate a decrease in the flow rate to the bundle – see Table 4.9 and Figure 4.3. These values are relative to the initial conditions given in Table 4.5 of Case 1a, which is why they are all close to 1.000. The time for this case goes up to 60 seconds.

Table 4.9: PB-2 Bundle Transient History

| Time (s) | Power | Pressure | Inlet temp | Flow rate |
|----------|-------|----------|------------|-----------|
| 0.00 | 1.000 | 1.000 | 1.000 | 1.000 |
| 1.00 | 0.994 | 1.004 | 1.000 | 1.000 |
| 2.00 | 0.988 | 1.000 | 1.000 | 1.001 |
| 3.00 | 0.990 | 1.000 | 1.000 | 1.001 |
| 4.00 | 0.990 | 0.997 | 1.000 | 1.000 |
| 5.00 | 0.990 | 1.003 | 1.000 | 1.001 |
| 6.00 | 0.990 | 1.000 | 1.000 | 1.002 |
| 7.00 | 0.990 | 1.002 | 1.000 | 1.000 |
| 8.00 | 0.989 | 0.999 | 1.000 | 1.000 |
| 9.00 | 0.988 | 1.002 | 1.000 | 1.001 |
| 10.00 | 0.987 | 1.000 | 1.000 | 1.001 |
| 11.00 | 0.934 | 1.000 | 1.000 | 0.726 |
| 12.00 | 0.719 | 1.000 | 1.000 | 0.311 |
| 13.00 | 0.692 | 0.985 | 1.000 | 0.309 |
| 14.00 | 0.687 | 0.992 | 1.000 | 0.310 |
| 15.00 | 0.689 | 0.984 | 1.000 | 0.310 |
| 16.00 | 0.689 | 0.985 | 1.000 | 0.310 |
| 17.00 | 0.690 | 0.987 | 1.000 | 0.310 |
| 18.00 | 0.691 | 0.984 | 1.000 | 0.310 |
| 19.00 | 0.692 | 0.988 | 1.000 | 0.310 |
| 20.00 | 0.692 | 0.980 | 1.000 | 0.309 |
| 21.00 | 0.692 | 0.980 | 1.000 | 0.309 |
| 22.00 | 0.692 | 0.990 | 1.000 | 0.309 |
| 23.00 | 0.691 | 0.985 | 1.000 | 0.309 |
| 24.00 | 0.692 | 0.980 | 1.000 | 0.309 |
| 25.00 | 0.691 | 0.986 | 1.000 | 0.309 |
| 26.00 | 0.692 | 0.983 | 1.000 | 0.309 |
| 27.00 | 0.692 | 0.980 | 1.000 | 0.309 |
| 28.00 | 0.692 | 0.981 | 1.000 | 0.309 |
| 29.00 | 0.692 | 0.982 | 1.000 | 0.309 |
| 30.00 | 0.692 | 0.980 | 1.000 | 0.309 |
| 31.00 | 0.690 | 0.981 | 0.999 | 0.309 |

| | | | | |
|-------|-------|-------|-------|-------|
| 32.00 | 0.672 | 0.982 | 0.999 | 0.309 |
| 33.00 | 0.663 | 0.980 | 1.000 | 0.309 |
| 34.00 | 0.663 | 0.982 | 1.000 | 0.310 |
| 35.00 | 0.664 | 0.976 | 1.000 | 0.309 |
| 36.00 | 0.664 | 0.978 | 1.000 | 0.309 |
| 37.00 | 0.663 | 0.978 | 1.000 | 0.309 |
| 38.00 | 0.663 | 0.975 | 1.000 | 0.309 |
| 39.00 | 0.663 | 0.980 | 1.000 | 0.310 |
| 40.00 | 0.663 | 0.977 | 1.000 | 0.309 |
| 41.00 | 0.663 | 0.978 | 1.000 | 0.368 |
| 42.00 | 0.664 | 0.978 | 1.000 | 0.456 |
| 43.00 | 0.664 | 0.978 | 1.000 | 0.546 |
| 44.00 | 0.665 | 0.980 | 1.001 | 0.672 |
| 45.00 | 0.665 | 0.982 | 1.001 | 0.802 |
| 46.00 | 0.665 | 0.985 | 1.001 | 0.853 |
| 47.00 | 0.664 | 0.986 | 1.001 | 0.885 |
| 48.00 | 0.664 | 0.984 | 1.002 | 0.915 |
| 49.00 | 0.664 | 0.988 | 1.002 | 0.938 |
| 50.00 | 0.662 | 0.984 | 1.002 | 0.954 |
| 51.00 | 0.662 | 0.990 | 1.003 | 0.968 |
| 52.00 | 0.659 | 0.988 | 1.003 | 0.975 |
| 53.00 | 0.664 | 0.985 | 1.004 | 0.979 |
| 54.00 | 0.672 | 0.989 | 1.004 | 0.990 |
| 55.00 | 0.682 | 0.988 | 1.005 | 0.992 |
| 56.00 | 0.695 | 0.989 | 1.005 | 0.992 |
| 57.00 | 0.709 | 0.990 | 1.005 | 0.990 |
| 58.00 | 0.728 | 0.983 | 1.005 | 0.987 |
| 59.00 | 0.746 | 0.983 | 1.006 | 0.987 |
| 60.00 | 0.760 | 0.989 | 1.006 | 0.984 |

Figure 4.3: PB-2 Bundle Transient History Plot

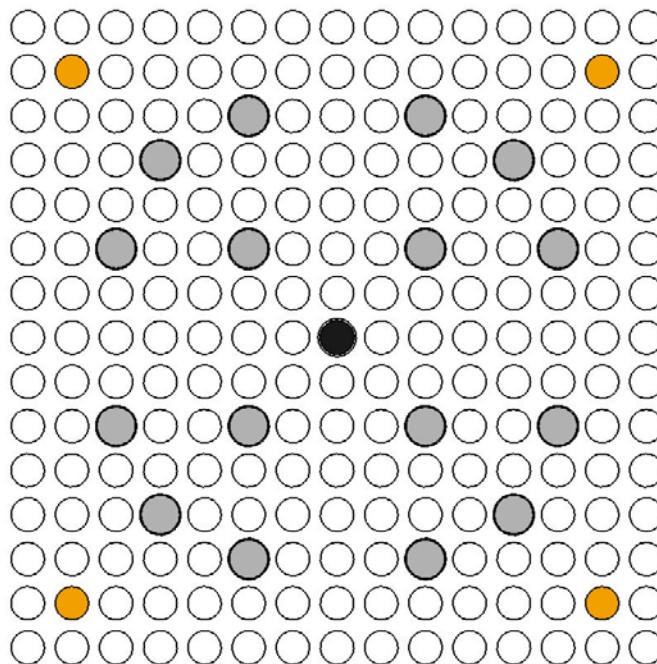


Case 2a – Steady-state PWR numerical test problems

This PWR case has been modelled for a fuel assembly from Three Mile Island Unit 1, and it is partially based on the data found in the PSBT benchmark. The geometry and dimensions are provided in Table 4.10 and Figure 4.4.

Table 4.10: TMI-1 Bundle Geometry

| Geometry | Value |
|---|-----------|
| Rod array | 15 x 15 |
| Number of fuel rods | 208 |
| Number of fuel rods with 2.0 w/o Gd2O3 (orange) | 4 |
| Fuel rod OD | 10.922 mm |
| Number of guide tubes (gray) | 16 |
| Guide tube OD | 13.462 mm |
| Guide tube ID | 12.650 mm |
| Number of instrumentation rods (black) | 1 |
| Instrumentation rod OD | 12.522 mm |
| Instrumentation rod ID | 11.202 mm |
| Fuel rod pitch | 14.427 mm |
| Fuel assembly pitch | 218.11 mm |
| Fuel rod length | 3657.6 mm |
| Number of MV spacers | 6 |
| Number of NMV spacers | 2 |

Figure 4.4: TMI-1 Bundle Image

The core boundary conditions are provided in Table 4.11 while the spacer grid locations are shown in Table 4.12.

Table 4.11: TMI-1 Bundle Boundary Conditions

| Core conditions | Value |
|---------------------------|-------------|
| Reactor power | 2 772 MWt |
| Core pressure | 15.2 MPa |
| Coolant inlet temperature | 565 K |
| Coolant flow rate | 16 050 kg/s |

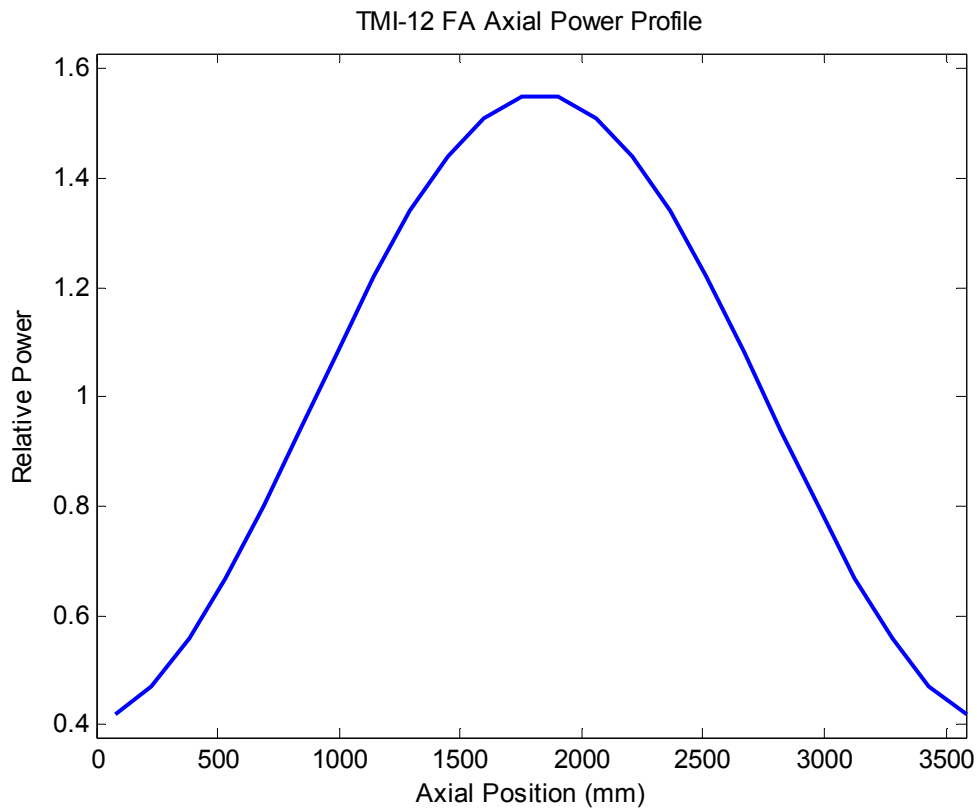
Table 4.12: TMI-1 Spacer Grid Locations

| Type - | Location (mm) |
|-----------|------------------|
| NMV | 0.0 |
| MV | 504.6 |
| MV | 1041.2 |
| MV | 1577.0 |
| MV | 2112.8 |
| MV | 2648.5 |
| MV | 3184.3 |
| NMV | 3657.6 |

The spacer grid and the axial power profile are measured from the bottom of the bundle. The axial power distribution is given in Table 4.13 and shown in Figure 4.5.

Table 4.13: TMI-1 Bundle Axial Power Profile

| Location (mm) | Relative power - | Location (mm) | Relative power - |
|------------------|---------------------|------------------|---------------------|
| 76.2 | 0.42 | 1905.0 | 1.55 |
| 228.6 | 0.47 | 2057.4 | 1.51 |
| 381.0 | 0.56 | 2209.8 | 1.44 |
| 533.4 | 0.67 | 2362.2 | 1.34 |
| 685.8 | 0.80 | 2514.6 | 1.22 |
| 838.2 | 0.94 | 2667.0 | 1.08 |
| 990.6 | 1.08 | 2819.4 | 0.94 |
| 1143.0 | 1.22 | 2971.8 | 0.80 |
| 1295.4 | 1.34 | 3124.2 | 0.67 |
| 1447.8 | 1.44 | 3276.6 | 0.56 |
| 1600.2 | 1.51 | 3429.0 | 0.47 |
| 1752.6 | 1.55 | 3581.4 | 0.42 |

Figure 4.5: TMI-1 Bundle Axial Power Profile Plot

The radial power distribution for this case was also obtained using CASMO-4. Details for the fuel pin types and locations can be found in the tables of Chapter 2. The radial power profile in Table 4.14 is 1/4 bundle symmetric, with the center of the fuel assembly corresponding to the orange-highlighted cell in the bottom-right of the table. The green value is a gadolinium pin location (4 total in the FA) and the blue highlights are for the guide tube locations (16 total in the FA). These values have been normalised to 1.000 (only if the entire bundle is taken into account, not the 1/4 symmetry as shown below).

Table 4.14: TMI-1 Bundle Radial Power Profile, 1/4 Bundle Symmetry

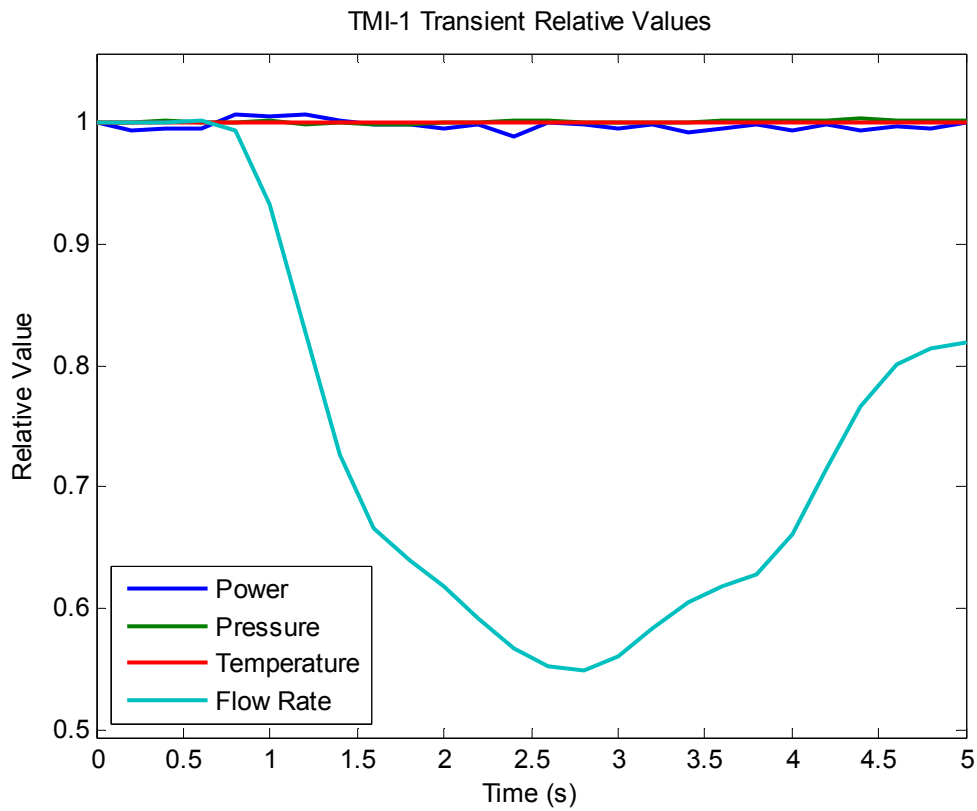
| | | | | | | | |
|-------|-------|-------|-------|-------|-------|-------|-------|
| 0.956 | 0.908 | 0.942 | 0.979 | 1.001 | 1.014 | 1.009 | 1.006 |
| 0.908 | 0.416 | 0.903 | 0.967 | 1.005 | 1.045 | 1.006 | 0.988 |
| 0.942 | 0.903 | 0.961 | 1.038 | 1.071 | 0.000 | 1.044 | 0.995 |
| 0.979 | 0.967 | 1.038 | 0.000 | 1.085 | 1.073 | 1.015 | 0.994 |
| 1.001 | 1.005 | 1.071 | 1.085 | 1.059 | 1.072 | 1.020 | 0.993 |
| 1.014 | 1.045 | 0.000 | 1.073 | 1.072 | 0.000 | 1.057 | 1.016 |
| 1.009 | 1.006 | 1.044 | 1.015 | 1.020 | 1.057 | 1.046 | 1.062 |
| 1.006 | 0.988 | 0.995 | 0.994 | 0.993 | 1.016 | 1.062 | 0.000 |

Case 2b - Transient PWR numerical test problem

This case utilises the same bundle geometry as in Case 2a and the transient history data are shown in Table 4.15 and Figure 4.6. This case is from the PSBT benchmark, which simulated a drop in the coolant flow rate. These values are also given as relative values, and are again based on the initial boundary conditions given in Table 4.5 of Case 1a.

Table 4.15: TMI-1 Bundle Transient History

| Time (s) | Power | Pressure | Inlet temp | Flow rate |
|----------|--------|----------|------------|-----------|
| 0.0 | 1.0000 | 1.0000 | 1.0000 | 1.0000 |
| 0.2 | 0.9929 | 1.0007 | 1.0000 | 1.0000 |
| 0.4 | 0.9955 | 1.0013 | 1.0000 | 1.0008 |
| 0.6 | 0.9951 | 1.0007 | 1.0000 | 1.0017 |
| 0.8 | 1.0067 | 1.0007 | 0.9997 | 0.9941 |
| 1.0 | 1.0053 | 1.0013 | 0.9997 | 0.9329 |
| 1.2 | 1.0067 | 0.9993 | 1.0000 | 0.8282 |
| 1.4 | 1.0027 | 1.0000 | 1.0000 | 0.7276 |
| 1.6 | 0.9987 | 0.9993 | 1.0000 | 0.6655 |
| 1.8 | 0.9991 | 0.9987 | 0.9997 | 0.6396 |
| 2.0 | 0.9951 | 1.0000 | 1.0000 | 0.6186 |
| 2.2 | 0.9982 | 1.0007 | 0.9997 | 0.5918 |
| 2.4 | 0.9889 | 1.0013 | 1.0000 | 0.5675 |
| 2.6 | 1.0009 | 1.0013 | 0.9997 | 0.5524 |
| 2.8 | 0.9982 | 1.0000 | 1.0000 | 0.5490 |
| 3.0 | 0.9955 | 1.0000 | 1.0000 | 0.5608 |
| 3.2 | 0.9978 | 1.0007 | 1.0000 | 0.5834 |
| 3.4 | 0.9915 | 1.0007 | 1.0000 | 0.6052 |
| 3.6 | 0.9951 | 1.0013 | 0.9997 | 0.6186 |
| 3.8 | 0.9982 | 1.0020 | 1.0000 | 0.6278 |
| 4.0 | 0.9929 | 1.0020 | 1.0000 | 0.6605 |
| 4.2 | 0.9978 | 1.0026 | 1.0000 | 0.7150 |
| 4.4 | 0.9929 | 1.0033 | 1.0000 | 0.7670 |
| 4.6 | 0.9964 | 1.0020 | 1.0000 | 0.8005 |
| 4.8 | 0.9955 | 1.0026 | 1.0003 | 0.8139 |
| 5.0 | 0.9996 | 1.0026 | 1.0000 | 0.8189 |

Figure 4.6: TMI-1 Bundle Transient History Plot

Case 3a – Steady-state VVER numerical test problem

This case is representative of a VVER-1000 fuel assembly, and the necessary parameters needed to simulate this scenario are provided in Tables 4.16 through 4.19 and Figures 4.7 through 4.9.

Table 4.16: VVER-1000 Bundle Geometry

| Geometry | Value |
|---|----------|
| Number of fuel rods | 312 |
| Fuel rods with 3.0 w/o ²³⁵ U (gray) | 78 |
| Fuel rods with 3.3 w/o ²³⁵ U (white) | 234 |
| Fuel rod OD | 9.10 mm |
| Number of guide tubes | 18 |
| Guide tube OD | 12.60 mm |
| Guide tube ID | 11.00 mm |
| Number of water rods | 1 |
| Water rod OD | 11.20 mm |
| Water rod ID | 9.60 mm |
| Fuel rod pitch | 12.75 mm |
| Fuel assembly pitch | 236 mm |
| Fuel rod length | 3 550 mm |
| Number of MV spacers | 13 |
| Number of NMV spacers | 0 |

Figure 4.7: VVER-1000 Bundle Image

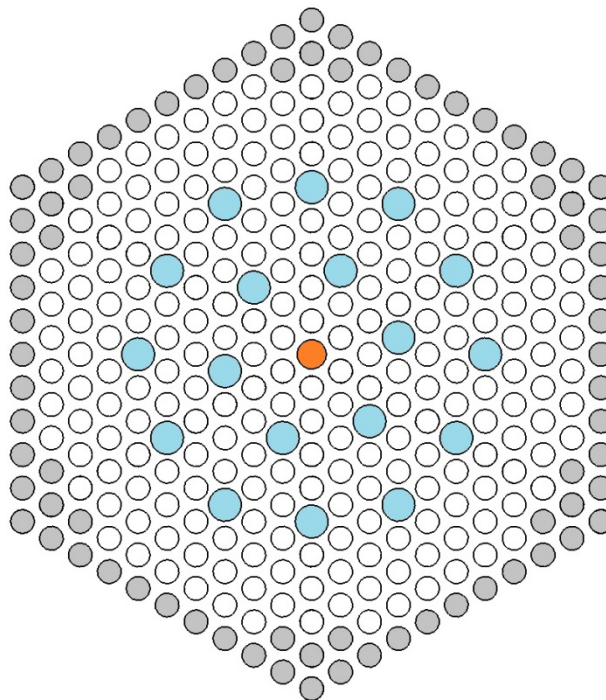


Table 4.17: VVER-1000 Bundle Boundary Conditions

| Core conditions | Value |
|---------------------------|--------------|
| Reactor power | 3 000 MWt |
| Core pressure | 15.7 MPa |
| Coolant inlet temperature | 560 K |
| Coolant flow rate | 17 600 kg/s |

Table 4.18: VVER-1000 Spacer Grid Locations

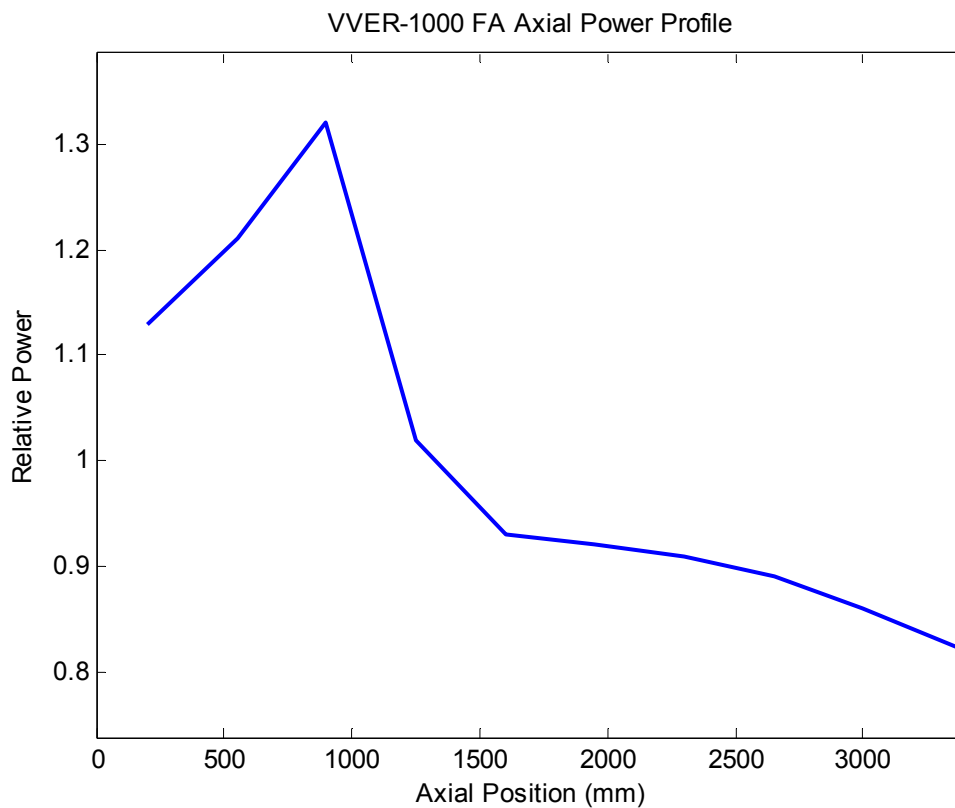
| Type - | Location (mm) |
|------------------|--------------------------------|
| MV | 232 |
| MV | 487 |
| MV | 742 |
| MV | 997 |
| MV | 1 252 |
| MV | 1 507 |
| MV | 1 762 |
| MV | 2 017 |
| MV | 2 272 |
| MV | 2 527 |
| MV | 2 782 |
| MV | 3 037 |
| MV | 3 292 |

Again, the spacer grid and the axial power profile values are measured from the bottom of the bundle. The axial power profile is a little rougher than the usual cosine curves because it is taken from the VVER-1000 Coolant Transient Benchmark.

Table 4.19: VVER-1000 Bundle Axial Power Profile

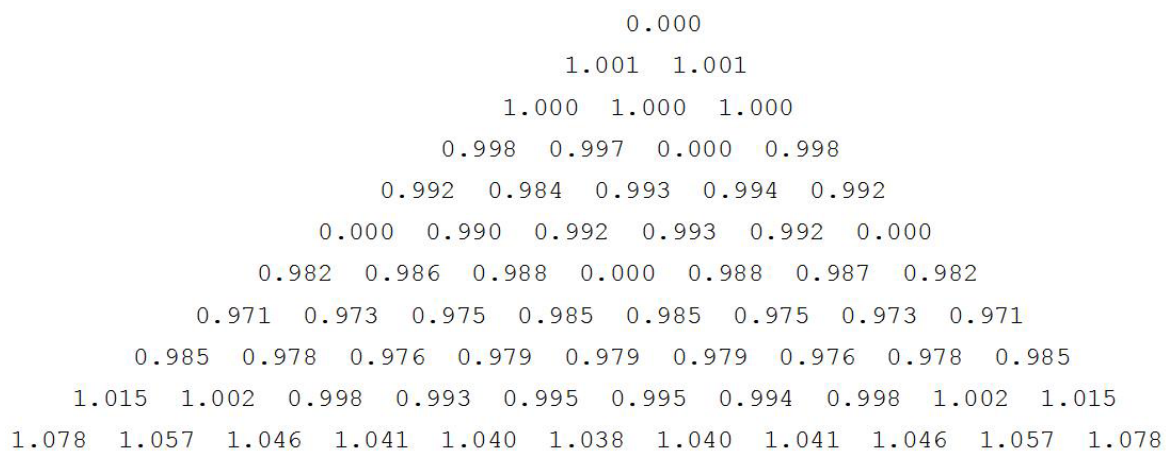
| Location (mm) | Relative power - |
|--------------------------------|----------------------------|
| 200 | 1.13 |
| 550 | 1.21 |
| 900 | 1.32 |
| 1 250 | 1.02 |
| 1 600 | 0.93 |
| 1 950 | 0.92 |
| 2 300 | 0.91 |
| 2 650 | 0.89 |
| 3 000 | 0.86 |
| 3 400 | 0.82 |

Figure 4.8: VVER-1000 Bundle Axial Power Profile Plot



The radial power profile for this particular profiled fuel assembly (which means there are two different levels of fuel enrichment contained within the same assembly) was obtained using CASMO-4E, which can be adapted to hexagonal geometry. The power profile is reported in Figure 4.9 in 1/6 bundle geometry, where the center of the VVER-1000 fuel assembly corresponds to the top-most value in this figure. The four other values of 0.000 correspond to the guide tube locations (18 total in the FA).

Figure 4.9: VVER-1000 Radial Power Profile, 1/6 Bundle Symmetry

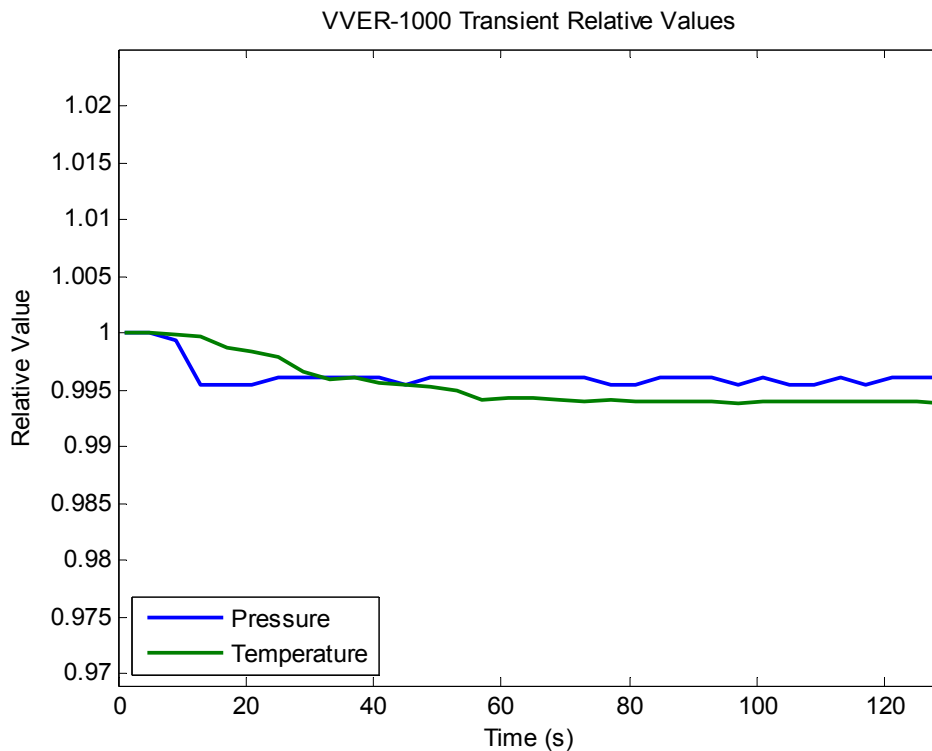


Case 3b - Transient VVER numerical test problem

This case, which is not quite complete enough, is derived from the VVER-1000 Coolant Transient Benchmark. The case involves a MCP coming online during lowered power operation and then observing the results. The data that are available currently are the pressure and inlet temperature values versus time – see Table 4.20 and Figure 4.10. The power and flow rates are not yet ready.

Table 4.20: VVER-1000 Bundle Transient History

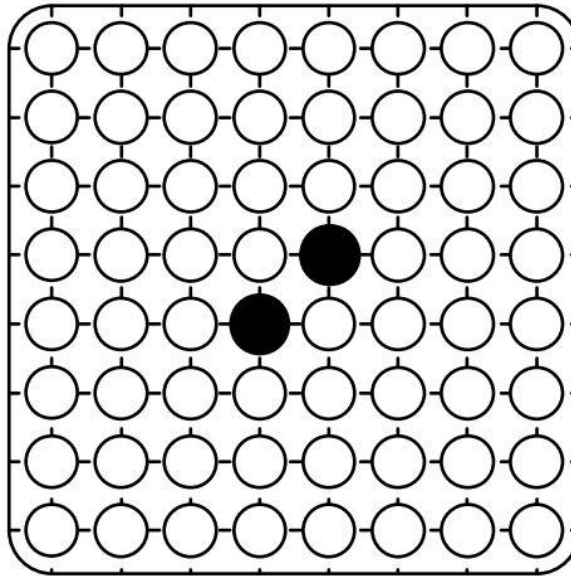
| Time (s) | Power | Pressure | Inlet temp | Flow rate |
|----------|-------|----------|------------|-----------|
| 0 | | 1.000 | 1.000 | |
| 4 | | 1.000 | 1.000 | |
| 8 | | 0.999 | 1.000 | |
| 12 | | 0.996 | 1.000 | |
| 16 | | 0.996 | 0.999 | |
| 20 | | 0.996 | 0.998 | |
| 24 | | 0.996 | 0.998 | |
| 28 | | 0.996 | 0.997 | |
| 32 | | 0.996 | 0.996 | |
| 36 | | 0.996 | 0.996 | |
| 40 | | 0.996 | 0.996 | |
| 44 | | 0.996 | 0.995 | |
| 48 | | 0.996 | 0.995 | |
| 52 | | 0.996 | 0.995 | |
| 56 | | 0.996 | 0.994 | |
| 60 | | 0.996 | 0.994 | |
| 64 | | 0.996 | 0.994 | |
| 68 | | 0.996 | 0.994 | |
| 72 | | 0.996 | 0.994 | |
| 76 | | 0.996 | 0.994 | |
| 80 | | 0.996 | 0.994 | |
| 84 | | 0.996 | 0.994 | |
| 88 | | 0.996 | 0.994 | |
| 92 | | 0.996 | 0.994 | |
| 96 | | 0.996 | 0.994 | |
| 100 | | 0.996 | 0.994 | |
| 104 | | 0.996 | 0.994 | |
| 108 | | 0.996 | 0.994 | |
| 112 | | 0.996 | 0.994 | |
| 116 | | 0.996 | 0.994 | |
| 120 | | 0.996 | 0.994 | |
| 124 | | 0.996 | 0.994 | |
| 128 | | 0.996 | 0.994 | |

Figure 4.10: VVER-1000 Bundle Transient History PlotCase 4a – Steady-state BWR experimental test problem

This test case is taken directly from the BFBT benchmark, and it includes a 8 x 8 bundle with electric heaters on its rods to simulate power. It is a full-scale bundle close in dimensions to the PB-2 assembly so it is applicable to the study of BWRs. There are two water rods within this bundle, which are not found on the PB-2 assembly used earlier in this exercise. The geometry of this test case is specified below, starting with various dimensions and parameters of Table 4.21 and Figure 4.11.

Table 4.21: BFBT Bundle Geometry

| Geometry | Value |
|----------------------------------|-----------------------|
| Rod array | 8 x 8 |
| Number of heated rods | 62 |
| Number of water rods | 2 |
| Heated rod OD | 12.3 mm |
| Heated rod pitch | 16.2 mm |
| Water rod OD | 15.0 mm |
| Axial heated length | 3708 mm |
| Flow channel inner width | 132.5 mm |
| Flow channel corner inner radius | 8 mm |
| Flow area | 9 781 mm ² |

Figure 4.11: BFBT Bundle Image

The case's boundary conditions are provided in Table 4.22.

Table 4.22: BFBT Bundle Boundary Conditions

| Test conditions | Value |
|--------------------------|------------|
| Power | 3.52 MW |
| Core pressure | 7.16 MPa |
| Coolant inlet subcooling | 50.3 kJ/kg |
| Coolant flow rate | 15.31 kg/s |

The spacer grids in this bundle are listed as type 'grid', and their locations (measured from the bottom of the bundle) are provided in Table 4.23.

Table 4.23: BFBT Spacer Grid Locations

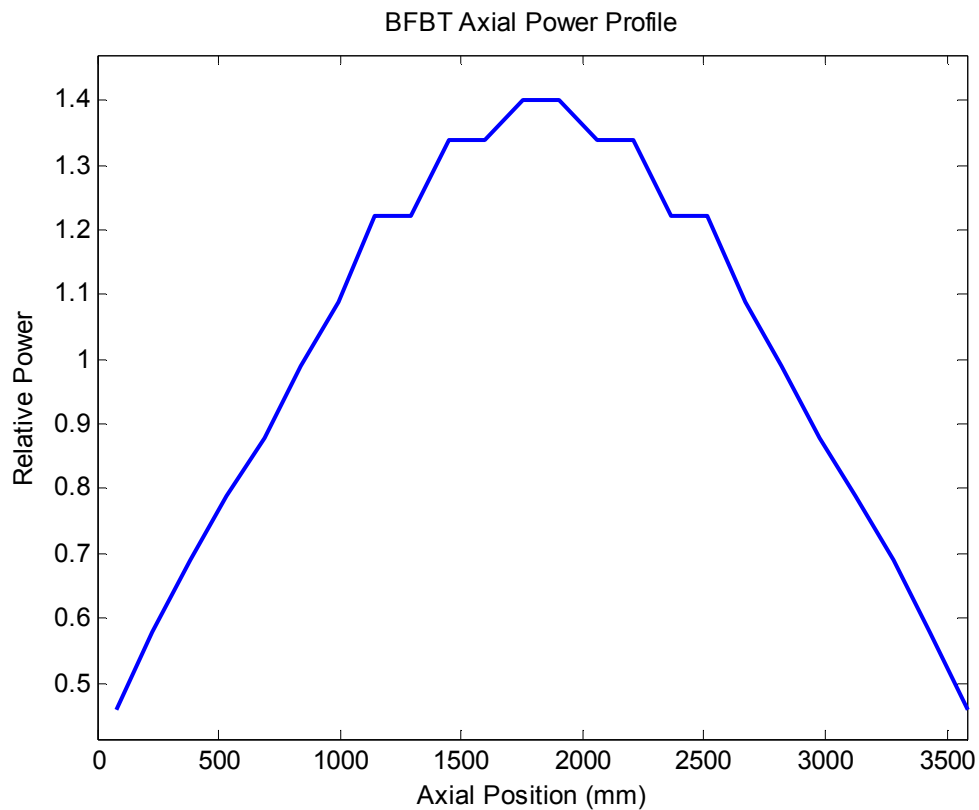
| Type | Location (mm) |
|------|---------------|
| - | |
| Grid | 455 |
| Grid | 967 |
| Grid | 1 479 |
| Grid | 1 991 |
| Grid | 2 503 |
| Grid | 3 015 |
| Grid | 3 527 |

The axial power profile is a 24-node shape as found in the BFBT benchmark specifications – see Table 4.24 and Figure 4.12.

Table 4.24: BFBT Bundle Axial Power Profile

| Location (mm) | Relative power - | Location (mm) | Relative power - |
|---------------|------------------|---------------|------------------|
| 77.25 | 0.46 | 1931.3 | 1.40 |
| 231.8 | 0.58 | 2085.8 | 1.34 |
| 386.3 | 0.69 | 2240.3 | 1.34 |
| 540.8 | 0.79 | 2394.8 | 1.22 |
| 695.3 | 0.88 | 2549.3 | 1.22 |
| 849.8 | 0.99 | 2703.8 | 1.09 |
| 1004.3 | 1.09 | 2858.3 | 0.99 |
| 1158.8 | 1.22 | 3012.8 | 0.88 |
| 1313.3 | 1.22 | 3167.3 | 0.79 |
| 1467.8 | 1.34 | 3321.8 | 0.69 |
| 1622.3 | 1.34 | 3476.3 | 0.58 |
| 1776.8 | 1.40 | 3630.8 | 0.46 |

Figure 4.12: BFBT Bundle Axial Power Profile Plot



The radial power profile includes the two water rods (indicated by ‘-’) and is shown in Table 4.25.

Table 4.25: BFBT Bundle Radial Power Profile

| + | 1 | 2 | 3 | 4 | 5 | 6 | 7 | 8 |
|---|------|------|------|------|------|------|------|------|
| 1 | 1.15 | 1.30 | 1.15 | 1.30 | 1.30 | 1.15 | 1.30 | 1.15 |
| 2 | 1.30 | 0.45 | 0.89 | 0.89 | 0.89 | 0.45 | 1.15 | 1.30 |
| 3 | 1.15 | 0.89 | 0.89 | 0.89 | 0.89 | 0.89 | 0.45 | 1.15 |
| 4 | 1.30 | 0.89 | 0.89 | 0.89 | - | 0.89 | 0.89 | 1.15 |
| 5 | 1.30 | 0.89 | 0.89 | - | 0.89 | 0.89 | 0.89 | 1.15 |
| 6 | 1.15 | 0.45 | 0.89 | 0.89 | 0.89 | 0.89 | 0.45 | 1.15 |
| 7 | 1.30 | 1.15 | 0.45 | 0.89 | 0.89 | 0.45 | 1.15 | 1.30 |
| 8 | 1.15 | 1.30 | 1.15 | 1.15 | 1.15 | 1.15 | 1.30 | 1.15 |

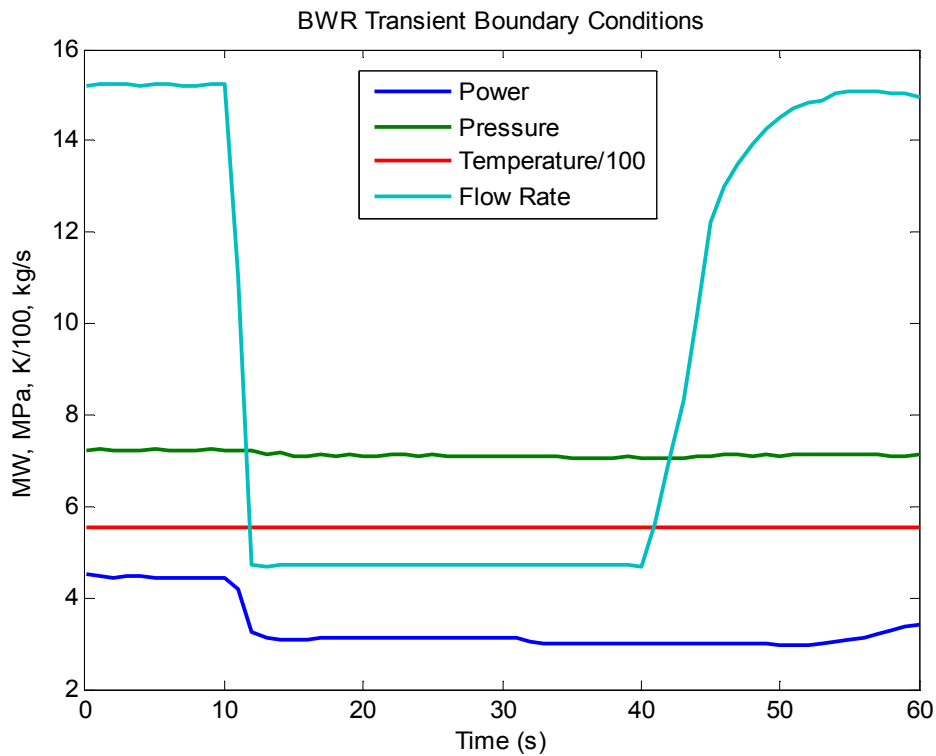
Case 4b - Transient BWR experimental test problem

This part of the test case is based on Test # 1071-58 performed in the BFBT benchmark. The bundle is the same as found in Case 4a and the transient time step values are given in Table 4.26 and Figure 4.13. This case is another decrease in flow rate, and goes for 60 seconds.

Table 4.26: BFBT Bundle Transient History

| Time (s) | Power (MW) | Pressure (MPa) | Inlet temp (K) | Flow rate (kg/s) |
|----------|------------|----------------|----------------|------------------|
| 0.00 | 4.50 | 7.227 | 554.18 | 15.22 |
| 1.00 | 4.47 | 7.252 | 554.19 | 15.22 |
| 2.00 | 4.45 | 7.224 | 554.16 | 15.23 |
| 3.00 | 4.46 | 7.227 | 554.19 | 15.23 |
| 4.00 | 4.46 | 7.206 | 554.22 | 15.21 |
| 5.00 | 4.45 | 7.246 | 554.17 | 15.22 |
| 6.00 | 4.45 | 7.226 | 554.18 | 15.24 |
| 7.00 | 4.45 | 7.239 | 554.18 | 15.22 |
| 8.00 | 4.45 | 7.221 | 554.16 | 15.21 |
| 9.00 | 4.45 | 7.244 | 554.18 | 15.23 |
| 10.00 | 4.44 | 7.230 | 554.19 | 15.22 |
| 11.00 | 4.20 | 7.226 | 554.17 | 11.04 |
| 12.00 | 3.23 | 7.228 | 554.15 | 4.73 |
| 13.00 | 3.12 | 7.119 | 554.17 | 4.70 |
| 14.00 | 3.09 | 7.171 | 554.17 | 4.71 |
| 15.00 | 3.10 | 7.109 | 554.13 | 4.71 |
| 16.00 | 3.10 | 7.116 | 554.16 | 4.72 |
| 17.00 | 3.11 | 7.130 | 554.15 | 4.71 |
| 18.00 | 3.11 | 7.114 | 554.15 | 4.71 |
| 19.00 | 3.12 | 7.137 | 554.16 | 4.71 |
| 20.00 | 3.12 | 7.086 | 554.15 | 4.71 |
| 21.00 | 3.11 | 7.084 | 554.15 | 4.71 |

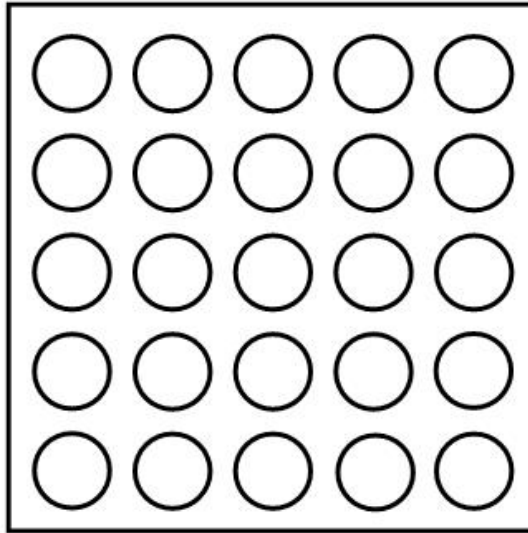
| | | | | |
|-------|------|-------|--------|-------|
| 22.00 | 3.11 | 7.151 | 554.12 | 4.71 |
| 23.00 | 3.11 | 7.121 | 554.13 | 4.71 |
| 24.00 | 3.12 | 7.080 | 554.09 | 4.71 |
| 25.00 | 3.11 | 7.124 | 554.12 | 4.71 |
| 26.00 | 3.12 | 7.102 | 554.09 | 4.71 |
| 27.00 | 3.12 | 7.081 | 554.09 | 4.71 |
| 28.00 | 3.11 | 7.092 | 554.08 | 4.71 |
| 29.00 | 3.11 | 7.096 | 554.07 | 4.71 |
| 30.00 | 3.11 | 7.081 | 554.07 | 4.71 |
| 31.00 | 3.11 | 7.087 | 554.03 | 4.71 |
| 32.00 | 3.02 | 7.098 | 554.03 | 4.71 |
| 33.00 | 2.98 | 7.080 | 554.05 | 4.71 |
| 34.00 | 2.99 | 7.097 | 554.08 | 4.71 |
| 35.00 | 2.99 | 7.057 | 554.08 | 4.71 |
| 36.00 | 2.99 | 7.071 | 554.08 | 4.71 |
| 37.00 | 2.99 | 7.071 | 554.09 | 4.71 |
| 38.00 | 2.98 | 7.044 | 554.13 | 4.70 |
| 39.00 | 2.99 | 7.081 | 554.17 | 4.71 |
| 40.00 | 2.98 | 7.058 | 554.18 | 4.70 |
| 41.00 | 2.99 | 7.064 | 554.21 | 5.60 |
| 42.00 | 2.99 | 7.066 | 554.23 | 6.94 |
| 43.00 | 2.99 | 7.070 | 554.28 | 8.31 |
| 44.00 | 2.99 | 7.084 | 554.34 | 10.23 |
| 45.00 | 2.99 | 7.097 | 554.39 | 12.21 |
| 46.00 | 2.99 | 7.119 | 554.45 | 12.97 |
| 47.00 | 2.99 | 7.123 | 554.53 | 13.47 |
| 48.00 | 2.99 | 7.110 | 554.62 | 13.93 |
| 49.00 | 2.99 | 7.139 | 554.71 | 14.28 |
| 50.00 | 2.98 | 7.111 | 554.84 | 14.52 |
| 51.00 | 2.98 | 7.151 | 554.96 | 14.72 |
| 52.00 | 2.96 | 7.143 | 555.06 | 14.84 |
| 53.00 | 2.99 | 7.120 | 555.19 | 14.89 |
| 54.00 | 3.02 | 7.150 | 555.36 | 15.06 |
| 55.00 | 3.07 | 7.138 | 555.46 | 15.09 |
| 56.00 | 3.13 | 7.148 | 555.54 | 15.09 |
| 57.00 | 3.19 | 7.152 | 555.67 | 15.06 |
| 58.00 | 3.28 | 7.104 | 555.72 | 15.02 |
| 59.00 | 3.36 | 7.104 | 555.82 | 15.02 |
| 60.00 | 3.42 | 7.144 | 555.87 | 14.98 |

Figure 4.13: BFBT Bundle Transient History Plot**Case 5a – Steady-state PWR experimental test problem**

This test case is based on the PSBT benchmark, which is very similar to the BFBT benchmark, but for pressurised water reactor studies instead. The bundle used during this exercise is only a 5 x 5 layout, which is small for a PWR (typically at least 15 x 15) but the boundary conditions are such that the experiment is useful for simulations. The geometry of the bundle is provided in Table 4.27 and shown in Figure 4.14.

Table 4.27: PSBT Bundle Geometry

| Geometry | Value |
|--------------------------|-----------------------|
| Rod array | 5 x 5 |
| Number of heated rods | 25 |
| Number of thimble rods | 0 |
| Heated rod OD | 9.5 mm |
| Heated rod pitch | 12.6 mm |
| Axial heated length | 3 658 mm |
| Flow channel inner width | 64.9 mm |
| Flow area | 2 440 mm ² |
| Number of MV spacers | 7 |
| Number of NMV spacers | 2 |
| Number of simple spacers | 8 |

Figure 4.14: PSBT Bundle Image

The bundle's boundary conditions define most of the parameters of the steady-state experiment. They are provided in Table 4.28.

Table 4.28: PSBT Bundle Boundary Conditions

| Test conditions | Value |
|---------------------------|------------|
| Power | 3.376 MW |
| Core pressure | 16.4 MPa |
| Coolant inlet temperature | 580 K |
| Coolant flow rate | 10.28 kg/s |

The locations of the various spacer grids are shown in Table 4.29. Note that there are three different types utilised within this bundle. The values of the distances are all measured from the bottom of the bundle.

Table 4.29: Spacer Grid Types and Locations

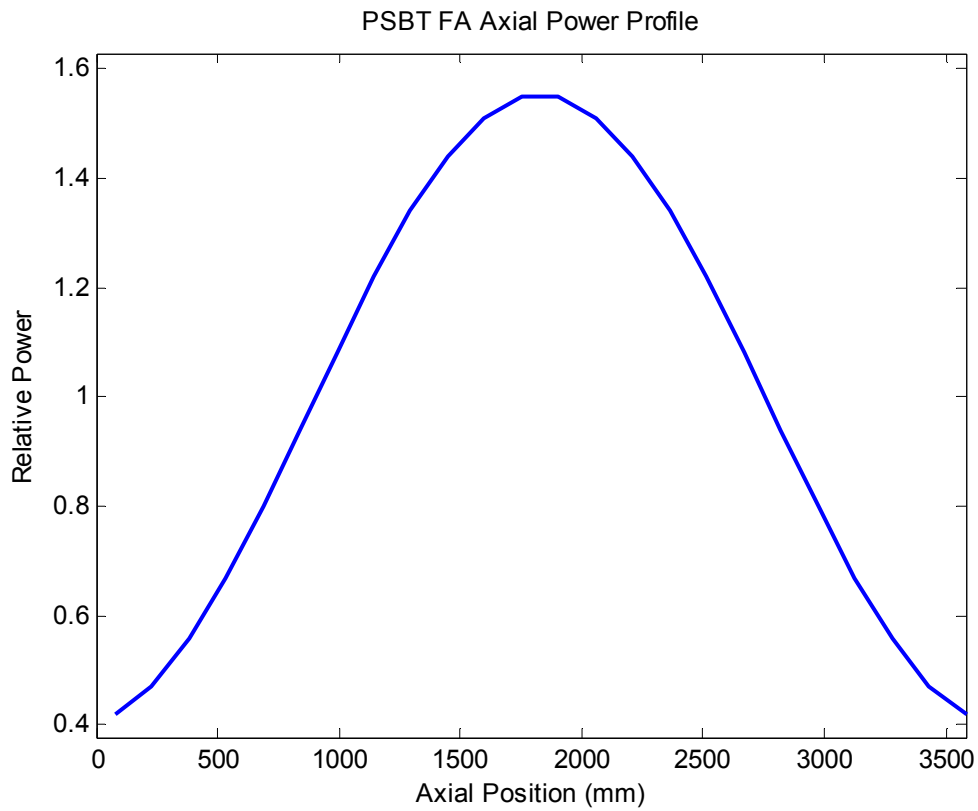
| Type - | Location (mm) |
|-----------|------------------|
| NMV | 2.5 |
| Simple | 237 |
| MV | 471 |
| Simple | 698 |
| MV | 925 |
| Simple | 1 151 |
| MV | 1 378 |
| Simple | 1 605 |
| MV | 1 832 |
| Simple | 2 059 |
| MV | 2 285 |
| Simple | 2 512 |
| MV | 2 739 |
| Simple | 2 993 |
| MV | 3 247 |
| Simple | 3 501 |
| MV | 3 247 |
| NMV | 3 755 |

The axial power profile is given in Table 4.30 and is shown in Figure 4.15.

Table 4.30: PSBT Bundle Axial Power Profile

| Location (mm) | Relative power - | Location (mm) | Relative power - |
|------------------|---------------------|------------------|---------------------|
| 76.2 | 0.42 | 1905.2 | 1.55 |
| 228.6 | 0.47 | 2057.6 | 1.51 |
| 381.0 | 0.56 | 2210.0 | 1.44 |
| 533.5 | 0.67 | 2362.5 | 1.34 |
| 685.9 | 0.80 | 2514.9 | 1.22 |
| 838.3 | 0.94 | 2667.3 | 1.08 |
| 990.7 | 1.08 | 2819.7 | 0.94 |
| 1143.1 | 1.22 | 2972.1 | 0.80 |
| 1295.5 | 1.34 | 3124.5 | 0.67 |
| 1448.0 | 1.44 | 3277.0 | 0.56 |
| 1600.4 | 1.51 | 3429.4 | 0.47 |
| 1752.8 | 1.55 | 3581.8 | 0.42 |

Figure 4.15: PSBT Bundle Axial Power Profile Plot



The radial power profile is provided in Table 4.31, as it is used in the PSBT benchmark. The values are not normalised, so the users must take care to do so if necessary.

Table 4.31: PSBT Bundle Radial Power Profile

| | 1 | 2 | 3 | 4 | 5 |
|---|------|------|------|------|------|
| 1 | 0.85 | 0.85 | 0.85 | 0.85 | 0.85 |
| 2 | 0.85 | 1.00 | 1.00 | 1.00 | 0.85 |
| 3 | 0.85 | 1.00 | 1.00 | 1.00 | 0.85 |
| 4 | 0.85 | 1.00 | 1.00 | 1.00 | 0.85 |
| 5 | 0.85 | 0.85 | 0.85 | 0.85 | 0.85 |

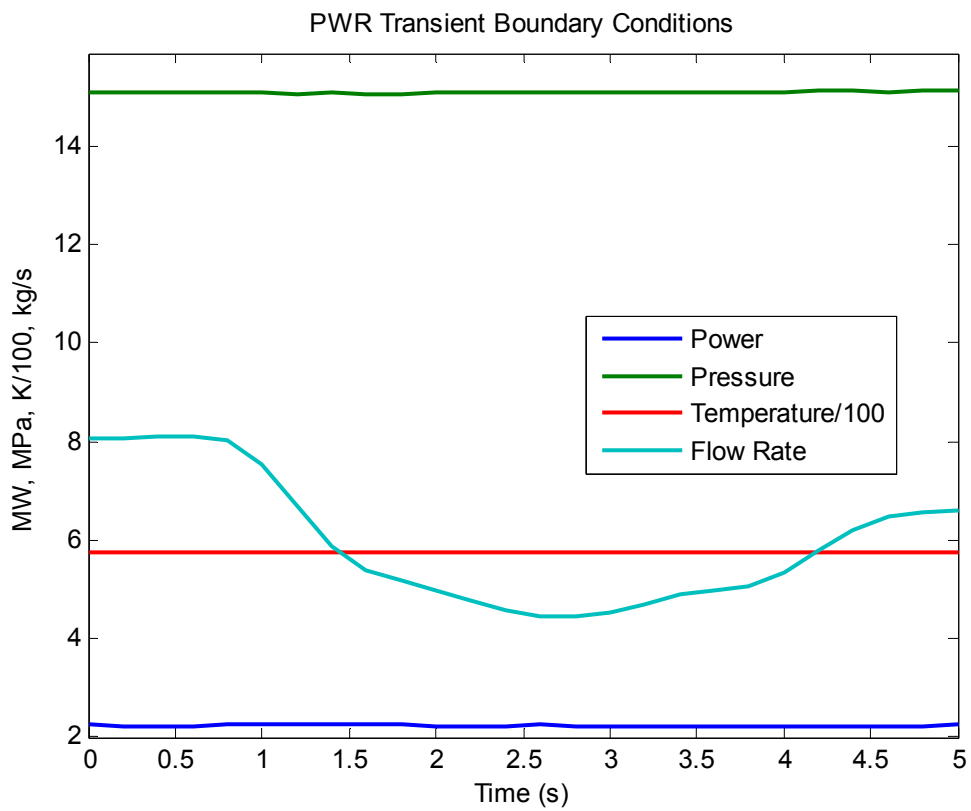
Case 5b – Transient PWR experimental test problem

The transient portion of this case includes another flow reduction, as performed as part of the PSBT benchmark. The boundary conditions at each time step are provided in Table 4.32 and shown in Figure 4.16. The transient runs for 5.0 seconds.

Table 4.32: PSBT Bundle Transient History

| Time (s) | Power (MW) | Inlet P (MPa) | Inlet T (K) | Flow rate (kg/s) |
|----------|------------|---------------|-------------|------------------|
| 0.0 | 2.244 | 15.08 | 574.4 | 8.09 |
| 0.2 | 2.228 | 15.09 | 574.4 | 8.09 |
| 0.4 | 2.234 | 15.10 | 574.4 | 8.09 |
| 0.6 | 2.233 | 15.09 | 574.4 | 8.10 |
| 0.8 | 2.259 | 15.09 | 574.3 | 8.04 |
| 1.0 | 2.256 | 15.10 | 574.3 | 7.54 |
| 1.2 | 2.259 | 15.07 | 574.4 | 6.70 |
| 1.4 | 2.250 | 15.08 | 574.4 | 5.88 |
| 1.6 | 2.241 | 15.07 | 574.4 | 5.38 |
| 1.8 | 2.242 | 15.06 | 574.3 | 5.17 |
| 2.0 | 2.233 | 15.08 | 574.4 | 5.00 |
| 2.2 | 2.240 | 15.09 | 574.3 | 4.79 |
| 2.4 | 2.219 | 15.10 | 574.4 | 4.59 |
| 2.6 | 2.246 | 15.10 | 574.3 | 4.47 |
| 2.8 | 2.240 | 15.08 | 574.4 | 4.44 |
| 3.0 | 2.234 | 15.08 | 574.4 | 4.53 |
| 3.2 | 2.239 | 15.09 | 574.4 | 4.72 |
| 3.4 | 2.225 | 15.09 | 574.4 | 4.89 |
| 3.6 | 2.233 | 15.10 | 574.3 | 5.00 |
| 3.8 | 2.240 | 15.11 | 574.4 | 5.08 |
| 4.0 | 2.228 | 15.11 | 574.4 | 5.34 |
| 4.2 | 2.239 | 15.12 | 574.4 | 5.78 |
| 4.4 | 2.228 | 15.13 | 574.4 | 6.20 |
| 4.6 | 2.236 | 15.11 | 574.4 | 6.47 |
| 4.8 | 2.234 | 15.12 | 574.5 | 6.58 |
| 5.0 | 2.243 | 15.12 | 574.4 | 6.62 |

Figure 4.16: PSBT Bundle Transient History Plot



Case 6a – Steady-state VVER experimental test problem and Case 6b - Transient VVER experimental test problems are not ready at this time and will be provided in Version 2.0 of the Specification.

Chapter 5: Requested output

5.1 Introduction

The analysis results of Phase II will be presented in a benchmark analysis report, which will be made available in both a hard copy and an electronic form.

Participants are asked to provide the output information with the given requirements:

- results should be submitted in an electronic format according to templates, which will be provided to participants by the benchmark team;
- all data should be in SI units or in the units indicated on the templates;
- Please provide any other information specific to the data.

5.2 Results for Exercise II-1

There are three types of variations applied to the fuel pin model test cases from Chapter 2. Both steady-state and transient cases will have similar changes, depending on the type of LWR in each study. The first of these variations is from the geometry of the fuel pin. The users are advised to run each of the cases taking the uncertainty in manufacturing tolerances into account. The obtained fuel temperature will vary from these tolerances and these variations will be studied for the sensitivity study. This will give an indication of how the different codes perform when running calculations under the same input parameters. The next type of uncertainty comes from the boundary condition variations, which are also applied to each case depending on the reactor type. Lastly, the code uncertainties are studied. The users are requested to perform their own study by modifying the source codes being used. A table of typical values is found in Chapter 2 but the users are able to determine which parameters are changed as well as the magnitude of these changes.

Steady-State Cases

For the first three numerical test problems, which are representative of PB-2, TMI-1, and Kozloduy-6 (Cases 1a through 3a) the users are requested to make the appropriate parameter variations and fill out a template similar to that shown in Table 5.1 below. The data requested are the centerline fuel temperature (and outer cladding temperature if possible) at the ending time step for the steady-state depletion case. The results go into the two columns shown below, underneath ‘Centerline Temperature (K)’ in Table 5.1, and the ‘nominal’ results are the mean values obtained, and the ‘st dev’ column represents the uncertainty due to the variation in the input parameters. The mean value and associated uncertainty are requested for each axial node value in the column. The number of axial nodes can also be changed for each of the different types of reactors, as given in the Test Cases section of Chapter 2. Once all the cases are run, the users are requested to provide the parameters, which caused the greatest amount of uncertainty in the propagated and output parameters. While the output does not need to exactly follow this format, any strategic method of displaying all the useful data over the various parameter changes could be deemed acceptable by the UAM team.

The distribution of the parameter is either flat or normal in this exercise. A flat (or uniform) distribution means that all values are equally likely across the given range. A normal distribution, known as a Gaussian distribution, has a mean value equal to the given nominal value and then extends outwards in the normal bell-curve shape for its distribution. A normal distribution is expected with most of these

manufacturing tolerances due to the fact that there is an expected value (which is equivalent to the nominal value provided).

Table 5.1: Exercise II-1 Steady-State Numerical Case Results Template

| | | |
|-------------------|----------------------------|---------|
| Case #: | 1a | |
| Case type: | Steady-state, numerical | |
| Reactor type: | BWR | |
| Reactor name: | PB-2 | |
| Scenario time: | 2230 | days |
| Target parameter: | Centerline temperature (K) | |
| Axial node | Nominal | st dev. |
| 1 (bottom) | | |
| 2 | | |
| 3 | | |
| 4 | | |
| 5 | | |
| 6 | | |
| 7 | | |
| 8 | | |
| 9 | | |
| 10 | | |
| 11 | | |
| 12 | | |
| 13 | | |
| 14 | | |
| 15 | | |
| 16 | | |
| 17 (top) | | |

Table 5.1 is an example for the first test case (1a) where the parameter of interest is the fuel centerline temperature. It is requested at each of the axial nodes as defined in Chapter 2 along with its associated uncertainty at each of these nodes, if possible. The ‘scenario time’ is the time after the start of the test case at which the results should be given. It is often at the ending time of the scenario for these steady-state depletion cases.

For the experimental cases, the temperatures are only requested at the same axial location as the measured values were taken. For example, if a research facility utilised a thermocouple at an elevation of 1 400 mm from the bottom to take outer cladding temperature readings, then the users should provide their results at the same elevation. This allows for a more accurate benchmark of the code and experimental values. This means that the results might be only one value for the given temperature due to the fact that only one thermocouple or temperature-measuring device was used during the original experiment. A sample template for this situation is provided in Table 5.2, as given for Case 4a, which is modelled on the IFA-432 experiment, as found in Chapter 2. This specific case had a thermocouple measuring the fuel temperature 100 mm from the bottom of the rod;

therefore the users are requested to report their calculated fuel temperatures and uncertainties at this location as well.

Table 5.2: Exercise II-1 Steady-State Experimental Case Results Template

| | | |
|-------------------|----------------------------|---------|
| Case #: | 4a | |
| Case type: | Steady-state, experimental | |
| Reactor type: | BWR | |
| Experiment name: | IFA-432, Rod 1 | |
| Scenario time: | 809.8 | days |
| Target parameter: | Centerline temperature (K) | |
| Axial location: | 100 | mm |
| | Value | st dev. |
| Calculated: | | |

It is important to note that this axial location is measured from the bottom of the IFA-432 rod used in the experiment.

Transient Cases

Part b of each of the six test cases is a transient scenario which involves a power pulse of short duration. The output from the transient cases will be more data due to the fact that the results are requested at various time steps during the simulation. This means that there will be multiple tables, similar to the one shown above, at each of the time steps specified. The first three test cases (1b through 3b) are the numerical cases, which are modelled for the reactors PB-2, TMI-1, and Kozloduy-6. The data requested for these three cases are the maximum centerline temperature experienced along the fuel rod at three different time steps. These results do not need to have an axial profile as in the steady-state cases; rather just the maximum value of fuel temperature needs to be reported. The three times chosen vary by case, but will be near the start of the power pulse, at the mid-point of the pulse, and at the end of the scenario (typically about one second). These times will be specified explicitly for each of the test cases in this exercise. Example of template for transient cases is shown in Table 5.3.

Table 5.3: Exercise II-1 Transient Numerical Case Results Template

| | | |
|-------------------|---|---------|
| Case #: | 1b | |
| Case type: | Transient, numerical | |
| Reactor type: | BWR | |
| Reactor name: | PB-2 | |
| Scenario time: | 0.206 | seconds |
| Target parameter: | Centerline temperature (K) (Maximum) | |
| | Value | st dev. |
| Calculated: | | |
| Axial location: | | mm |

Table 5.3 shows the scenario time as the center of the pulse (at 0.206 seconds) and would be the second of the three time steps at which data are requested. The other two times (for this particular scenario: Case 1b) would be the beginning of the pulse at 0.196 seconds, and at the end of the scenario, at 1.000 seconds. The specifications for the times at which to report data are shown in Chapter 2. The axial location

at which the maximum fuel temperature was calculated should also be reported, as shown in Table 5.3 above. This axial location may vary from each of the three different time steps.

If users wish to provide data of every time step along with the associated uncertainty for the parameters, then that is also acceptable. The time step sizes for the transient cases, as provided in Chapter 2, are relatively small (often 0.001 seconds or smaller) so this would be a large amount of data that the users are responsible for reasonably presenting.

The propagated and output parameter for the transient cases is still the centerline temperature, but as stated in the steady-state case explanation - if the users are able to also calculate values and associated uncertainty for the outer cladding temperature, then this would broaden the amount of experimental data with which the results can be compared. This is due to the relative difficulty in providing experimental centerline temperatures in comparison to measuring the temperature on the outside of the fuel rods (at the outer cladding surface) which is more common at most facilities. The target parameter will be clearly identified in each of the test cases in Chapter 2. For example, in the following results template, Table 5.4, the only measured parameter from the actual experiment was the cladding temperature for the FK-1 pulse case. Therefore, the users are requested to provide outer cladding temperatures at the same elevation as the measured data from the experiment.

Table 5.4: Exercise II-1 Transient Experimental Case Results Template

| | | |
|-------------------|--------------------------|---------|
| Case #: | 4b | |
| Case type: | Transient, experimental | |
| Reactor type: | BWR | |
| Experiment name: | FK-1 Pulse | |
| Scenario time: | 0.206 | seconds |
| Target parameter: | Cladding temperature (K) | |
| Axial location: | 21 | mm |
| | Value | st dev. |
| Calculated: | | |

The FK-1 pulse has its peak at 0.206 seconds, the same as the numerical case due to the fact that the numerical case is modelled on the FK-1 experiment and utilises the same power history. Similar to the numerical transient case, the output and propagated parameter will be requested at three different time steps (only one is shown in the template above).

5.3 Results for Exercise II-2

Chapter 3 of this report covers Exercise II-2, which focuses on neutron kinetics in LWRs. Similar to Exercise II-1 there are two types of test cases- depletion and kinetics. The depletion cases include long-term irradiations of fuel assemblies in order to determine k_{eff} , the nuclide concentrations, the power distribution, and the burn-up of the assembly. The kinetics cases, which are short-term power transients, are included in order for the users to calculate power versus time and reactivity versus time data, as well as 3-D power distributions at given time steps.

Depletion Cases

The three numerical depletion cases (Cases 1a through 3a in Chapter 3) are modelled for the PB-2, TMI-1, and Kozloduy-6 reactors in terms of dimensional parameters. All three include a flat power history for their irradiation period, and at the end of the depletion the nuclide concentrations, the burn-up, and k_{eff} are requested at the provided axial position. An example of the results template for these numerical cases is shown below in Table 5.5.

Table 5.5: Exercise II-2 Depletion Numerical Case Results Template

| | | |
|--------------------|------------------------|---------|
| Case #: | 1a | |
| Case type: | Depletion, numerical | |
| Reactor type: | BWR | |
| Reactor name: | PB-2 | |
| Scenario time: | 1400 | days |
| Target parameter: | Nuclide concentrations | |
| Axial location: | 1828.8 | mm |
| Nuclide: | Value | st dev. |
| ²³³ U | | |
| ²³⁵ U | | |
| ²³⁶ U | | |
| ²³⁸ U | | |
| ²³⁹ Pu | | |
| ²⁴⁰ Pu | | |
| ²⁴¹ Pu | | |
| ²⁴² Pu | | |
| ²⁴¹ Am | | |
| ²⁴³ Am | | |
| ²⁴² Cm | | |
| ²⁴⁴ Cm | | |
| ¹⁴² Nd | | |
| ¹⁴³ Nd | | |
| ¹⁴⁴ Nd | | |
| ¹⁴⁵ Nd | | |
| ¹⁴⁶ Nd | | |
| Burn-up (MWd/MTU): | | |
| K _{eff} : | | |

For the three experimental cases, there are post-irradiation examination (PIE) data with which to compare the calculated results. These data often include a list of various nuclides as found in the rods at various axial locations after the irradiation has been completed. The burn-up is also determined during this examination. The users will be requested to compare their calculated results for these nuclide concentrations and burn-up values during the experimental cases (Cases 4a through 6a). A sample of the experimental calculation results template is shown below in Table 5.6.

Table 5.6: Exercise II-2 Depletion Experimental Case Results Template

| | | |
|--------------------|-------------------------|---------|
| Case #: | 4a | |
| Case type: | Depletion, experimental | |
| Reactor type: | BWR | |
| Experiment name: | FK-2 PIE | |
| Scenario time: | 1402 | days |
| Target parameter: | Nuclide concentrations | |
| Axial location: | 2050 | mm |
| Nuclide: | Value | st dev. |
| ²³³ U | | |
| ²³⁵ U | | |
| ²³⁶ U | | |
| ²³⁸ U | | |
| ²³⁹ Pu | | |
| ²⁴⁰ Pu | | |
| ²⁴¹ Pu | | |
| ²⁴² Pu | | |
| ²⁴¹ Am | | |
| ²⁴³ Am | | |
| ²⁴² Cm | | |
| ²⁴⁴ Cm | | |
| ¹⁴² Nd | | |
| ¹⁴³ Nd | | |
| ¹⁴⁴ Nd | | |
| ¹⁴⁵ Nd | | |
| ¹⁴⁶ Nd | | |
| Burn-up (MWd/MTU): | | |
| K _{eff} : | | |

The axial location is measured from the bottom of the active length of the fuel rods. In some of these experimental cases, there are several axial locations for which experimental data exist, so the users are free to choose multiple locations as stated in the Chapter 3 test case definitions.

Kinetics Cases

During the transient cases, the fuel assemblies (as a mini-core) are exposed to a short-duration spike in reactivity change which causes a variation in the power and other parameters over the time steps. The uncertainties are mainly due to the control rod worth and insertion speed. These transients are not rapid enough to be similar to SCRAM cases, where the control rods move as quickly as possible, but they are still representative of an RIA with a fast control rod ejection or drop. For these cases, the important output parameter is the core power versus time. Since the scenario occurs over a relatively short period of time, the results are requested at several intervals along this time span. Table 5.7 below illustrates how a template for this type of case could be used to illustrate the calculated results of core power over time.

Table 5.7: Exercise II-2 Kinetics Numerical Case Results Template

| | | |
|-------------------|-----------------------|---------|
| Case #: | 2b | |
| Case type: | Kinetics, numerical | |
| Reactor type: | PWR | |
| Reactor name: | TMI-1 3 x 3 mini-core | |
| Target parameter: | Core power | |
| At time: | Value | st dev. |
| 0.0 s | | |
| 10.0 s | | |
| 20.0 s | | |
| 30.0 s | | |
| 60.0 s | | |

The experimental cases (Cases 4b through 6b) also require the users to determine the power versus time evolution of the mini-core. Example of template for these cases is given in Table 5.8.

Table 5.8: Exercise II-2 Kinetics Experimental Case Results Template

| | | |
|-------------------|------------------------|---------|
| Case #: | 5b | |
| Case type: | Kinetics, experimental | |
| Reactor type: | PWR | |
| Experiment name: | SPERT E-Core | |
| Target parameter: | Core power | |
| At time: | Value | st dev. |
| 0.0 s | | |
| 0.2 s | | |
| 0.5 s | | |
| 1.0 s | | |
| 5.0 s | | |

5.4 Results for Exercise II-3

The thermal-hydraulic test cases found in Chapter 4 of this report are utilised to determine results for the void distribution and moderator density along a fuel assembly. The cases all use a single fuel assembly bundle and give the appropriate boundary conditions used during the simulation. The variations are made in these boundary conditions as well as with several of the geometric parameters in order to cover the effects of manufacturing tolerances. The power profiles can also have some changes applied.

Steady-State Cases

The first three cases are the steady-state numerical test problems (Cases 1a through 3a) and they are designed with the calculation of the void fraction distribution in mind. Reporting this distribution will be done with respect to the axial location of the calculated results, as shown in Table 5.9.

Table 5.9: Exercise II-3 Steady-state Numerical Case Results Template

| | | |
|-------------------|-------------------------|---------|
| Case #: | 1a | |
| Case type: | Steady-state, numerical | |
| Reactor type: | BWR | |
| Reactor name: | PB-2 | |
| Target parameter: | Void fraction | |
| Axial node | Value | st dev. |
| 1 (bottom) | | |
| 2 | | |
| 3 | | |
| 4 | | |
| 5 | | |
| 6 | | |
| 7 | | |
| 8 | | |
| 9 | | |
| 10 | | |
| 11 | | |
| 12 | | |
| 13 | | |
| 14 | | |
| 15 | | |
| 16 | | |
| 17 | | |
| 18 | | |
| 19 | | |
| 20 | | |
| 21 | | |
| 22 | | |
| 23 | | |
| 24 (top) | | |

The experimental cases (Cases 4a through 6a) also involve calculating void distribution, so the template will be very similar to the one shown in Table 5.9.

Transient Cases

The six transient test problems involve some sort of change applied to the boundary conditions of the bundle over time, usually a change in the flow rate, which in turn causes changes in the other related parameters. These tests have been designed to allow the users to calculate parameters such as the void distribution over time, just as in the steady-state cases. The template is then very similar, but it is important to note the time at which the results occur. This is shown in Table 5.10 below, which uses the example of 15.0 seconds into the transient scenario for this set of results.

Table 5.10: Exercise II-3 Transient Numerical Case Results Template

| | | |
|-------------------|----------------------|---------|
| Case #: | 1b | |
| Case type: | Transient, numerical | |
| Reactor type: | BWR | |
| Reactor name: | PB-2 | |
| Scenario time: | 15.0 | seconds |
| Target parameter: | Void fraction | |
| Axial node | Value | st dev. |
| 1 (bottom) | | |
| 2 | | |
| 3 | | |
| 4 | | |
| 5 | | |
| 6 | | |
| 7 | | |
| 8 | | |
| 9 | | |
| 10 | | |
| 11 | | |
| 12 | | |
| 13 | | |
| 14 | | |
| 15 | | |
| 16 | | |
| 17 | | |
| 18 | | |
| 19 | | |
| 20 | | |
| 21 | | |
| 22 | | |
| 23 | | |
| 24 (top) | | |

Chapter 6: Conclusions

The objective of the OECD LWR UAM activity is to establish an internationally accepted benchmark framework to compare, assess and further develop different uncertainty analysis methods associated with the design, operation and safety of LWRs. As a result, the LWR UAM benchmark will help to address current nuclear power generation industry and regulation needs and issues related to practical implementation of risk informed regulation. The realistic evaluation of consequences must be made with best-estimate coupled codes, but to be meaningful, such results should be supplemented by an uncertainty analysis. The use of coupled codes allows to avoid unnecessary penalties due to incoherent approximations in the traditional decoupled calculations, and to obtain more accurate evaluation of margins regarding licensing limit. This becomes important for licensing power upgrades, improved fuel assembly and control rod designs, higher burn-up and others issues related to operating LWRs as well as to the new Generation 3+ designs being licensed now (ESBWR, AP-1000, EPR-1600 and etc.). Establishing such internationally accepted LWR UAM benchmark framework offers the possibility to accelerate the licensing process when using best-estimate methods.

The proposed technical approach is to establish a benchmark for uncertainty analysis in best-estimate modelling and coupled multi-physics and multi-scale LWR analysis, using as bases a series of well-defined problems with complete sets of input specifications and reference experimental data. The objective is to determine the uncertainty in LWR system calculations at all stages of coupled reactor physics/thermal hydraulics calculation. The full chain of uncertainty propagation from basic data, engineering uncertainties, across different scales (multi-scale), and physics phenomena (multi-physics) will be tested on a number of benchmark exercises for which experimental data are available and for which the power plant details have been released.

This report presents benchmark specifications for Phase II (Core Phase) of the OECD LWR UAM benchmark in a format similar to the previous OECD/NRC benchmark specifications. The Phase II consists of the following exercises:

- Exercise II-1: “Fuel Physics”: Fuel thermal properties relevant to steady-state and transient performance.
- Exercise II-2: “Time-Dependent Neutronics”: Neutron kinetics and fuel depletion stand-alone performance.
- Exercise II-3: “Bundle Thermal-Hydraulics”: Thermal-hydraulic fuel bundle performance.

These exercises take into account other physics involved in reactor core simulation, i.e. thermal-hydraulics and fuel physics as well as the time-dependent neutronics phenomenon. The output and target uncertainties of interest in Phase II are related to the following parameters:

- dynamic reactivity (dynamic control rod worth, boron worth and scram);
- time-dependent total power evolution, decay heat, power shapes;
- core/FA pressure drop;
- CHF/DNB ratio;
- moderator density, temperature and void distribution;
- pellet (fuel) and cladding temperature;
- geometry (thermal and mechanical deformation).

These exercises follow those established in the industry and regulation routine calculation scheme for LWR design and safety analysis. This phase is focused on understanding uncertainties in the prediction of key reactor core parameters associated with LWR stand-alone fuel modelling, bundle thermal-hydraulics and time-dependent neutronics core simulation. Such uncertainties occur due to input data uncertainties, modelling errors, and numerical approximations. The chosen approach in Phase II is to select/propagate for each exercise the most important contributors, which can be treated in a practical manner.

Depending on the availability of different methods in the computer code of choice for a given exercise, the related methodological uncertainties can play a smaller or larger role. The participants are responsible for performing convergence studies with their computer codes in order to remove the uncertainties associated with numerical approximations (numerical method uncertainties) and reduce the uncertainties associated with the methods (physics uncertainties) used in their codes. The method related contribution of uncertainty can be derived from earlier benchmarks conducted within NEA/OECD or from the verification (mathematics) and validation (physics) studies performed with the computer code of choice.

In the current LWR standard calculation scheme (utilised in industry and regulation) usually different modelling approximations are used at different stages of the calculation. These approximations are the second important source of input uncertainty. In order to assess the uncertainties due to utilisation of the above-mentioned approximations, one has to decompose and evaluate the errors of these approximations. Evaluation of the uncertainties introduced with such modelling approximations is important because in some situations these approximations work well and in others they do not. This is accomplished by designing appropriate test problems for a given exercise.

Geometry, material properties and manufacturing uncertainties are also an important source of calculation uncertainty. Information for these uncertainties for the different test models as well as on their propagation is provided in this specification.

It is important to understand the uncertainties in key output reactor core parameters associated with steady-state core simulation with regard to introducing appropriate design margins and deciding where efforts should be directed to reduce uncertainties. The obtained output uncertainties from Phase II of the OECD LWR UAM benchmark will be utilised as input uncertainties in the remaining phase – Phase II Phase III (System Phase).

Phase III will include system thermal-hydraulics and coupling between fuel, neutronics and thermal-hydraulics for steady-state, depletion and transient analysis. The target uncertainties for Phase III are as follows:

- Exercise III-1 - U-7 (uncertainties in coupled history (depletion) and instantaneous feedback (transient) modelling);
- Exercise III-2 - U-8 (uncertainties in thermal-hydraulics boundary conditions);
- Exercise III-3 - U-9 (uncertainties in safety related parameters and margins);
- Exercise III-4: “Comparison of Best Estimate Plus Uncertainty (BEPU) vs. Conservative Calculations”.

In Phase III the interactions between the prediction uncertainties and modelled control system actions will be taken also into account. It is very important to select appropriate transients with available measured data of good quality to be analysed in Phase III. The final objective is to compare the code predictions, uncertainties with measured data and uncertainties. PB-2 Turbine Trip data and Kalinin-3 VVER coolant transient data are appropriate. For appropriate TMI-1 transient data the CRISSUE database can be utilised.

References

1. “Neutronics/Thermal-hydraulics Coupling in LWR Technology”, Vol. 3, CRISSUE-S-WP3: Achievements and Recommendations Report, ISBN 92-64-02085-3, NEA No. 5434, OECD 2004.
2. “Uncertainty Analysis in Modeling UAM-2006 Workshop”, Summary Record, NEA/NSC/DOC (2006)15.
3. “Expert Group on Uncertainty Analysis in Modeling”, Mandate and Programme of Work, NEA/NSC/DOC (2006)17.
4. “Uncertainty Analysis in Modeling First Workshop (UAM-1)”, Summary Record, NEA/NSC/DOC (2007)17.
5. Technology Relevance of the “Uncertainty Analysis In Modeling” Project for Nuclear Reactor Safety, NEA/NSC/DOC (2007)15.
6. J. Solis, K. Ivanov, B. Sarikaya, A. Olson, and K. Hunt, “BWR TT Benchmark. Volume I: Final Specifications”, NEA/NSC/DOC (2001)1.
7. K. Ivanov, T. Beam, A. Baratta, A. Irani, and N. Trikouros, “PWR MSLB Benchmark. Volume 1: Final Specifications”, NEA/NSC/DOC (99)8, April 1999.
8. B. Ivanov, K. Ivanov, P. Groudev, M. Pavlova, and V. Hadjiev, “VVER-1000 Coolant Transient Benchmark (V1000-CT). Phase 1 – Final Specification”. NEA/NSC/DOC (2002)6.
9. B. Neykov, F. Aydogan, L. Hochreiter, K. Ivanov (PSU), H. Utsuno, F. Kasahara (JNES), E. Sartori (OECD/NEA), M. Martin (CEA), “OECD-NEA/US-NRC/NUPEC BWR Full-size Fine-mesh Bundle Test (BFBT) Benchmark”, Volume I: Specifications, © OECD 2006, NEA No. 6212, [NEA/NSC/DOC\(2005\)5](#).
10. A. Rubin, A. Schoedel, M. Avramova, *et al.* “OECD/NRC Benchmark Based on NUPEC PWR Subchannel and Bundle Tests; Vol. I: Experimental Database and Final Problem Specifications”, [NEA/NSC/DOC\(2010\)1](#) (November 2010).
11. “Core Design and Operating Data for Cycles 1 and 2 of Peach Bottom 2”, EPRI NP-563, June 1978.
12. “Transient and Stability Tests at Peach Bottom Atomic Power Station Unit 2 at End of Cycle 2”, EPRI NP-564, June 1978.
13. A. M. Olson, “Methods for Performing BWR System Transient Analysis”, Philadelphia Electric Company, Topical Report PECo-FMS-0004-A (1988).
14. F. Aydogan, L. Hochreiter, K. Ivanov (PSU), M. Martin (CEA), H. Utsuno (JNES), E. Sartori (OECD/NEA), “OECD-NEA/US-NRC/NUPEC BWR Full-size Fine-mesh Bundle Test (BFBT) Benchmark”, Volume II: Uncertainty and Sensitivity Analyses of Void Distribution and Critical Power - Specification, © OECD 2007, [NEA/NSC/DOC\(2007\)21](#).
15. J. Papin, B. Cazalis, J. M. Frizonnet, E. Federici, F. Lemoine (IRSN/DPAM), “Synthesis of CABRI-RIA Tests Interpretation”, Forum Eurosafe, Paris, November 2003.
16. “Neutronics/Thermal-hydraulics Coupling in LWR Technology”, Vol. 1, CRISSUE-S-WP1: Data Requirements and Databases Needed for Transient Simulations and Qualification, ISBN 92-64-02083-7, NEA No. 4452, OECD 2004.

17. “Neutronics/Thermal-hydraulics Coupling in LWR Technology”, Vol. 2, CRISSUE-S-WP2: State-of-the-art Report (REAC-SOAR), ISBN 92-64-02084-5, NEA No. 5436, OECD 2004.
18. P. M. Chantoin (CEA), E. Sartori (OECD/NEA), J. A. Turnbull, “The Compilation of a Public Domain Database on Nuclear Fuel Performance for the purpose of Code Development and Validation”, OECD/NEA, IFPE Database, June 1997.
19. G. M. O’Donnell, H. H. Scott, R. O. Meyer, “A New Comparative Analysis of LWR Fuel Designs”, NUREG-1754, USNRC, 2001.
20. A. Avvakumov, V. Malofeev, V. Sidorov, “Analysis of Pin-by-Pin Effects for LWR Rod Ejection Accident”, NUREG/IA-0175, USNRC, 2000.
21. I. Panka, A. Kereszturi, C. Maraczy, “Selected Examples on Multiphysics Researches at KFKI AEKI- Results for Phase I of the OECD/NEA UAM Benchmark”, Hungarian Academy of Sciences, 2010.
22. L. Yegorova, K. Lioutov, N. Jouravkova (KI), *et al.* “Experimental Study of Narrow Pulse Effects on the Behavior of High Burnup Fuel Rods with Zr-1% Nb Cladding and UO₂ Fuel (VVER Type) under Reactivity-Initiated Accident Conditions: Program Approach and Analysis of Results”, NUREG/IA-0213, Vol. 1, 2006.
23. L. Yegorova, K. Lioutov, N. Jouravkova (KI), *et al.* “Experimental Study of Narrow Pulse Effects on the Behavior of High Burn-up Fuel Rods with Zr-1% Nb Cladding and UO₂ Fuel (VVER Type) under Reactivity-Initiated Accident Conditions: Test Conditions and Results”, NUREG/IA-0213, Vol. 2, 2006.
24. A. Avvakumov, V. Malofeev, V. Sidorov (KI), H. H. Scott (NRC), “Spatial Effects and Uncertainty Analysis for Rod Ejection Accidents in a PWR, NUREG/IA-0215, USNRC, 2007.
25. D. B. Scott, “Physical and Mechanical Properties of Zircaloy 2 and 4”, Westinghouse Electric Corporation, Pittsburgh, PA, 1965.
26. K. J. Geelhood, W. G. Luscher, C. E. Beyer et al., “Predictive Bias and Sensitivity in NRC Fuel Performance Codes”, NUREG/CR-7001, PNNL-17644, PNNL, Richland, WA, 2009.
27. L. Pagani, “On the Quantification of Safety Margins”, Massachusetts Institute of Technology, Cambridge, MA, 2004.
28. K. Ivanov, M. Avramova, S. Kamerow, I. Kodeli, E. Sartori, E. Ivanov, O. Cabellos, “Benchmark for Uncertainty Analysis in Modeling (UAM) for Design, Operation, and Safety Analysis of LWRs, Volume I: Specification and Support Data for the Neutronics Cases (Phase I)”, Version 2.0, March 2012.
29. G. A. Berna (GABC), C. E. Beyer (PNNL), K. L. Davis (INEEL), D. D. Lanning (PNNL), “FRAPCON-3: A Computer Code for the Calculation of Steady-State, Thermal-Mechanical Behavior of Oxide Fuel Rods for High Burn-up”, NUREG/CR-6534 Vol. 2, PNNL-11513, 1997.
30. M. E. Cunningham, C. E. Beyer, P. G. Medvedev (PNNL), G. A. Berna (GABC), H. Scott (NRC), “FRAPTRAN” A Computer Code for the Transient Analysis of Oxide Fuel Rods”, NUREG/CR-6739, Vol. 1, PNNL-13576, 2001.
31. D. D. Lanning, C. E. Beyer (PNNL), G. A. Berna (GABC), “FRAPCON-3: Integral Assessment”, NUREG/CR-6534, Volume 3, PNNL-11513, 1997.
32. M. E. Cunningham, C. E. Beyer, F. E. Panisko, P. G. Medvedev (PNNL), G. A. Berna (GABC), H. H. Scott (NRC), “FRAPTRAN: Integral Assessment”, NUREG/CR-6739, Vol. 2, PNNL-13576, 2001.

33. B. Collins, A. Yanov, T. Downar (UMich), M. Klein, W. Zwermann (GRS), M. Jessee, M. Williamns (ORNL), “Application of PARCS to Uncertainty Analysis of TMI Minicore”, Presented at the UAM-5 Meeting, Stockholm, April 2011.
34. D. D. Lanning, E. R. Bradley, “Final Irradiation and Post-irradiation Data from the NRC/PNL Instrumented Assembly IFA-432”, HPR-329/7.
35. T. Sugiyama, T. Nakamura, K. Kusagaya, H. Sasajima, F. Nagase, T. Fuketa, “Behavior of Irradiation BWR Fuel under Reactivity-Initiated-Accident Results of Tests FK-1, -2, and -3”, JAERI-Research 2003-033, January 2004.
36. H. Devold, H. Wallin, “PIE Results from the High Burn-up Rods CD/CH (IFA-429) and Comparison with In-Pile Data”, HWR-409, October 1994.
37. U. Mertyurek, M. W. Francis, I. C. Gauld, “SCALE 5 Analysis of BWR Spent Nuclear Fuel Isotopic Compositions for Safety Studies”, ORNL/TM-2010/286, December 2010.
38. Y. Nakahara, K. Suyama, T. Suzaki, “Technical Development on Burn-up Credit for Spent LWR Fuels [Translated]”, JAERI-Tech 2000-071, ORNL/TR-2001/01, January 2002.
39. Y. Nakahara, K. Suyama, J. Inagawa, R. Nagaishi, S. Kurosawa, N. Kohno, M. Onunki, H. Mochizuki, “Nuclide Composition Benchmark Data for Verifying Burn-up Codes on Spent Light Water Reactor Fuels”, *Nuclear Technology*, Vol. 137, pg. 111-126, February 2002.
40. B. Roque, P. Marimbeau, J. P. Grouiller, A. Tsilanizara, T. D. Huynh, “Specification for the Phase 1 of a Depletion Calculation Benchmark Devoted to Fuel Cycles”, [NEA/NSC/DOC\(2004\)11](#), NEA/OECD, 2004.
41. C. E. Sanders, I. C. Gauld, “Isotopic Analysis of High-Burn-up PWR Spent Fuel Samples from the Takahama-3 Reactor”, NUREG/CR-6798, ORNL/TM-2001/259, 2003.
42. H. M. Dalle, “Monte Carlo Burn-up Simulation of the Takahama-3 Benchmark Simulation”, ISBN 978-85-99141-03-8, INAC Rio de Janeiro, Brazil, 2009.
43. Committee on the Safety of Nuclear Installations, “VVER-Specific Features Regarding Core Degradation - Status Report”, [NEA/CSNI/R\(98\)20](#), NEA/OECD September 1998.
44. B. D. Murphy (ORNL), J. Kravchenko, A. Lazarenko, A. Pavlovitchev, V. Sidorenko (KI), A. Chetverikov (State Scientific Center Research Institute of Atomic Reactors), “Simulation of Low-Enriched Uranium (LEU) Burn-up in Russian VVER Reactors with the Helios Code Package”, ORNL/TM-1999/168, March 2000.
45. U. Grundmann, S. Mittag, “DYN3D Calculations for the V-1000 Test Facility and Comparisons with the Measurements”, Research Centre Rossendorf, Institute of Safety Research, PHYSOR Chicago, 2004.
46. S. Mittag, U. Grundmann *et al.* “Validation of Coupled Neutronic/Thermal-hydraulic Codes for VVER Reactors”, FIKS-CT-2001-00166, FZR-408, Forschungszentrum Rossendorf, 2004.
47. G. Grandi, L. Moberg, “Qualification of CASMO5/Simulate-3K against the SPERT-III E-Core Cold Start-up Experiments”, Studsvik Scandpower, Inc., PHYSOR 2012, Knoxville, TN.
48. J. Dugone, “SPERT III Reactor Facility: E-Core Revision”, IDO-17036, Reactor Technology TID-4500 (44th Ed.), U.S. Atomic Energy Commission, November 1965.
49. R. E. Heffner, T. R. Wilson, “SPERT III Reactor Facility”, U.S. Atomic Energy Commission, Idaho Falls, ID, 1961.